CONTRACT NO. A132-167
FINAL REPORT
DECEMBER 1993

Development of an Objective Classification Procedure for Bay Area Flow Types Representing Ozone-Related Source-Receptor Relationships

CALIFORNIA ENVIRONMENTAL PROTECTION AGENCY
AIR RESOURCES BOARD
Research Division

Development of an Objective Classification Procedure for Bay Area Flow Types Representing Ozone-Related Source-Receptor Relationships

Final Report

Contract No. A132-167

Prepared for:

California Air Resources Board
Research Division
2020 L Street
Sacramento, California 95814

Prepared by:

Till E. Stoeckenius

Systems Applications International
101 Lucas Valley Road
San Rafael, California 94903

and

Paul T. Roberts
Lyle R. Chinkin

Sonoma Technology, Inc.
5510 Skylane Blvd., Suite 101
Santa Rosa, California 95403-1083

December 1993

Disclaimer

The statements and conclusions in this report are those of the contractor and not necessarily those of the California Air Resources Board. The mention of commercial products, their source, or their use in connection with material reported herein is not to be construed as actual or implied endorsement of such products.

Acknowledgments

A number of people beside the authors contributed significant amounts of time and energy to the completion of this project. Art Noda of Systems Applications International wrote and compiled the results of all of the SAS data analysis routines that provided the bulk of the results reported herein. Additional SAS results were provided by Art Carpenter of CalOxy Consultants, who conducted the discriminant analyses. Hilary Main and Stefan Musarra of Sonoma Technology performed the surface trajectory analyses. An extensive set of meteorological data for the Bay Area was provided by Jih-Yih Jiang of the Bay Area Air Quality Management District. Additional data was provided by Dorothy Miller at the Western Regional Climate Center. Data for Moss Landing was provided by Stephen Holets of Pacific Gas and Electric. Steve Sidawi of Valley Research Corporation, working under the direction of Dr. Yuji Horie, processed most of the meteorological and air quality data collected for the project and created the database files used in subsequent analyses. Dr. Ted Smith provided many helpful comments on a draft version of this report. Finally, Sharon Douglas of Systems Applications International provided the introductory overview of meteorological conditions in the San Francisco Bay Area.

This report was submitted in fulfillment of Contract No. A132-167, "Development of an Objective Classification Procedure for Bay Area Air Flow Types Representing Ozone-Related Source-Receptor Relationships," by Systems Applications International under the sponsorship of the California Air Resources Board. Work was completed as of 4/15/94.

Abstract

Air quality and meteorological data collected during a three-year period (1989–1991) in the San Francisco Bay Area and surrounding air basins (Broader Sacramento Valley, northern and central portions of the San Joaquin Valley, and the North Central Coast) were analyzed to determine air flow patterns and accompanying meteorological conditions associated with high ozone concentrations in the region. A set of six unique "source-receptor scenarios" were identified. The distinguishing meteorological features of each scenario were explored and used as the basis for the development of an objective procedure for identifying the most appropriate scenario for any given day based on the values of a few key routinely collected meteorological variables. Trajectory analyses were performed for selected days representative of the more common scenarios to determine the principal source-receptor relationships. Favored locations of high ozone concentrations under each scenario were also identified and diurnal profiles of ozone concentrations examined for evidence of interbasin transport of ozone and precursor material. These results provide an improved understanding of the mechanisms that control ozone concentrations in various portions of the study region. The results are particularly useful for the analysis of interbasin transport, air quality trends, and the selection of episodes to be used for photochemical modeling studies.

Contents

Figures

Tables

EXECUTIVE SUMMARY

INTRODUCTION

Air quality and meteorological data collected during a three-year period (1989–1991) in the San Francisco Bay Area and surrounding air basins (Broader Sacramento Valley, northern and central portions of the San Joaquin Valley, and the North Central Coast) were analyzed to determine air flow patterns and accompanying meteorological conditions associated with high ozone concentrations in the region. Information on the various types of conditions occurring in conjunction with ozone episodes can be used to gain a better understanding of the mechanisms that control ozone concentrations. In particular, a procedure for classifying days into groups based on similarities in flow patterns and accompanying meteorological and air quality conditions can provide information useful in the analysis of interbasin transport and air quality trends, and can be used to develop criteria for the selection of episodes for photochemical modeling studies.

Seven principal surface air flow patterns in the Bay Area were identified by Hayes et al. (1984). As in previous studies of this region, we found that five of these patterns are associated with high ozone concentrations somewhere within the study region[1]. Although the flow patterns evolve during the course of the day, our analysis and that of Douglas et al. (1989) indicates that mid-morning conditions, when precursor concentrations increase and rapid ozone formation begins, are closely related both to the magnitude and spatial distribution of afternoon maximum ozone concentrations and to meteorological conditions in the area. Thus, the 10:00 a.m. flow patterns provide a good initial indication of the most likely source-receptor scenario for the day.

PROCEDURES

Flow patterns assigned by ARB meteorologists to each episode day during the study period were compared with the daily ARB streamline charts and an independent assessment of the flow pattern over the coastal waters. These nearshore winds were

[1] The five flow patterns are Northwest, Northeast, Bay Outflow, Southerly, and Calm as depicted in Figure 3-2. For the purposes of this analysis, ozone episodes were defined by the occurrence of concentrations greater than 9 pphm in the San Francisco Bay Area Air Quality Management District or the North Central Coast, or concentrations greater than 12 pphm in the Broader Sacramento Valley or the northern or central San Joaquin Valley.

found to differ frequently from the onshore flow described by the ARB patterns. In addition, the distributions of ozone concentrations associated with each significant onshore-offshore flow pattern combination was examined. Based on these analyses, a set of candidate "source-receptor scenarios" was defined that describe the principal combinations of flow patterns, other meteorological conditions, and air quality conditions observed on episode days. Each episode day during the study period for which ARB streamline analyses were available was assigned to one of these scenarios. This tentative grouping of episodes was used to explore the principal features of each scenario through a series of analyses:

- A set of forward and backward surface air parcel trajectories were calculated on selected days representing each scenario. The trajectories provide an indication of the source regions impacting each downwind receptor area and the principal transport routes.

- Meteorological conditions associated with each candidate source-receptor scenario were analyzed to determine the principal features of each scenario. Box plots were used to compare the distributions of key meteorological variables between source-receptor scenarios on episode days and between episode and non-episode days.

- Exploratory cluster and discriminant analyses were conducted to provide quantitative measures of the principal meteorological features of each source-receptor scenario and to identify days that did not seem to fit well into the initial scenario to which they were assigned. Meteorological conditions on these days were examined, and days that appeared to be a better match with a different scenario were reassigned.

- Revised scenario assignments for episode days were used to develop a final set of linear discriminant functions. These functions form the basis of an objective source-receptor scenario classification procedure. A screening procedure was also developed to assist in identifying days that meet the basic meteorological requirements for the formation of high ozone concentrations. The objective classification procedure was used to determine the most likely source-receptor scenario for all such days. Application of the classification procedure is most appropriate for these days since conditions on other days may not match the general features of the source-receptor scenarios assigned by the procedure.

- Spatial patterns in ozone concentrations associated with each source-receptor scenario as assigned by the objective classification procedure were examined to identify locations where high concentrations occur most frequently. Diurnal ozone concentration patterns were examined for evidence of local production vs. transport of ozone and precursor material from upwind sources.

RESULTS

Results obtained from the analyses described above indicate that ozone episodes in the San Francisco Bay Area and surrounding air basins occur under a variety of meteorological conditions. However, low, strong subsidence inversions—as evidenced by high 850 mb temperatures, low inversion base heights, high temperatures at inland locations, and higher sea-level pressures at Reno than at San Francisco—are a common denominator. In most cases, temperatures along the coast remain cool, indicating at least localized onshore flow that can transport material inland. All of the episode days examined exhibit some or all of these characteristics. However, grouping episodes by source-receptor category reveals several unique features of each pattern:

- Northwest days are the most numerous and the most diverse group, representing a mix of conditions typical of episode days in general. Of all the episode days, this group has, on average, the least negative San Francisco-to-Reno surface pressure gradient (the gradient is near zero or negative on nearly all episode days). This suggests a relatively vigorous sea breeze and a deeper marine layer that maintains low ozone concentrations along the coast and around the Bay but provides for transport of precursor material inland where high concentrations can form. Trajectory analyses on Northwest days indicate that the transport of material from the Bay Area through the Delta primarily moves material to the south of Sacramento and into the northern San Joaquin Valley due to the presence of a northerly wind component within the Central Valley. More significant transport to Sacramento may occur under a weak northwest pattern when northerly component winds are not present as far south as Sacramento. Transport of material from the major Bay Area source regions to Livermore and Gilroy is consistent with the Northwest pattern.

- Northeast days are quite distinct with significantly higher pressure to the north and east of San Francisco (large negative San Francisco-to-Redding and San Francisco-to-Reno pressure gradients). This results in a north to northeasterly flow in the Southern Sacramento Valley and Delta region which can, but does not always, extend into the inland valleys of the Bay Area (e.g., Livermore). Thus, this scenario is not consistent with transport from the Bay Area to the Broader Sacramento Valley. However, strong offshore winds are not present over the Bay Area under this scenario since the presence of such winds generally eliminates any high ozone concentrations.[2] Instead, flow within the Bay Area is similar to that found under the Bay Outflow scenario. The Northeast pattern is also characterized by relatively warm temperatures along the coast.

- Bay Outflow days are similar in many respects to Northwest days, but with higher temperatures aloft and inland and weaker 700 mb and 500 mb height gradients.

---

[2] We note, however, that Douglas et al. (1989) studied a northeast flow event during 1980 during which the northeasterly winds penetrated into the Bay Area and produced exceedances in the South Bay. An event of this type was not observed during the 1989–1991 study period.

This indicates the presence of a broad, flat high pressure system with strong subsidence inversion and a weaker, primarily thermally driven surface circulation pattern that sets up in the absence of any synoptic-scale forcing. Under these conditions, winds are light and variable and the current wind monitoring network does not provide sufficient resolution to allow for the calculation of reliable trajectories. Streamline analyses indicate northerly winds in Sacramento at least during the morning hours, preventing transport from the Bay Area. However, transport from the Bay Area to Sacramento may be possible under this scenario if southwest Delta winds form early enough during the day.

- Calm days were only observed twice in conjunction with ozone episodes, making it difficult to draw any general conclusions regarding their principal meteorological characteristics. However, both days were characterized by generally weak surface and aloft pressure gradients, as one would expect.

- Southerly days are not normally associated with high ozone concentrations in the study region. Two episodes with very different meteorological conditions were classified as having southerly flow. In both cases, the only ozone exceedances were 13 pphm concentrations in Sacramento.

- Northwest-South days exhibited a variety of conditions similar to those associated with both Northwest and Bay Outflow patterns. Exceedances occurred at several monitors throughout the Bay Area on one of these days, but only at Livermore on another and only at Pinnacles on the remaining two. These results suggest that the characteristics of this flow pattern are quite diverse.

Surface trajectory analysis results indicate that transport from the Bay Area into the North Central Coast is possible under all but the Northwest-South scenario. However, routinely available data do not allow for distinguishing between those scenarios in which a convergence zone is or is not present in the vicinity of Gilroy. When present, this convergence zone effectively blocks surface transport between the South Bay and receptors to the south in the North Central Coast air basin, although transport aloft may still occur.

An objective procedure for assigning the most appropriate of the above source-receptor scenarios to any given day was developed on the basis of the unique meteorological features of each scenario. A linear discriminant analysis was used to derive a set of six linear functions of 13 key daily meteorological variables with one function corresponding to each source-receptor scenario. Each function is evaluated for a given day, and the scenario corresponding to the function with the largest value is taken as the most appropriate scenario for that day. Function coefficients for each meteorological variable are listed in Table 3-14; the variable names are defined in Table 3-6. The 850 mb temperature as measured by the morning Oakland radiosonde, afternoon maximum temperatures along the coast and in the Central Valley, and surface and aloft pressure differences between San Francisco and points to the north, south, and east provide the information needed to differentiate between scenarios.

When applied to the ozone episode days from which it was developed, the fraction of days assigned by the objective classification procedure to a scenario other than the one originally identified (i.e., the misclassification rate) was just 7 percent. Since the procedure is "tuned" to some extent to the peculiarities of these episode days, misclassification rates may be higher when an independent data set is used. Such a data set was not available for use in this study. However, estimates of the misclassification rate which might apply to an independent data set were obtained via crossvalidation. Crossvalidation results reveal that the procedure is usually able to correctly identify Northwest days. However, the procedure appears to be limited in its ability to distinguish Bay Outflow days from Northwest days: our crossvalidation estimate of the misclassification rate is on the order of 50 percent for this scenario. Not enough episode days belonging to any of the other source-receptor scenarios (Northeast, Calm, South, and Northwest-South) were observed during the study period to derive a meaningful crossvalidation estimate of the misclassification rate. The Northeast scenario is quite distinct and is likely to be identified correctly; meteorological conditions distinguishing the other scenarios are not as clearcut.

Meteorological conditions on ozone episode days represent a subset of the full range of conditions which may be observed in the study region. Combinations of wind flow patterns and meteorological conditions other than those represented by the six source-receptor scenarios described above may occur on non-episode days. Thus, application of the objective classification procedure to non-episode days may produce misleading results. Unfortunately, it is difficult to devise a classification procedure that correctly separates episode days from non-episode days on the basis of meteorological conditions. Procedures based on classification trees and discriminant analysis incorrectly classify a high percentage of the episode days as non-episode days. Therefore, a simple screening procedure was devised which defines "potential ozone days" as any day meeting the following requirements:

> Oakland morning 850 mb temperature $\geq$ 17.5° C, and
> Sacramento and Fresno surface temperatures $\geq$ 85° F, and
> San Francisco-to-Reno surface pressure difference $\leq$ 10 mb.

Nearly all (86 percent) of episode days meet these requirements while 85 percent of non-episode days do not. The six source-receptor scenarios described above as predicted by the objective classification procedure should provide reasonably accurate descriptions of the wind flow patterns and meteorological conditions on potential ozone days; conditions on other days may be quite different.

The objective source-receptor scenario classification procedure was applied to all potential ozone days during the study period to determine the most appropriate scenario for each day. Daily maximum ozone concentrations for days assigned to each scenario were examined to evaluate differences in the spatial distribution of ozone concentrations between scenarios. In addition, diurnal profiles of average hourly ozone concentrations on episode days were computed for key monitoring sites to evaluate the potential for transport under each scenario; an extended period of high ozone concentrations during the afternoon or a second peak in late afternoon is a telltale indication of transport impacts.

The principal features of spatial ozone distributions associated with each scenario, as revealed by these analyses, are:

- Concentrations in the immediate vicinity of San Francisco Bay are generally highest under the Northeast and Bay Outflow scenarios, when the sea breeze is weakest. Similarly, concentrations in San Jose are highest under Northeast and Calm scenarios.

- Peak concentrations at Livermore are highest under Northwest and Bay Outflow scenarios, and exceedances of 9 pphm are most frequent under Bay Outflow conditions. Diurnal profiles show little difference in the timing of the afternoon peak between scenarios.

- Concentrations in the Sacramento area are lowest under the Northeast scenario, when transport from the Bay Area is cut off by northerly component winds in the valley and local emissions are transported away from the area. Much higher concentrations are observed under the Bay Outflow and Northwest scenarios and exceedances of 9 pphm are most common under Bay Outflow conditions, most likely as a result of increased stagnation, high temperatures, and reduced vertical mixing, both in the Bay Area and in Sacramento. Our trajectory analyses on Northwest episode days showed no evidence of transport from the Bay Area due to northerly component flow in the Broader Sacramento Valley. However, such transport may occur on some days included in the Northwest category when conditions allow southwest Delta winds to extend into the Sacramento metropolitan area. While data on Bay Outflow days was insufficient for calculating trajectories, streamline analyses prepared for a few such days indicate northerly winds in the Sacramento area (which would prevent transport from the Bay Area) at least during the morning hours. Diurnal profiles show little difference between scenarios in the timing of the late afternoon ozone maximum in Sacramento, thus providing no clear indication of transport under any scenario.

- Highest ozone concentrations in the northern and central San Joaquin Valley are associated with the Bay Outflow scenario. Diurnal profiles at Stockton and Modesto reveal higher late afternoon concentrations under this scenario, indicating possible transport from the Bay Area and, in some cases, Sacramento. This feature is not evident at Fresno.

CONCLUSIONS AND RECOMMENDATIONS

Results from this study provide a good basic description of the major categories of meteorological conditions, including wind flow patterns, most commonly associated with high ozone concentrations in the San Francisco Bay Area and surrounding air basins, and the resulting spatial and temporal distribution of ozone concentrations. In addition, the objective classification procedure developed here can be used to identify the most likely scenario for any given day based on the value of a few key meteorological measurements which are available on a routine basis. This information will be useful for isolating

meteorological conditions in trends analyses, assessing the potential for interbasin transport, and selecting episodes to be used in photochemical modeling exercises.

Further refinement of the unique meteorological and air quality features of each source-receptor scenario we have identified would enhance the usefulness of our results. Additional study of transport between air basins under each scenario is especially needed. Currently available data are only sufficient to suggest the possibility of transport in some cases, but not to confirm the occurrence or quantify the magnitude of transport. Some wind profiler data have been collected at key locations to help address this need; however, these data were not available in time for use in our study.

Crossvalidation results of the objective source-receptor scenario classification procedure developed in this study indicate that improvements in the identification of Bay Outflow days may be needed. In addition, more examples of Northeast, Calm, and Northwest-South scenarios are needed to confirm the proper identification of these scenarios. Air quality and meteorological conditions on Northwest-South days in particular require further study. These needs could be met through the assembly and analysis of additional air quality and meteorological data. Extending the analysis to include at least an additional three years of data (say, 1992, 1993, and, when available, 1994) is recommended.

The objective classification procedure presented in this report is based on a set of 13 meteorological variables. Preliminary stepwise discriminant analyses indicate that a procedure based on just four of these variables would perform almost as well. Reducing the number of variables would simplify the procedure and reduce problems encountered when one or more of the variables are missing. This possibility should be explored in more detail.

1 INTRODUCTION

BACKGROUND

Ozone concentrations in the San Francisco Bay Area, North Central Coast, Northern San Joaquin Valley, and Broader (i.e., southern) Sacramento Valley occasionally exceed state (and, in some cases, federal) air quality standards. As a result, much effort has been devoted towards gaining an understanding of the conditions resulting in high ozone concentrations in these air basins.

Ozone formation is the result of complex photochemical reactions of precursors in the atmosphere. The observed ozone concentration in an area depends on (1) the concentration levels of ozone and precursors swept into the region by the wind, (2) precursors emitted within the region, (3) the rate at which reactions leading to ozone formation take place, (4) the rate of dilution due to vertical and horizontal dispersion, and (5) the rate at which reaction products are advected out of the region. All of these factors are heavily influenced by meteorological conditions. Therefore, to understand the underlying causes of high ozone concentrations, one must study the mechanisms by which meteorological conditions affect each factor. Meteorological effects are important in many applications, including:

- **Transport:** Ozone and precursors may be transported from one air basin to the next or from one part of an air basin to another, thus contributing to exceedances in the downwind location. The direction of transport and its impact relative to ozone formed from local emissions is controlled by meteorological conditions. If these conditions can be identified, then the overall contribution of emissions in upwind areas to ozone impacts downwind can be quantified.

- **Trends:** Many studies have established that changing meteorological conditions contribute significantly to day-to-day and year-to-year variations in ozone concentrations. These variations make it difficult to detect long-term ozone trends such as might reflect trends in precursor emissions. If an accurate statistical model relating meteorological conditions and ozone concentrations can be developed, then meteorologically adjusted ozone trends can be calculated by applying the model to a standardized set of meteorological conditions.

- **Episode Selection for Modeling:** Mathematical models that describe the dispersion and chemical reactions of ozone and precursors are a major tool in the development of ozone control strategies. Due to the specialized nature and large amount of input data required, it is only practical to model a handful of ozone

episodes. Estimates of the ozone distribution under future emission control scenarios (needed to estimate future design values and population exposures) can be accurate only if that handful of episodes adequately represents the range of meteorological conditions associated with high ozone concentrations and if the frequency of occurrence of each type of episode is known.

STUDY OBJECTIVES

From the above discussion it is clear that the diversity and frequency of meteorological conditions associated with high ozone concentrations must be understood to develop efficient emission control strategies and to track progress in reducing ozone concentrations. To fulfill this need, a method for classifying ozone episodes according to meteorological conditions is needed.

The primary goal of this study is to develop an objective procedure, based on routinely available meteorological data, for classifying ozone episodes in the Bay Area and adjacent air basins according to source-receptor scenarios. A source-receptor scenario describes a group of spatially and temporally varying meteorological conditions that determine the trajectories that air parcels follow from source regions to receptor regions, along with the environmental conditions the parcels encounter as they travel along these trajectories. Air flow patterns[1] alone determine the parcel trajectories, and hence the source-receptor couples, but they do not fully describe the other meteorological factors that can affect ozone concentrations within the parcels. Thus, source-receptor scenarios can be thought of as subsets of air flow patterns representing different combinations of meteorological conditions (e.g., temperature, mixing height) that may be associated with a given flow pattern. This distinction between air flow patterns and source-receptor scenarios is useful in spite of the correlation of wind fields with other meteorological variables since, in practice, flow pattern specifications must be stated in broad terms which allow for considerable within-pattern variations.

A useful source-receptor classification system must take into account requirements imposed by the following potential applications:

- **Transport Assessment:** Days with similar directions, speeds and magnitudes of ozone and precursor transport between air basins should be grouped together.

  Previous studies have shown that interbasin transport of ozone and precursor pollutants from the San Francisco Bay Area to adjacent air basins occurs from time to time (Roberts et al., 1992). The 1988 California Clean Air Act requires that the ARB assess the relative contribution of upwind emissions to downwind pollutant concentrations in areas where transported pollutants have been identified to cause or contribute to violations of the state ozone standard. An objective

[1] An air flow pattern is defined here as a pattern in both time and space. Thus an air flow pattern represents a particular temporally and spatially varying pattern of winds.

source-receptor scenario classification procedure is needed to provide information on the frequency of occurrence of meteorological conditions that are associated with such interbasin transport.

- **Trends Analysis:** Days on which the meteorological variables that control the amount of ozone transported into and formed in each receptor region (winds, temperature, mixing height, etc.) are at similar levels should be grouped together.

  Underlying trends in ozone concentrations expected to be associated with year-to-year changes in precursor emission levels are difficult to detect due to the great meteorologically induced variability in annual ozone summary statistics. A classification of days by source-receptor scenario can be used as the foundation of a procedure for developing ozone trends that have been adjusted to account for variations in meteorological conditions, thus exposing the underlying trends.

- **Episode Selection for Modeling:** Days for which a particular emission control scenario would produce similar changes (considering both magnitude and location) in ozone concentrations should be grouped together.

  The requirements that the selected ozone episodes be representative and that the frequency of occurrence of all source-receptor scenarios be known can be fulfilled through an objective source-receptor scenario classification system. With such a system, model episodes can be selected from among those found to be representative of each source-receptor scenario and design values expected under simulated control scenarios can be estimated by weighting the simulation results for each episode according to the frequency of occurrence of the scenario it represents.

OVERVIEW OF APPROACH

The approach we used for analyzing source-receptor scenarios in the San Francisco Bay Area and surrounding air basins applies a number of ideas gained from a similar study of the South Coast Air Basin (Stoeckenius et al., 1991) and several recent analyses of photochemical modeling, trends analysis and transport issues in the Bay Area and adjacent air basins (Roberts et al., 1992). Principal source-receptor scenarios were identified and examined in a series of steps:

- A brief review of previous analyses of ozone episode conditions in and around the Bay Area was conducted (see below).

- An extensive database of aerometric and meteorological variables was collected (see Section 2). These data were selected to represent conditions in the San Francisco Bay Area (SFBA), Broader Sacramento Valley (BSAC), the Northern San Joaquin Valley (NSJV), and the North Central Coast (NCC) as far south as Pinnacles National Monument (see Figure 2-1). The most recent three-year period for which data were available when our study began was used (1989–1991).

- Principal air flow patterns within the study region were examined and categorized (see Section 3). The spatial distributions of daily maximum ozone concentrations under these flow patterns were compared to determine the major ozone receptor areas under each pattern. A trajectory analysis was used to identify the major source regions associated with each receptor area and the routes by which material was transported to the receptors.

- Meteorological conditions associated with ozone episodes were identified as were variations in these conditions from one flow pattern to the next (see Section 3). These results provide an indication of the environmental conditions experienced by air parcels as they travel from source regions to the receptor areas.

Taken together, the results of these analyses provide a comprehensive picture of the nature of each of the principal source-receptor scenarios in the study region.

REVIEW OF PREVIOUS ANALYSES OF THE METEOROLOGICAL ASPECTS OF BAY AREA OZONE EPISODES

Flow Patterns Under Episode Conditions

The San Francisco Bay Area is a meteorologically and topographically complex region. The semipermanent Pacific High, which reaches its northernmost latitude in July and August, dominates the weather in the Bay Area during the summer months (the primary ozone season). Another persistent feature during this time is the thermal trough that envelops California's Central Valley. Together, these large-scale features produce an onshore (west to east) pressure gradient force and typically onshore flow.

Superimposed on this large-scale meteorology are mesoscale perturbations that produce the local weather and flow patterns. The typical onshore pressure gradient is enhanced during the day by the unequal heating of the land and water surfaces and gives rise to a sea breeze. The strength of the sea breeze depends on the magnitude of the pressure gradient. Penetration of the sea breeze inland into the Bay Area and the Central Valley is controlled by the coastal and inland mountain ranges, a series of north-south ridges running parallel to the coastline. The sea breeze penetrates inland through gaps in these mountain ranges.

The mesoscale airflow is channeled and deflected by the terrain and transformed by upslope and downslope flows along the terrain. The effects of terrain and the local thermal gradients differ under varying synoptic conditions. Strong synoptic pressure gradients render local gradients and terrain less effective in determining the local flow patterns. It is the interaction between the synoptic-scale and mesoscale meteorology that produces the widely varying local weather patterns of the Bay Area.

A meteorological classification scheme for Northern California was developed by Smith and co-workers (1985). Local flow patterns have also been classified according to the general direction of low-level flow over the area (Smalley, 1970; Hayes et al., 1984).

Seven types of characteristic flow patterns were identified by Hayes and co-workers (see Figure 3-2): northwesterly flow (moderate to strong and weak), southerly flow, southeasterly flow, northeasterly flow, bay inflow, bay outflow, and light and variable (not shown). The bay inflow and bay outflow patterns describe the development of local onshore and offshore breezes that develop around the bay due to temperature gradients between the land and water surfaces.

Douglas and co-workers (1989) used the classification system of Hayes and co-workers to categorize all ozone exceedance days within the period 1983-1987 according to wind flow pattern. During this period the one-hour national ambient ozone standard (12 pphm) was exceeded in the Bay Air Quality Management District (BAAQMD) on 70 days. The ozone exceedance days were grouped into five categories based on analyses of the wind flow patterns at 0400, 1000, 1600 and 2200 PST. Although airflow at virtually all hours can influence the source-receptor relationship, Douglas et al. determined that the air flow pattern at 1000 PST was most important in the categorization of the episodes as this roughly corresponds to the time of maximum morning emissions and transport. The primary time for ozone formation from its precursors is between 0900 and 1400 PST. Since nighttime and early morning winds are usually light on episode days, the 1000 PST wind flow pattern can predominate in the establishment of the spatial pattern of ozone exceedances in the mid-afternoon. The 1600 pst flow patterns are dominated by strong northwesterly flows and do not provide much information with which to differentiate patterns in ozone exceedances. As defined by Douglas and co-workers, Group 1 contains all days that have primarily northwesterly flow throughout the day (periods of stagnation may be interspersed with the northwesterly flow). Group 2 includes days dominated by the bay outflow pattern. All days within this group can be classified as having a bay outflow pattern at 1000 PST. Bay outflow is combined with periods of northwesterly flow as well as calm periods throughout the day. Group 3 includes all exceedance days with southerly flow. Group 4 contains those exceedance days with northeasterly flow, and Group 5 represents bay inflow. Group 1 accounts for 33 percent of ozone exceedance days, Group 2 for 34 percent, Group 3 for 24 percent, Group 4 for 6 percent, and Group 5 for 3 percent.

A comparison of this distribution of exceedance days with the Smith et al. (1985) 500 mb height patterns on the same days (as reported by Douglas and co-workers) shows only a very weak relationship between the surface and upper-air patterns with the "Broad Ridge" pattern slightly more common than expected under bay outflow conditions. This finding reflects the generally flat 500 mb height gradients found over Northern California during episode events.

Meteorological Conditions Associated with Bay Area Episodes

Zeldin and Meisel (1978) reviewed an early study by the Bay Area Air Quality Management District which identified daily maximum temperature and inversion base height as being strongly correlated with daily maximum ozone concentrations. An analysis by Sandberg et al. (1978) revealed a connection between summer ozone levels and rainfall over the preceding two winters. This relationship may be a unique result of

California's mediterranean climate (unpublished accounts have been given of similar relationships in the South Coast). Douglas et al. (1989) demonstrated that high ozone events in the Bay Area are associated with a negative San Francisco-to-Reno surface pressure gradient, high temperatures, strong inversions, and lower than normal wind speeds. These conditions are consistent with a weaker than normal sea breeze, which keeps ozone and precursors over the Bay Area for longer periods and provides warm, sunny conditions that contribute to high ozone concentrations. However, other conditions (in particular, stronger sea breezes), although lowering ozone concentrations in the immediate vicinity of the Bay, can contribute to high concentrations in downwind areas.

Bay Area Transport Patterns

Four ARB-sponsored studies of interbasin transport involving the Bay Area have been completed in recent years (ARB, 1990; Douglas et al., 1991; Roberts et al., 1992; Roberts et al., 1993). Transport of ozone and precursors originating in the Bay Area has also been examined in connection with several other studies (Dabberdt, 1983; Roberts and Main, 1989; Douglas et al., 1989). These studies have shown that significant amounts of material are occasionally transported out of the Bay Area via three main exits:

(1) The Sacramento River Delta area, from which pollutants can be transported into the Sacramento Valley and the San Joaquin Valley

(2) The San Ramon and Livermore Valleys and eventually the Altamont Pass area, from which pollutants can be transported into the San Joaquin Valley

(3) The south bay and San Jose areas and eventually the Gilroy/Hollister area, from which pollutants can be transported into Monterey County.

Ozone and precursors may be transported near the surface and aloft along these paths. Additional aloft transport paths may exist, especially in the San Martin/Gilroy area where a convergence zone can inject pollutants aloft into the northwesterly flow which then moves them into the San Joaquin Valley. Material from the Bay Area may also be transported offshore and then southeast along the coast and eventually onshore again into the North Central Coast Air Basin.

Transport along the routes described above does not necessarily occur under all of the meteorological regimes associated with high ozone concentrations. Therefore, sources in the Bay Area may contribute to exceedances in downwind basins on some days but not on others. Formulation of appropriate emission control measures requires estimates of the frequency with which interbasin transport occurs and the relative contribution of such transport to downwind ozone concentrations. These considerations also apply to transport from one portion of the Bay Area to another.

2 DATA GATHERING

Identifying source-receptor scenarios for the SFBA and surrounding air basins requires a comprehensive set of air quality and meteorological data that details the formation of ozone and the transport of ozone and precursor material under a variety of conditions associated with exceedances of the state and federal ozone standards. In this section, we describe the procedures used in collecting and processing the necessary data. Tables and figures for this section begin on page 2-5.

SELECTION OF STUDY PERIOD

The data must cover a period long enough to capture the full range of meteorological scenarios associated with high-ozone events. Long periods of record are also desirable for the analysis of air quality trends. On the other hand, insofar as aerometric data are used to identify source-receptor scenarios, the analysis requires a period during which the magnitude and spatial distribution of emissions are approximately constant. But too short a period of record will not include enough data to yield statistically meaningful results. In past studies, three years of data has generally been selected as a compromise between these conflicting requirements. Since recent data are of most interest and since special efforts to collect aerometric and meteorological data were made during 1990 and 1991 (including data from the special NOAA/WPL radar wind profiler monitoring network for the analysis of wind fields), the period 1989-1991 was selected for analysis.

Since our study is concerned with high-ozone episodes, we restricted our attention to the months April-October. Our previous analysis of ozone episode characteristics in the South Coast Air Basin (Stoeckenius et al., 1991) raised a concern about the potential effects of differences in emission patterns between weekdays and weekends (documented by Horie, 1988). As a result, that analysis was restricted to Tuesdays, Wednesdays, and Thursdays, which left a relatively small number of episodes available for analysis and ignored many episodes occurring on other days, especially Saturdays. While planning the current analysis, we first decided to restrict attention to weekdays only, but after developing a definition of an ozone episode for our analysis we found the number of weekday episodes to be quite limited, and therefore we decided to include weekends.

DATA SOURCES

We gathered a large amount of air quality and meteorological data for this study, including:

- Hourly average ambient ozone, NO, NO_2, and NO_x concentrations for all routinely reporting monitors in the San Francisco Bay Area, Northern San Joaquin Valley (from Fresno County northward), North Central Coast, and Sacramento Valley air basins. Stations included in the study are listed in Table 2-1. Site locations are indicated in Figure 2-1. These data were provided by the ARB.

- Hourly wind speed and direction, temperature, relative humidity, sigma-theta, and solar insolation observations at all BAAQMD 10-m tower sites (sites are listed in Table 2-2). These data were provided by the BAAQMD.

- Geopotential height, temperature, and wind speed and direction data for five levels (surface, 1000 mb, 900 mb, 850 mb, and 500 mb) from the twice-daily upper air soundings at Oakland, Los Angeles (LMU), Winnemucca, and Medford. These data were obtained from the Western Regional Climate Center and processed for this study by the BAAQMD.

- Inversion base height, top height, and temperature difference for the twice-daily Oakland upper air soundings (provided by Jih-Yih Jiang of the BAAQMD).

- Hourly surface meteorological observations (wind speed and direction, ceiling height, dry bulb temperature, wet bulb temperature, relative humidity, sea level pressure, total opaque sky cover, precipitation indicator) for San Francisco, Reno, Redding, Sacramento, Monterey, Stockton, and Fresno. These data were obtained from the Western Regional Climate Center.

- Surface meteorological data (wind direction, speed, temperature, relative humidity) from a 60-foot tower located at Pacific Gas and Electric's Moss Landing power plant (these data provided by Stephen Holets of PG&E).

Data from the NOAA/WPL radar wind profilers, which were operated at key locations during a portion of the study period, were unavailable in time for use in this study.

All of the above data were examined for completeness, outliers, proper formatting, and proper identification of units before being entered into the project database.

PROCESSING OF OZONE DATA

Daily maximum hourly average ozone concentrations were calculated for each day at each site. Values from days with less than nine hourly averages between 0900 and 2100 PST were ruled invalid. Table 2-1 lists the number of valid daily maximum concentrations, the number of days exceeding 9 pphm, and the minimum, maximum, and mean daily maximum concentrations at each site. Note that these summary statistics were compiled for weekdays only since the initial study design called for excluding weekends; however, the analyses in Section 3 are based on all days, not just weekdays. Monitors listed in Table 2-1 as having more than about 430 valid daily maximum concentrations can be considered to have essentially complete data records for 1989-1991.

Analysis of ozone concentration data is facilitated by dividing the study area into subregions, each containing one or more monitors with highly correlated readings. The formation of subregions—small clusters of monitors that experience similar ozone levels and respond similarly to changing meteorological factors—both reduces the volume of data to be analyzed and reduces the influence of micro-scale factors that may affect individual monitors but are of little importance in identifying source-receptor scenarios.

A preliminary grouping of monitors into subregions was based on discussions with BAAQMD personnel responsible for daily air quality forecasting. This grouping was then evaluated via an interstation correlation analysis on daily maximum ozone concentrations to assess the degree of covariance between the monitoring sites. This analysis led to the final grouping of monitors into subregions. Patterns of missing data were analyzed to identify cases in which subregion averages may be adversely affected by changes in the number of stations reporting. For subregions with sufficient numbers of stations with mostly complete data records, stations with frequently missing data were dropped from the analysis. This procedure resulted in adequate spatial coverage by monitors with nearly complete data records in all subregions except for the Western Alameda and Southwestern Sacramento Valley subregions.

For the Western Alameda subregion, two monitors in San Leandro are included: Station 60328 (San Leandro), for which data are available for 1989 only, and station 60343 (San Leandro County Hospital), for which data are available from August 1990 through October 1991. The two other monitors in this subregion (Fremont and Hayward) have nearly complete data records throughout the study period. San Leandro ozone readings were found to be sufficiently different from those in Fremont and Hayward to warrant including some measure of San Leandro ozone in the subregion average. A linear regression analysis was performed with the County Hospital monitor daily maximum ozone as the dependent variable and the Fremont and Hayward ozone as the predictors. The resulting regression equation ($r^2 = 0.69$) was used to calculate the San Leandro daily maximum ozone concentration for the entire study period. These concentrations were then averaged with those from Fremont and Hayward to arrive at the Western Alameda subregion average daily maximum ozone concentration. This is the only subregion for which such a regression technique was applied.

Stations in the Southwestern Sacramento Valley subregion generally had poor data coverage, and correlations between stations were low. Spatial averages for this subregion should be interpreted with caution and values at individual stations consulted before drawing any final conclusions about the behavior of ozone concentrations in this area.

The final set of monitoring sites included in each subregion is listed in Table 2-3. Note that Pinnacles and Hollister were grouped together for the purpose of defining subregions although the Pinnacles monitor is located at an elevated site and does not correlate particularly well with any nearby sites (highest correlation, 0.688, is with Gilroy; correlation with Hollister is 0.606). Jiang (1992) noted that Pinnacles is more closely correlated with other elevated sites in southern Monterey County, even though these sites are located much farther away. A physical explanation for this relationship is not apparent, although it has been suggested that the correlations result from ozone trapped

above the inversion layer. Further research on this important finding is recommended. Only monitors in Sacramento and the immediate vicinity are included in the Sacramento Area subregion. Auburn and Rocklin, which often exhibit the peak concentration in the Broader Sacramento Valley, are not included to avoid focusing on peaks that may be due primarily to emissions from Sacramento alone. The Folsom monitor, which is closer to Sacramento than Auburn or Rocklin, is included in the subregion as this site may be influenced by Bay Area emissions on some days when the ozone peak produced by Sacramento emissions lies to the northeast. Two monitors in Fresno (Olive and 3425 First St.) were combined to obtain one site with a complete data record.

Subregion average daily maximum ozone concentrations (SADMOCs) were computed from valid daily maximums at the monitors listed in Table 2-3. Relative SADMOCs were then calculated for each subregion by taking the ratio of the SADMOC to the daily maximum concentration averaged over all subregions. These ratios were used to identify groups of days with similar spatial distributions of relative ozone concentrations, as described in Section 3.

Meteorological Data

All meteorological data collected for the study were processed by Valley Research Inc. into a series of Paradox database files. These files were further processed into SAS data sets, and key daily meteorological variables were constructed and merged with the daily subregion ozone data set. The selection of key daily meteorological variables is described in Section 3.

TABLE 2-1. Ambient air quality monitoring sites and ozone concentration summary statistics.

Station No.	Station Location	No. Valid Days	No. Days > 9 pphm	Daily Maximum Min.	Daily Maximum Max.	Daily Maximum Mean
San Francisco Bay Area						
07442	Bethel Island	628	19	2	12	5.6
07440	Concord	632	13	2	11	4.9
48875	Fairfield	634	8	2	11	4.7
60336	Fremont	637	20	2	13	4.7
43389	Gilroy	636	20	2	13	5.8
60337	Hayward	607	3	1	11	3.5
43380	Los Gatos	631	13	1	12	4.9
43387	Mountain View	629	9	2	12	4.4
28783	Napa	621	5	2	11	4.3
60339	Oakland	591	0	1	8	2.7
07430	Pittsburg	638	9	2	11	5.0
41541	Redwood City	636	1	1	10	3.6
07433	Richmond	639	1	1	10	3.3
90306	San Francisco	634	0	1	8	2.8
43382	San Jose, 4th Street	632	20	1	13	4.9
43386	San Jose, Piedmont Rd.	415	10	2	12	5.0
43390	San Jose, W. San Carlos	541	7	1	13	4.2
60328, 60343	San Leandro	456	2	1	12	3.4
21451	San Rafael	634	0	1	8	3.0
49893	Santa Rosa	612	0	1	9	3.7
49887	Sonoma	615	6	2	10	4.7
48879	Vallejo	628	6	2	12	4.3
60340	Livermore	632	34	2	14	5.4

TABLE 2-1. Continued

Station No.	Station Location	No. Valid Days	No. Days > 9 pphm	Daily Maximum Min.	Daily Maximum Max.	Daily Maximum Mean
North Central Coast						
27550	Carmel Valley	608	4	2	13	4.8
44851	Davenport	594	1	1	10	3.7
27544	Salinas	636	0	2	8	3.8
44850	Santa Cruz	617	1	2	12	4.4
35823	Hollister	618	4	2	11	5.1
—	Pinnacles*	—	—	—	—	—
Sacramento Valley						
31813	Auburn	498	81	3	15	7.5
57578	Broderick	379	11	1	14	5.5
34293	Citrus Heights	631	55	2	15	6.2
57577	Davis	372	6	2	11	5.9
34287	Folsom	612	102	2	19	7.0
34294	North Highlands	377	18	1	13	6.0
31810, 31820	Rocklin	590	52	2	15	6.5
34286	Sacramento, Meadowview	585	53	3	14	7.1
34295	Sacramento, Del Paso Manor	629	57	2	18	6.5
34305	Sacramento, 1309 T St.	620	14	0	14	5.3
34307	Sacramento, Earhart Dr.	520	33	0	15	5.7
48881	Vacaville	280	5	2	12	5.1
57569	Woodland	462	8	2	11	5.6
—	Lambic Road*	—	—	—	—	—

* Summary statistics not available for this site.

TABLE 2-1. Continued

Station No.	Station Location	No. Valid Days	No. Days > 9 pphm	Daily Maximum Min.	Daily Maximum Max.	Daily Maximum Mean
San Joaquin Valley						
10248	Clovis	254	47	3	13	7.4
50571	Crows Landing	442	41	2	15	6.7
10234	Fresno, Olive	202	50	3	14	7.5
10244	Fresno, 4706 E. Drummond	588	127	3	15	7.7
10245	Fresno, Sierra Skypark 2	500	80	2	15	7.4
10246	Fresno, 3425 First St.	411	108	3	18	8.1
20003	Madera	538	40	2	13	6.9
50568	Modesto	629	55	2	13	6.2
10230	Parlier	599	202	3	15	8.5
39252	Stockton, Hazelton St.	632	22	2	12	5.4
39267	Stockton, 13521 E. Mariposa	526	43	1	13	6.4
50562	Turlock	597	69	2	13	6.9
50572	Westley	240	12	3	13	6.1

TABLE 2-2. Meteorological data availability from 10 m towers in the San Francisco Bay Area.*

Tower Location	Measurement Start Date
Union City	September 1987
Fremont	August 1989
Chabot	September 1989
Sunol	September 1989
Pleasanton	May 1991
Bethel Island	July 1987
Danville	August 1989
Concord	September 1990
Highland	September 1989
Kregor	September 1989
Vollmer Peak	September 1989
Pt. San Pablo	September 1989
Mt. Tamalpais	July 1989
Alviso	November 1989
Rio Vista	July 1989
Valley Ford	August 1989
Napa	May 1987
Ft. Funston	April 1988
San Carlos	April 1991
Mt. Pise	September 1989
San Martin	May 1987
San Jose (airport)	September 1987
Gilroy	August 1989
Mt. Hamilton	September 1989
Petaluma	May 1987
Santa Rosa	May 1987
Sonoma Baylands	October 1989

* Each tower measures hourly average wind speed, direction, temperature, and relative humidity at the 9 m level.

TABLE 2-3. Ozone monitoring stations contained within each subregion.

ARB Bay Area Ozone Study
Subregion Definitions

Subregion	Stations	Comments
North Bay (NBAY)	Napa, Sonoma, Vallejo, Fairfield	Ignore Santa Rosa
Contra Costa Co. (CONT)	Bethel Is., Concord, Pittsburg	
Inner Bay (IBAY)	San Rafael, Richmond, Oakland, San Francisco, Redwood City	Significantly higher readings at Redwood City but these do not correlate well with San Jose
Western Alameda County (WALA)	San Leandro, Hayward, Fremont	
Livermore Valley (LVRM)	Livermore	
South Bay (SBAY)	Los Gatos, Mountain View, San Jose (4th St), Gilroy	Peak concentrations at Gilroy frequently much higher than at other sites; analyze Gilroy separately where appropriate
Monterey Bay (MBAY)	Davenport, Santa Cruz, Salinas, Carmel Valley	All sites have major marine influence
Southern Santa Clara Valley (SSAN)	Hollister, Pinnacles	Pinnacles is at 335 m elevation; may need to analyze separately (see text)
Southwestern Sacramento Valley (WSAC)	Woodland, Davis, Vacaville, Lambie Road	Lower interstation correlations and incomplete data characterize this subregion
Sacramento Area (SAC)	Citrus Heights, Folsom, North Highlands, Sacramento (Meadowview, Del Paso Manor, 1309 T St., Earhart Dr.)	Auburn, Rocklin not included to avoid focus on peak due to Sacramento emissions
Northern San Joaquin Valley (NSJV)	Modesto, Stockton (Hazelton St., 13521 E. Mariposa), Turlock	
Central San Joaquin Valley (CSJV)	Fresno (Olive, 3425 First St., 4706 E. Drummond), Parlier	Combine Olive and 3425 First St. sites into one

FIGURE 2-1a. San Francisco Bay Area Air Basin routine monitoring stations. (Source: ARB/TSD)

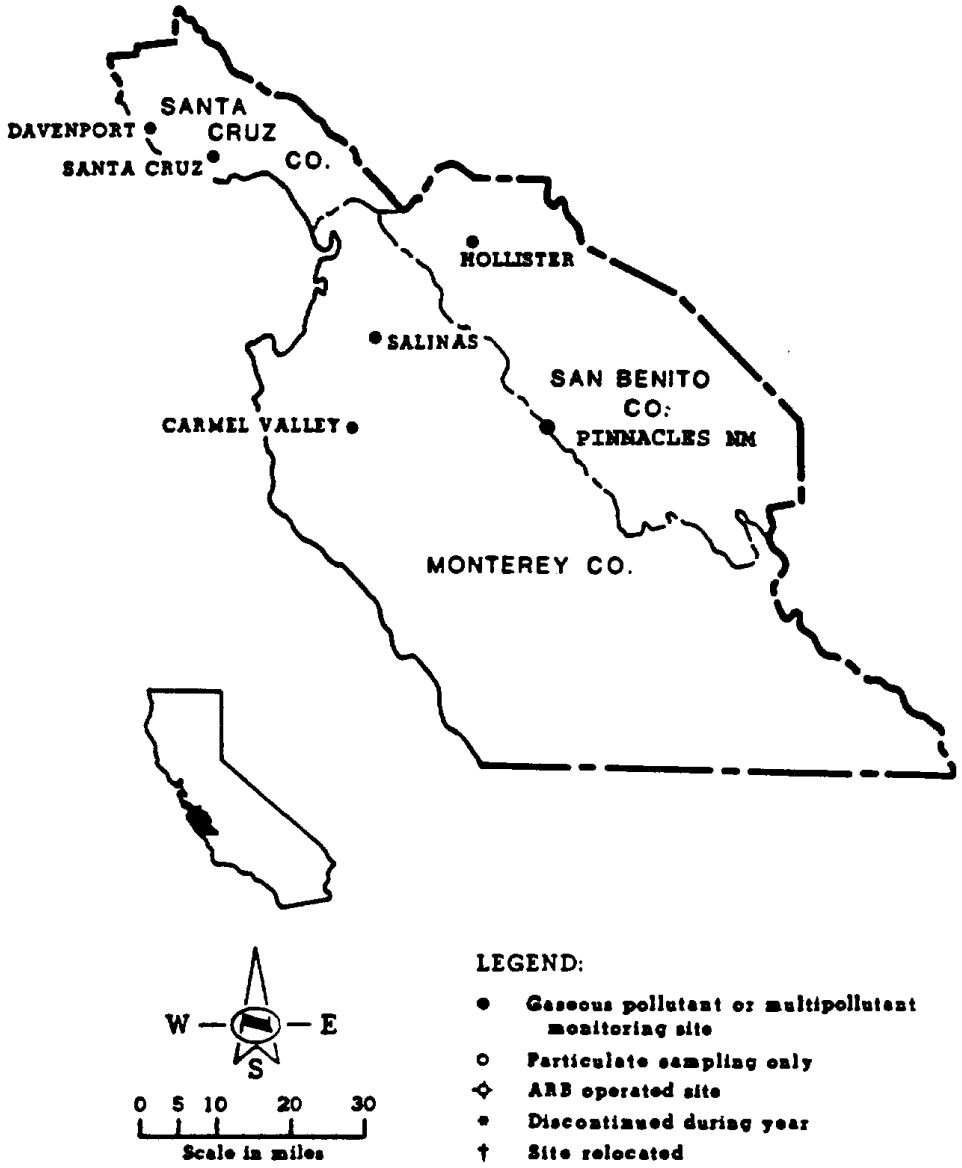

91156
94022

FIGURE 2-1b. North Central Coast Air Basin routine monitoring stations. (Source: ARB/TSD)

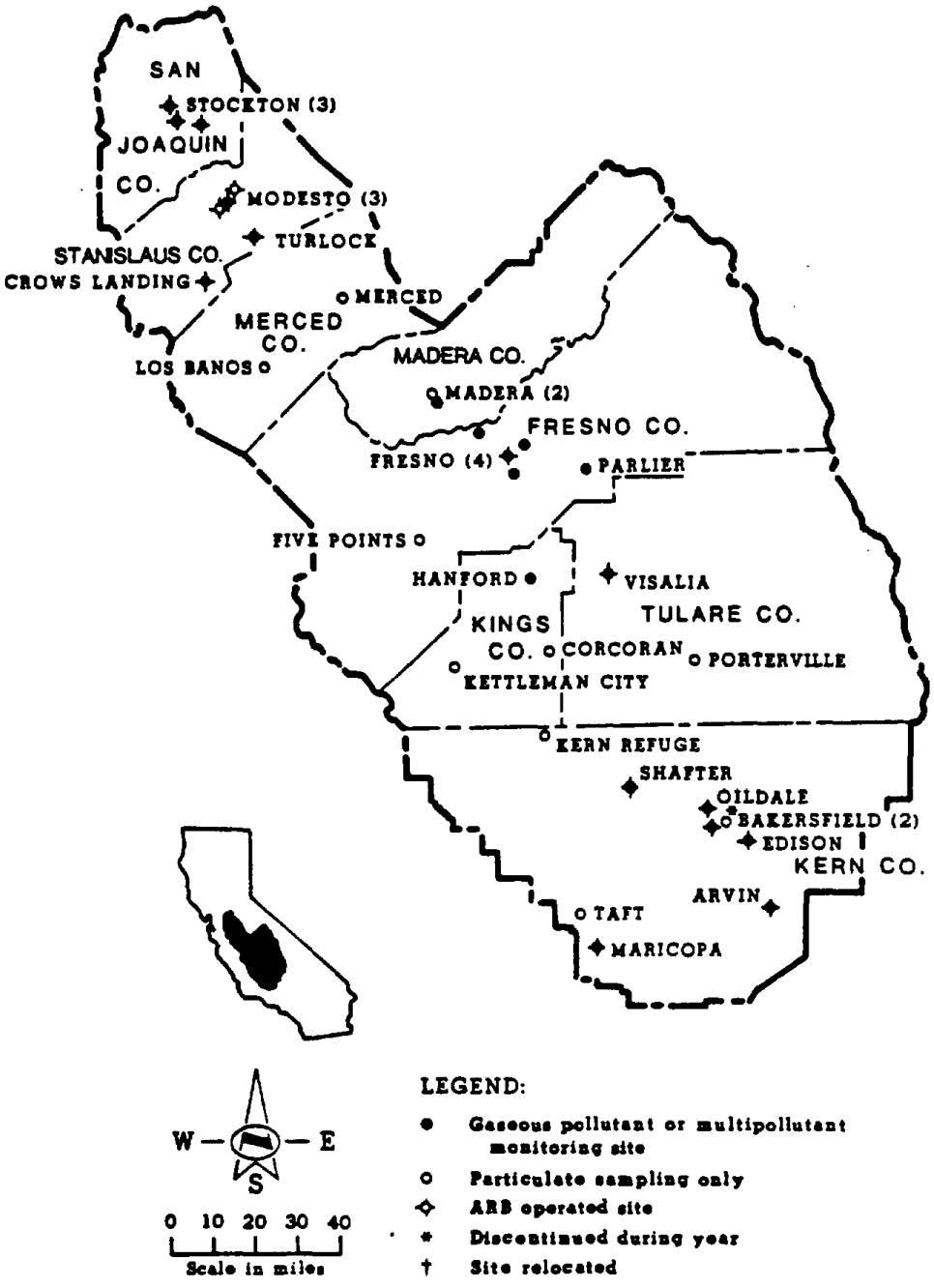

91156
94022

FIGURE 2-1c. San Joaquin Valley Air Basin routine monitoring stations. (Source: ARB/TSD)

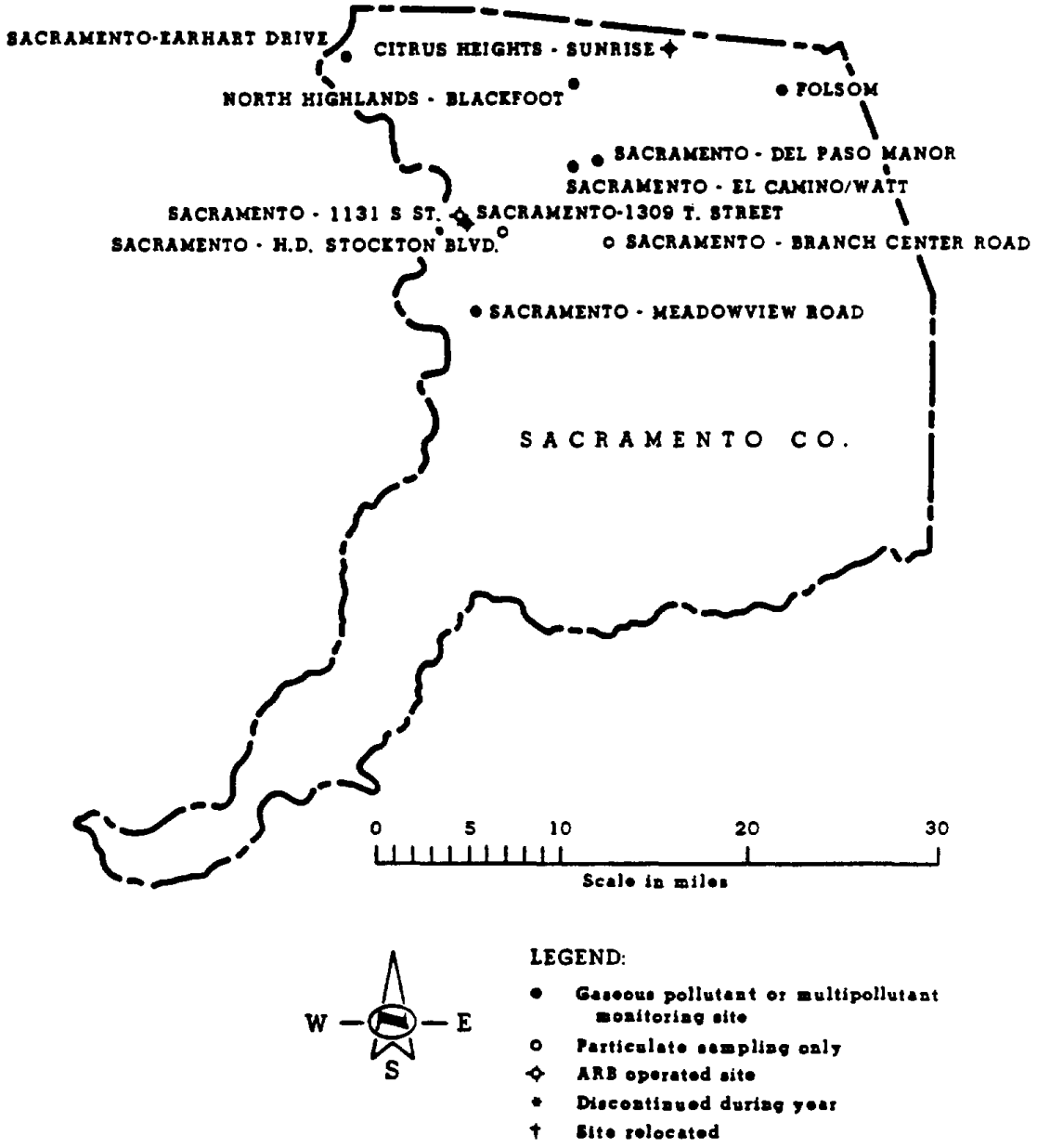

FIGURE 2-1d. Sacramento County routine monitoring stations. (Source: ARB/TSD)

94022

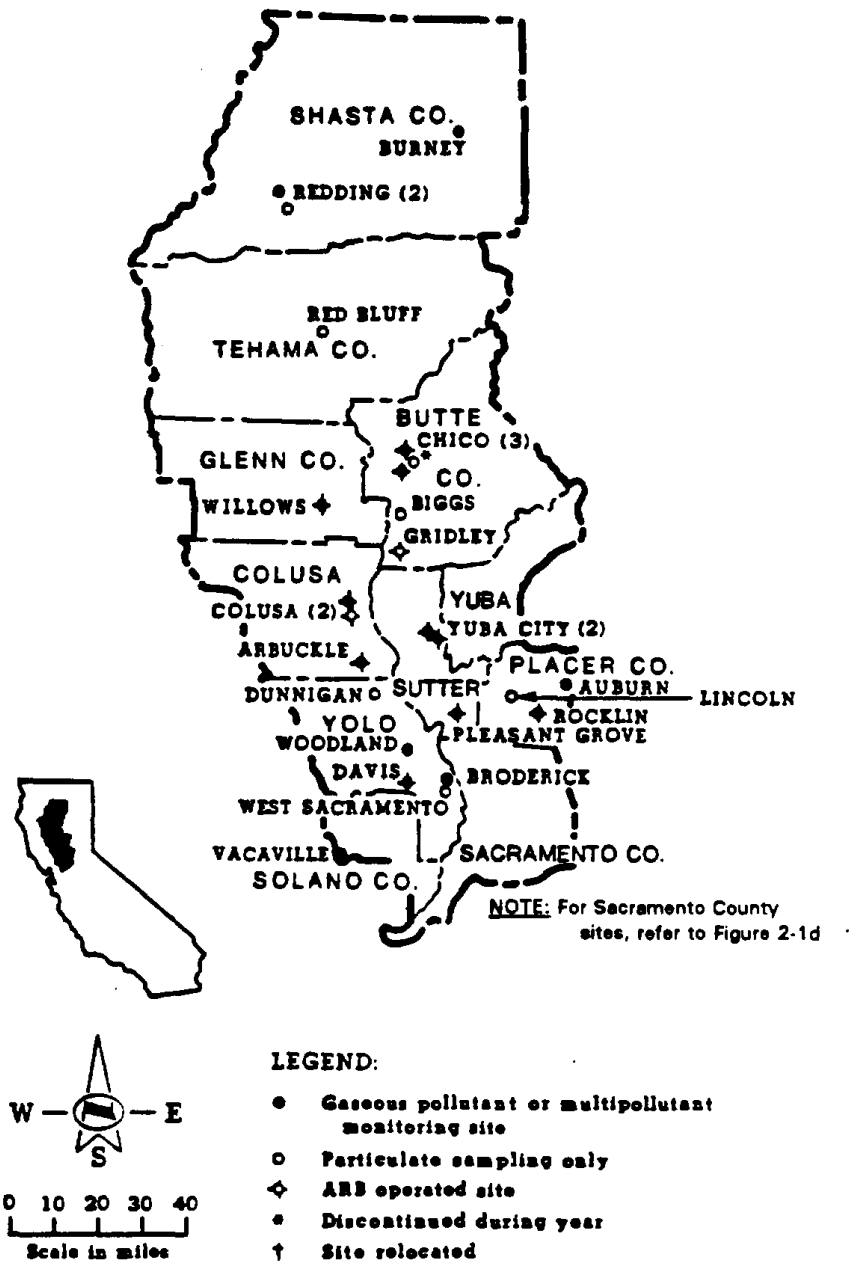

91156
94022

FIGURE 2-1e. Sacramento Valley Air Basin routine monitoring stations. (Source: ARB/TSD)

3 ANALYSIS

This section presents our analyses of the air quality and meteorological database described in the previous section. These analyses were designed to determine the principal flow patterns and associated meteorological conditions (i.e., the source-receptor scenarios) associated with ozone episodes in the study region and to develop an objective procedure for classifying days by scenario on the basis of a few key routinely collected meteorological measurements. The section is divided into four main topics:

A flow pattern analysis in which existing flow pattern information compiled by the ARB is supplemented with our own analysis of flow over the nearshore waters. Spatial patterns of ozone concentrations under each flow pattern are examined to identify the characteristic spatial ozone concentration distributions, including the locations of high ozone concentrations. Results of these analyses and previous studies are then used to derive a set of conceptual (idealized) flow patterns used as a guide for the remainder of the study.

A trajectory analysis performed on selected ozone episodes to identify the significant transport routes and source-receptor couples associated with each conceptual flow pattern.

An analysis of the relationship of meteorological conditions to flow patterns and ozone concentrations. This analysis identified the key meteorological features of each flow pattern and thus the final source-receptor scenarios.

Development of the objective source-receptor scenario classification procedure, including procedure development, evaluation, and application.

FLOW PATTERN ANALYSIS

Analysis of Wind Fields and Associated Air Quality

The ARB prepares streamline analyses from northern and southern California wind data four times daily. A typical streamline analysis is shown in Figure 3-1 (figures begin on page 3-46). Daily streamlines for the San Francisco Bay Area are classified by the ARB according to a set of eight typical flow patterns described by Hayes (1984), as illustrated in Figure 3-2. Due to the nearly infinite variety of possible flow geometries, assigning a particular streamline analysis to one of the categories in Figure 3-2 is an imperfect process, and the details of the flow at any given time may differ from the idealized flows

shown. Flow patterns are assigned by the ARB on the basis of which of the eight patterns represents the best possible fit to the data within the San Francisco Bay Area Air Quality Management District. Wind data from stations outside of the district that might indicate flow along the boundaries of the District are not considered (Wilson, 1994).

Roberts (1992) noted that the Bay Area flow type assignments were not suitable for analysis of flow into the Broader Sacramento Valley (BSAC) due to differences in the details of the flow through the Delta. As a result of this experience, it was decided that the ARB streamline analyses for the study period would be reviewed and the flow typing repeated independently.

A complete set of the ARB's 00:00, 12:00, and 18:00 UTC (16:00, 04:00, and 10:00 PST) streamline analyses were obtained for weekdays, June-October of 1989, 1990, and 1991. These maps were used to check on and more fully characterize typical flow patterns associated with each of the eight ARB flow pattern types. Although in many cases local features of the streamline analysis (or of the underlying wind data) differed significantly from the idealized flow pattern type to which the case was assigned, our review determined that in the vast majority of cases, the assigned flow pattern represented the best possible overall fit to the actual streamlines, and no changes were made to the designated flow patterns as a result of this review.

One key finding of this review was that flow along the coast and over the coastal waters differed dramatically from one day to the next, even for days assigned to the same ARB flow category, and it appeared that the "nearshore" flow direction may be correlated with certain key features of the onshore flow. We therefore categorized each weekday 10:00 PST streamline analysis as belonging to one of several nearshore flow patterns defined by the predominant flow direction north and south of San Francisco Bay (using the Golden Gate as an approximate dividing line). The analysis of nearshore flows resulted in the following classifications:

NW	Flow with northerly component (i.e., approximately WNW to N)
S	Flow with southerly component (i.e., approximately WSW to SE)
E	Northeasterly or easterly flow (offshore)
W	Flow almost directly out of the west
C	Calm
U	Unclassifiable due to either insufficient observations or no identifiable pattern
M	Missing streamline map

In some cases, flow in the northern half of the region differed from that in the southern half. For example, "NW-S" was assigned to days with northwesterly flow in the north

and southerly flow in the south, leading to a convergence zone in the vicinity of the Golden Gate (the most commonly occurring "hybrid" flow category).

As expected, tabulation of the nearshore flows revealed that the most common category was NW (55%) followed by S (20%). The remaining days were dominated by the NW-S, S-NW, W, and U categories.

Table 3-1 shows the joint frequencies of occurrence of the 10:00 PST nearshore and onshore flow patterns for 1989-1991. (Tables begin on page 3-27.) As expected, most nearshore flows are NW, and most of these correspond to either the strong or weak northwesterly (Type 1A and 1B) onshore flow regimes. Furthermore, nearly all (27 out of 33) of the onshore Type 2 (southerly) cases were associated with southerly nearshore winds. However, 17 percent of the onshore Type 1A and 1B cases had offshore wind patterns with at least some southerly component (S, NW-S, S-C, S-NW, W-S), suggesting that southerly nearshore winds are an important variation on the typical northwesterly pattern.

Table 3-1 indicates a few cases with unlikely combinations of onshore and nearshore flow types, such as the four cases classified as onshore Type 2 (southerly) that had northwesterly nearshore winds. Onshore flow type assignments on these days were reviewed again, and the flow type assignments on three days were changed as a result.

Spatial Patterns of Ozone Concentrations

Different flow patterns can be expected to result in different spatial distributions of ozone concentrations. In this section, we present an analysis of the relationship between the flow patterns described above and spatial patterns in ozone. We begin with a general description of ozone distributions over all days. This is followed by a comparison of the distributions associated with each flow pattern.

All Days

Box plots summarizing the distributions of subregion average daily maximum ozone concentrations over the study period were prepared. A key to the box plot symbols is presented in Figure 3-3; the box plots themselves are displayed in Figure 3-4 and subregions are defined in Table 2-1. Subregion average concentrations exceeded the federal ozone standard (12 pphm) at Livermore, the Southern Santa Clara Valley, and in the Broader Sacramento, and Northern and Central San Joaquin Valleys. The highest peak and average concentrations occurred in the Central San Joaquin Valley. The distribution of concentrations is similar in Livermore and the South Bay with the exception of two days above the federal standard in Livermore. Lowest concentrations typically occur in the Inner Bay, Western Alameda County, and the North Bay.

Stoeckenius et al. (1991) identified groups of similar days in the South Coast Air Basin via the spatial distribution of *relative* subregion average daily maximum ozone

concentrations, where the relative concentration for a subregion is defined as the ratio of the subregion average to the average over all subregions. Figure 3-5 presents box plots of the relative subregion average daily maximum ozone concentrations for the study period. As expected, the patterns of relative concentrations and absolute concentrations are similar, being highest in the Central Valley, Livermore, and Southern Santa Clara Valley and lowest in the Inner Bay and Monterey Bay. On a relative basis, concentrations in the South Bay tend to be lower than those at Livermore or in the Southern Santa Clara Valley.

In the following section, we describe how the typical spatial patterns of relative and absolute concentrations differ from one flow pattern to the next.

Spatial Ozone Distributions by Flow Pattern

Spatial ozone patterns associated with each flow pattern were explored through examination of side-by-side box plots of subregion average daily maximum ozone concentrations for each onshore-nearshore flow pattern combination that occurred on 10 or more days. Box plots were also prepared for all days of onshore type 1A/B, 2, 4, 6, and 7, regardless of the nearshore pattern. A key to the box plot symbol is presented in Figure 3-3; the box plots themselves are presented in Figure 3-6 (plots for onshore-nearshore combination patterns appear in Figure 3-6a to 3-6f; plots for onshore patterns appear in Figures 3-6g to 3-6l)[1]. A comparison of plots for each pattern to plots for the predominant onshore 1A-nearshore NW (1A-NW) pattern reveals the following features (strictly speaking, these comparisons refer only to the 50th and 75th percentiles of the distribution of daily maximums, unless otherwise noted):

The 1B/NW pattern is very similar to the 1A-NW, except for slightly lower concentrations in the San Joaquin, Southern Santa Clara, and Livermore Valleys.

The 1A-S pattern is associated with higher concentrations in Livermore, the South Bay, and the Sacramento and San Joaquin valleys, and slightly lower concentrations in the Monterey Bay and Southern Santa Clara Valley.

The 2-S pattern is associated with lower concentrations in the southern Santa Clara Valley, Sacramento, West Sacramento Valley, and Contra Costa County and higher concentrations around the Inner Bay region. Contrary to what one might expect, the 75 percentile and more extreme values are slightly (1-1.5 pphm) higher in the Monterey Bay region under this pattern. The significance of this, if any, is not clear.

Days classified in the ARB scheme as pattern 4 (northeasterly) have lower concentrations in the Sacramento Area and generally higher concentrations

[1] Only days for which ARB flow patterns were available (weekday, June-October 1989-1991) are included in the box plots in Figures 3-6 and 3-7.

everywhere outside of the Central Valley. This is especially noticeable in the Monterey Bay, South Bay, Western Alameda County, and Inner Bay areas where even the extreme values are higher than under the 1A-NW pattern.

The 6-S pattern is associated with higher concentrations (including extreme values) in the Central Valley, higher values in Livermore and the South Bay, and somewhat higher values at other Bay Area locations (except the Inner Bay), and lower values in Monterey and the Southern Santa Clara Valley.

Concentrations generally tend to be higher on type 6 days than on type 1A/B days, although extreme values in the BAAQMD on type 1 days are similar to those on type 6 days. The 6-NW pattern differs from the 6-S pattern in that concentrations in the Monterey Bay area and the Southern Santa Clara Valley are lower under the 6-S pattern while concentrations in the Central Valley are typically higher. Northeasterly days are distinct in that they are associated with lower concentrations inland and higher concentrations around the Bay and in the coastal valleys.

The above analysis was repeated for the relative subregion average ozone concentrations, constructing side-by-side box plots for each onshore-nearshore flow pattern combination that occurred on 10 or more days and for all onshore type 1A/B, 2, 4, 6, and 7 days (Figure 3-7). The most obvious flow pattern effects on relative concentrations are lower values in the North Central Coast, Southern Santa Clara Valley, and Inner Bay and higher values in Livermore and BSAC during the 6-S regime as compared to the 1A-NW regime. Significantly higher relative concentrations occurred in the Monterey Bay area under all Type 4 (northeasterly) conditions than under the northwesterly flow conditions. Comparison of 1A-NW with 1A-S days showed no differences except for somewhat lower relative concentrations in the Southern Santa Clara Valley and higher relative concentrations in the Western Alameda County subregions during the southerly offshore days, suggesting a more frequent incidence of southerly flow over the San Jose area on 1A-S days. These features are generally consistent with those identified in the absolute ozone concentrations. No other major differences between flow categories are evident in the spatial distribution of relative daily maximum concentrations.

These analyses provide an indication of the overall differences in the spatial distribution of ozone concentrations from one flow category to the next. Below we focus on the spatial distribution of ozone under episode conditions and the associated flow patterns.

Air Flow Patterns on Episode Days

The distribution of ozone concentrations and air flow patterns during ozone episode events was analyzed. Ozone episode events were defined as days on which either the maximum ozone concentration at any monitoring site in the BAAQMD or the MBUAPCD exceeded 9 pphm or any monitor in the BSAC exceeded 12 pphm. Days with high ozone in the Northern or Central San Joaquin Valley (where such events are relatively common) but low ozone elsewhere were not included due to the possible

confounding influence of Sacramento emissions in such cases. The higher cutoff for concentrations in BSAC (12 pphm) was selected to restrict attention to extreme ozone events.

Table 3-2 lists the percent of all days and of episode days by onshore flow category as determined from the 10:00 PST wind field analysis. For northwest, northeast, and calm flows, episodes occur roughly in proportion to the number of days with these flow types. Episodes are disproportionately infrequent on southerly days and proportionately more frequent under bay outflow conditions.

Table 3-3 lists the 10:00 PST onshore and nearshore flow types, along with the maximum ozone concentration in each subregion for each episode day during the study period meeting these criteria. A summary of this information is provided in Table 3-4 which lists the number of days on which concentrations exceeded 9 pphm (12 pphm in BSAC) for each onshore flow type. Also shown in Table 3-4 are the number of such exceedance days that we would expect to have observed based solely on the relative frequencies of occurrence of each flow type on episode days (i.e., if there is no relationship between flow type and subregion exceedances on episode days). The number of exceedances in each subregion under the northwest flow type was roughly as expected, while somewhat more than the expected number of exceedances occurred in Livermore and BSAC under bay outflow conditions. Since only a few episode days exhibited southerly, northeasterly, or calm flow types, it is difficult to draw firm conclusions about the pattern of exceedances on these days. However, it is interesting to note that no BSAC exceedances occurred under the seven northeast and calm flow types whereas exceedances in the South Bay occurred on five of these days, together with the only Inner Bay exceedance and 3 of the 13 exceedances in Western Alameda. Both days with the southerly flow type had exceedances in BSAC, and no other exceedances occurred on these two days. With the exception of this latter feature, these results are generally consistent with the box plots described above.

Development of Conceptual Flow Patterns

Based on the onshore and nearshore flow patterns analyzed above and on previous studies of transport from the Bay Area to surrounding air basins, a set of flow patterns representative of conditions on episode days was postulated. A key feature of these patterns is the presence or absence of a low-level convergence zone in the vicinity of Gilroy which controls the transport of material to the North Central Coast via the Santa Clara Valley: transport, at least at the surface, is possible only when the convergence zone is not present. Eight patterns were defined as follows:

Ic: Northwesterly flow with convergence zone

Inc: Northwesterly flow without convergence zone

II: Southerly flow

IVc: Northeasterly flow with convergence zone

IVnc: Northeasterly flow without convergence zone

VIc: Bay outflow with convergence zone

VInc: Bay outflow without convergence zone

VIII: North bay northwesterly - south bay southerly

The postulated patterns are schematically illustrated in Figure 3-8. Patterns I, II, IV, and VI are similar to the corresponding onshore flow categories defined for the San Francisco Bay Area by the ARB. Pattern VIII is not used by the ARB; days with this pattern are typically categorized into either the northwesterly or southerly ARB flow types. Roberts (1993, personal communication) suggests that ozone exceedances have been known to be associated with this "mixed" flow type. However, the frequency of occurrence of this type is not known since a daily tabulation is unavailable.

Unfortunately, routine data needed to determine the presence or absence of a convergence zone near Gilroy were not available for this study. Nevertheless, the postulated flow patterns described above provide a useful working hypothesis for the identification of key source-receptor scenarios in the study area. Using the postulated flow patterns as a guide, each ozone episode day was assigned to one of six flow categories: Northwest (NW), Southerly (S), Northwest in north bay - Southerly in south bay (NW-S), Northeast (NE), Calm (C), and Bay Outflow (BO). Assignment of days to these categories was based primarily on the 10:00 PST onshore flow pattern assigned by the ARB and the corresponding nearshore flow pattern determined in the manner described above. Interpolated wind fields used in the trajectory analysis described in the next section were also consulted for days for which they were available.

Onshore and nearshore flow patterns and the assigned flow categories for each episode day are listed in Table 3-3. For the most part, the flow category assignments followed the onshore flow patterns. Days for which either the onshore or the nearshore flow patterns were not available were not assigned to a flow category, except for August 4-5, 1990, which were assigned to the northwest category based on the windfield analysis reported by Roberts et al. (1992). Days with uncertain nearshore flow patterns were assigned on the basis of the onshore flow pattern. Days with onshore NW and nearshore NW-S flow patterns were assigned to the NW-S flow category. The onshore flow pattern for June 21, 1989, was V (Bay Inflow), a condition usually associated with nocturnal drainage flow. This day was assigned to the northeast flow category based on the observation of easterly winds in Carquinez Strait.

TRAJECTORY ANALYSIS[2]

To further analyze flow patterns on episode days and to develop a picture of the principal source-receptor relationships on these days, a large number of backward and forward air parcel trajectories were calculated for selected ozone episodes. These trajectories estimate the path of a hypothetical air parcel over a selected time period. Back trajectories follow an air parcel backwards from the time and place of the observed daily maximum ozone concentration to illustrate where the air mass associated with the peak ozone concentration might have come from; forward trajectories follow an air parcel originating from major source regions in the morning to illustrate where the emissions might impact downstream.

Methodology

The following sections discuss the selection of days for trajectory analysis, the available wind data, and the procedures used to prepare wind fields and calculate trajectories.

Data Preparation

To evaluate transport to the North Central Coast (NCC) air basin, the Northern San Joaquin Valley (NSJV), and the BSAC, the domain shown in Figure 3-9 was selected. This domain included receptor sites in the NCC, NSJV, and BSAC, and the major upwind air basin, the San Francisco Bay Area. Wind fields were generated from hourly-averaged wind speed and direction data collected at a large number of surface monitoring sites as shown in Figure 3-9 (Roberts et al., 1992). Data were obtained from several sources, including the ARB; Weather Network, Inc. for the Sacramento Valley; the Sacramento Area Ozone Study (sponsored in the summers of 1989 and 1990 by the Sacramento Area Council of Governments); SJV Air Quality Study and AUSPEX (SJVAQS/AUSPEX) for the summer of 1990; Bay Area Air Quality Management District (BAAQMD) 10-meter tower network; National Ocean Buoy Center for data collected from offshore northern California by the Minerals Management Service, the U.S. Coast Guard, the Army Corps of Engineers, and the National Weather Service (NWS); and the CIMIS network. Data availability varies from site to site; many of the 10-meter towers installed by the BAAQMD did not begin operation until some time after 1989.

Wind data were interpolated onto a 10 km by 10 km grid covering the modeling domain using the Caltech 2-D wind interpolation procedure as modified and documented by Kit Wagner of the ARB (see Roberts et al., 1992). Model settings included a radius of influence of 20 km and a 2000 meter depth of the layer associated with terrain influence. Examination of preliminary interpolated wind fields indicated a potential problem with winds on one side of the mountain ridge separating the Salinas and San Benito Valleys

---

[2] Some of the material in this section is based on work done on a previous ARB project (Roberts et al., 1992).

exerting an unrealistic influence on interpolated winds on the other side. Therefore, the final interpolated wind fields were generated with a barrier along this ridge to prevent interpolation of winds from one side with winds from the other side. Offshore, pseudo wind measurement sites were placed between several of the buoys to better represent offshore wind conditions. Without these pseudo sites, the model generated unrealistic winds in several offshore areas due to the influence of coastal wind sites which were locally, but not regionally, representative.

Trajectories were generated from the hourly interpolated wind fields at 30-minute time steps. Backward and forward trajectories were generated for hours of peak ozone concentrations and precursor emissions, respectively, on ozone exceedance days from selected monitoring sites in the BSAC, NCC, and San Francisco Bay Area. Ensembles of trajectories were used to define typical transport paths. Since a barrier was placed across the mountain ridge between the Salinas and San Benito Valleys in the wind field model, a barrier was not used in the trajectory model. In this way, the model allowed a trajectory to cross the mountain ridge if the winds were sufficiently strong or persistent, but interpolated winds on the downwind side of the ridge did not influence the air parcel until it crossed the ridge line.

In general, transport paths determined from individual trajectories are not as reliable as transport paths determined from many trajectories under similar conditions. Thus, we attempted to determine typical transport paths as a consensus based on many forward and backward trajectories.

Selection of Wind Field Dates and Available Data

As discussed below, gaps in the availability of wind data presented a major limitation, forcing us to concentrate primarily on ozone episodes during 1990. Based on an analysis of ozone violations in the NCC, Roberts et al. (1992) selected seven ozone exceedance days from 1987 to 1990 for analysis. The selections were based on days with the highest ozone concentrations at NCC air basin monitoring sites, plus the availability of surface meteorological data. Data were missing for the Moss Landing surface meteorological site on all 1987-1989 days. Also, the BAAQMD 10-meter towers were not installed at San Martin and Gilroy until May 1987 and August 1989, respectively, and a meteorological site at Hollister was not installed until early 1990. These data gaps are a major limitation of any wind analysis because without good data in this part of the Santa Clara Valley, flow in the area where the convergence zone may form will not be properly represented. To test the importance of this, Roberts et al. (1992) prepared wind fields for several of the pre-1990 exceedance days and found flow in this area of the domain to be unrealistic. That area must be properly represented to understand the potential transport up the Santa Clara Valley to the Hollister monitoring site. There were several exceedances during 1991; however, wind data were also insufficient to properly represent flow in the NCC during these periods.

Selection of Trajectories

Roberts et al. (1992) prepared wind fields for nine days in 1990: July 9-12 and August 3-7. Peak ozone concentrations and the onshore and nearshore wind flow patterns on these dates are listed in Table 3-5. Forward and backward trajectories were calculated starting from the key locations listed in Table 3-5. Backward trajectories were initiated from receptor or downwind locations at 1300, 1500, and 1700 PST, which typically encompassed the time of peak ozone concentrations at these sites. When the peak ozone concentration at a particular receptor occurred before 1300 or after 1700 PST, we also estimated a trajectory at that time (e.g., 1000 or 1800 PST). Forward trajectories were initiated from source or upwind locations at 0500 and 0700 PST to estimate the transport of early morning emissions. Forward trajectories were also prepared beginning at 1500 and 1700 PST to estimate the transport of the peak ozone concentrations and afternoon emissions overnight.

Uncertainties

Surface trajectory analyses prepared in the manner described above are subject to various sources of uncertainty. The following caveats should be kept in mind when reviewing the trajectory plots:

- Data measurement error and errors introduced by the spatial and temporal interpolation of the wind data may contribute to errors in the trajectory paths.

- Vertical mixing and elevated transport are not represented with surface trajectories. Therefore, these trajectories do not account for material that may be transported aloft (possibly in a different direction from the surface flow) and later mixed down to the surface. On a few days during which upper air data were available for the Upper Sacramento Valley, trajectories were computed using data collected at 400 and 800 m above ground by Roberts et al., 1992. Aloft trajectory paths and transport times often differed significantly from surface trajectories.

- Wind data from 88 sites were used to generate the wind fields; however, not all grid squares in the domain are represented by a station. Due to the effects of complex terrain and sparse data in some areas, some flow paths may not be properly represented.

- True 3-dimensional flow across mountain ranges is often poorly represented by a surface, 2-D model such as the one we used. In addition, winds on either side of a mountain ridge can often be different. For most cases in this study, the spatial distribution of wind sites and the strength of wind flow in the coastal valleys produced quite realistic surface trajectories, even near mountains. However, in one case, a barrier was needed to reduce the influence of wind measurements from the other side of the mountain ridge on the interpolated winds. Although this procedure resulted in more realistic wind fields, some trajectories were calculated to cross the ridge under the influence of sufficiently strong flow normal to the

barrier. Since vertical motions are not treated by the model, these cross-barrier trajectories may not be realistic in all cases.

Results

A total of over 1500 trajectories were prepared. The trajectory analyses were used to obtain consensus wind flows for the selected exceedance days, and these flows were compared to the conceptual wind flow patterns shown in Figure 3-8. Wind fields were compiled for nine days in 1990 during which northwesterly (the most common wind flow type on exceedance days) and southerly flow occurred. A set of additional analyses were conducted to evaluate conditions under the northeast and bay outflow patterns, as described in the following subsections. The following discussion illustrates the general characteristics of the trajectories calculated for the northwest and southerly days.

Northwesterly Flow Without Convergence

Figure 3-10 shows surface backward trajectories beginning on July 11 at several locations. The start times of the trajectories varied; for this figure we chose start times based on the time of the peak ozone concentrations at each site. Figure 3-11 shows a forward trajectory beginning at 0700 PST at San Jose on July 11 to illustrate flow from the southern Bay Area to the NCC. Except for the trajectory from Pinnacles, these trajectories match well with the conceptual northwesterly flow pattern without convergence (see Figure 3-8). The forward trajectory from San Jose may be positioned slightly further north than the actual air flow. Note that the Gilroy, Hollister, and Santa Cruz trajectories were traced back over the coastal range, which may not be realistic. On July 11, ozone exceedances occurred at Pinnacles, Hollister, Gilroy, San Jose, the NSJV, and the BSAC.

The most noticeable difference between the trajectory pattern and the conceptual drawing is that the backward trajectory from Pinnacles was traced back to the Monterey Bay. An early morning ozone peak was observed at 1000 PST at Pinnacles on July 11. The backward trajectory beginning at this time indicated that the air parcels were traced from the west via Monterey. Note, however, that the trajectory was traced across a ridge of the coastal mountains; this seems unlikely. The wind field model was formulated with a barrier along this ridge (Roberts et al., 1992), but trajectory paths are allowed across the barrier. It is possible that the early ozone peak is the result of mixing down of ozone from aloft which might have been transported into the Pinnacles area overnight, or the result of overnight transport aloft arriving at the high elevation of the Pinnacles monitoring site. Without aloft meteorological data, we cannot document the mechanism that produced this early peak at Pinnacles. At 1800 PST on July 11, 1990, surface backward trajectories from Pinnacles indicated that air parcels were traced back to the South Bay/San Jose area, as we would expect under this flow pattern (not shown).

A second example of the northwesterly flow, in Figure 3-12, shows surface backward trajectories beginning on August 5 at various times and locations. Figure 3-13 shows a

forward trajectory beginning at 0700 PST at San Jose to illustrate flow from the southern Bay Area to the NCC. These trajectories also match relatively well with the conceptual northwesterly flow pattern, although the wind flow on August 5 contained a stronger northerly component than on July 11. Note that on August 5, the surface backward trajectories from Pinnacles in the afternoon indicated that air parcels were traced to the South Bay/San Jose area, as we would expect. The trajectory traced back from Santa Cruz crosses over the coastal range and may be unrealistic. Ozone exceedances occurred at Pinnacles, Hollister, Gilroy, and the NSJV on this day.

Northwesterly Flow With Convergence

Figure 3-14 shows surface backward trajectories beginning on July 10 at several locations. Trajectory start times were based on the time of the peak ozone concentrations at each site. Backward trajectories were terminated at 1800 PST on July 9. Forward trajectories beginning at 0500 PST at San Jose and Moss Landing on July 10 are shown in Figure 3-15. The forward trajectory from San Jose indicates that flow reversed near Gilroy in the afternoon. While the backward trajectory from Gilroy was traced to the South Bay/San Jose area, the backward trajectory from Hollister was quite different. The Hollister air parcels had been in the Hollister area for a number of hours and were then traced to the west. The backward trajectory from Pinnacles was very similar to the Hollister trajectory. These trajectories indicate that there may have been a convergence zone between Hollister and Gilroy on July 10.

A comparison of the trajectories on July 10 with the conceptual northwesterly flow pattern with convergence (Figure 3-8) shows that in general, the trajectory paths were similar to the conceptual model, although the flow was more westerly than indicated in the conceptual drawing. The trajectory traced back from Santa Cruz crosses over the coastal range and may be unrealistic. Ozone exceedances occurred at Gilroy, San Jose, Livermore, and the NSJV on July 10. Several hours of ozone data at Hollister were missing during the time that peak concentrations generally occur at this site.

Southerly Flow

Figure 3-16 shows surface backward trajectories beginning at various times on August 7, 1990 from several locations. Although the ARB classified the wind flow on August 7, 1990 as a weak northwesterly flow, these backward trajectories show that the wind flow had a strong southerly component. Forward trajectories on this day showed a mixture of southerly and westerly flow (not shown). Ozone exceedances occurred at Pinnacles, the BSAC, and the NSJV on August 7.

A comparison of the trajectories in Figure 3-16 with the conceptual southerly flow pattern (Figure 3-8) shows generally good agreement, although the northward flow from Gilroy to San Jose was not evident in this case and the trajectories from Sacramento Valley and Stockton suggest that flow from offshore through the Bay Area is possible under this regime, contrary to what is indicated in Figure 3-8.

Northeasterly Flow

Table 3-2 showed that ozone exceedances rarely occurred under northeasterly wind flow during 1989-1991 and not at all during 1990 when adequate data were available for wind fields. However, in a previous study, Douglas et al. (1989) computed particle trajectories for a northeasterly event associated with ozone exceedances (September 30–October 1, 1983). Forward particle trajectories initiated in the Carquinez Strait showed that the flow during this period was northeasterly (see Figure 3-17). The trajectories showed flow from the strait toward the Golden Gate and then to the south, similar to the conceptual drawings for northeasterly flow shown in Figure 3-8. Wind data were insufficient to evaluate the presence or absence of a convergence zone near Gilroy. Ozone concentrations on September 30 and October 1 were as high as 20 pphm at some locations in the Bay Area during this event.

Sensitivity Analysis of Trajectories

Start times and locations for trajectories discussed above were selected on the basis of their usefulness in investigating the source-receptor relationships identified earlier and for building consensus trajectory paths. Since the trajectory paths may be sensitive to the particular start time selected, we also analyzed some supplementary trajectory start times and locations as part of a sensitivity analysis. This sensitivity analysis had the following objectives:

- To investigate the sensitivity of the receptor location coordinates. Do trajectories beginning at locations in nearby grid cells generally agree with one another?

- To investigate the sensitivity of trajectory paths to the start time. Do trajectories initiated two to three hours apart follow similar paths?

We estimated backward trajectories beginning on July 12 and August 7, 1990 for particles released from the locations listed in Table 3-5 and for particles located one grid cell (10 km) to the north, south, east, and west of the nominal starting locations. In addition, a few forward trajectories were made on July 12 and selected backward trajectories were made on July 10 for the same clusters of locations. In nearly all cases, the trajectories from the five grid cells had similar paths. Figures 3-18 and 3-19 show examples of trajectories starting at 1300 PST on July 12, 1990. Backward trajectories from the six sites and surrounding grid cells shown in the figures were traced along similar paths. Note that in some cases, the air parcels were traced back across a ridge of the coastal mountains (i.e., see Pinnacles trajectories north of Santa Cruz, Figure 3-11). We formulated the wind field model with a barrier along this ridge, but trajectory paths are allowed across the barrier as previously discussed. For most of the test cases, the five trajectories originating from a cluster followed similar paths to one another even though changes in wind speed were noted.

In contrast, Figures 3-20 through 3-22 show some of the differences that were observed in the backward trajectories. Figure 3-20 shows that backward trajectories begun to the

north and west of Livermore at 1500 PST on July 10 were traced along somewhat different paths than the backward trajectories begun from the grid cells to the north and east. In Figure 3-21, the backward trajectories begun in all the grid cells near Crows Landing at 1500 PST on August 7 were traced along significantly different paths. Finally, Figure 3-22 shows that the backward trajectory from the northern grid cell near Pinnacles begun at 1300 PST on August 7 was traced along a different path over the hills than the other trajectories.

In summary, while the trajectories begun in adjacent grid cells typically followed similar paths, there were a few exceptions, generally at locations situated near complex terrain such as Pinnacles, Los Banos, and Crows Landing. In these cases, trajectories need to be interpreted with caution in light of the surrounding terrain.

To investigate the sensitivity of trajectory paths to the start time, backward trajectories were typically initiated at 1300, 1500, and 1700 PST while forward trajectories were initiated at 0500, 0700, 1500, and 1700 PST. In most cases for the nine selected days, the trajectories begun within these time windows had similar paths. However, on the morning of August 6, the forward trajectories initiated at 0500 and 0700 PST followed significantly different paths. Figure 3-23 shows that the forward trajectories started from several locations at 0500 PST on August 6, 1990 traveled to the east. By 0700 PST the same day (Figure 3-24), most of the air parcels traveled to the southeast. One of the most striking differences is the paths of air parcels released from San Jose at the two different times: the air parcel released at 0500 PST was transported into the SJV while the air parcel released at 0700 PST was transported into the NCC.

Clearly, trajectories begun two to three hours apart could follow very different paths. However, on most days which we studied, differences in the trajectories starting within a few hours of each other were small.

Analysis of Wind Fields for Northeasterly and Bay Outflow Conditions

Detailed trajectory calculations for the study period could not be made for days with northeasterly and bay outflow flow patterns for several reasons. Most notably, data were insufficient to properly represent flow in the NCC under these conditions. Furthermore, bay outflow conditions are very localized, with low wind speeds and variable wind directions. As a result, trajectory analysis under these conditions is very difficult and subject to unacceptable uncertainties as changes in wind direction and speed may occur on a scale much smaller than the grid size of the wind model.

Since we could not prepare meaningful trajectories for bay outflow conditions and since there were no northeasterly ozone exceedance days with sufficient wind data to prepare trajectories during the study period, we performed an alternative analyses for selected ozone episode days associated with these two flow patterns. This consisted of (1) obtaining ARB streamline charts (which also show the wind observations at individual stations) for the preceding afternoon (16:00 PST), early morning (04:00 PST) and mid-morning (10:00 PST); (2) annotating each chart with additional wind data obtained for

this study (e.g., Bear Valley near Pinnacles, Tracy, and two sites near Travis); and (3) reanalyzing the streamline charts and preparing new flow diagrams on the base maps of the study region. Results of this procedure are presented in Figures 3-25 through 3-31.

Several findings can be made on the basis of this reanalysis of the surface streamlines on these ozone episode days. In general, during the three years examined, northeasterly winds at the surface did not penetrate into the central Bay Area under episode conditions in contrast to the conceptual northeasterly flow shown in Figures 3-8d and 3-8e. Rather, on those days with northeasterly flow, northeasterly winds were only observed in the delta and near Livermore, while a pattern very similar to the bay outflow pattern was often observed over the Bay Area itself. Lastly, bay outflow conditions were found to be coupled with a variety of nearshore wind flow patterns (e.g., southerly, weak northwesterly, or a convergence of southerly and northwesterly off the San Mateo County coast).

The above findings suggest several things about the likely transport of ozone and ozone precursors in and out of the Bay Area. Specifically, under bay outflow conditions, transport to the NCC is likely, while transport to the BSAC and NSJV is unlikely, and transport to Livermore is possible, depending on the strength of winds. When coupled with northeasterly flow, bay outflow cannot transport ozone or precursors into the BSAC or SJV. Also, although not evident in any of the days analyzed here, we believe, based on the work of Douglas et al. (1989) and the isolated nature of ozone exceedances in the NCC (e.g., Davenport, Santa Cruz), that it is possible that ozone or precursors may be transported from the Bay Area to the NCC via an offshore route or possibly over the Santa Cruz Mountains.

Conclusions and Recommendations

Over 1500 air parcel trajectories were calculated to estimate the general paths of ozone and ozone precursor transport between upwind and downwind areas. Additional analyses testing the sensitivity of the trajectory paths to the starting times and locations selected ensure that the results obtained are meaningful and representative of general flow conditions. Based on these analyses, we draw the following conclusions:

- Trajectory analyses are useful for illustrating the relationships between upwind and downwind areas under most of the wind flow patterns, including the predominant northwesterly pattern. For the most part, backward and forward trajectories for the selected days show good agreement with the conceptual drawings of northwesterly flow with and without a convergence zone near Gilroy.

- Backward and forward trajectories for one modeled day show relatively good agreement with the conceptual drawing for southerly flow, although the trajectories show that air parcels originating offshore of the Bay Area could penetrate through to the NSJV and BSAC under this pattern.

- While the trajectories begun in adjacent grid cells typically follow similar paths, there are a few exceptions, generally at locations near complex terrain such as Pinnacles, Los Banos, and Crows Landing. In those cases, the results of trajectories need to be interpreted with caution to obtain the most reasonable trajectories based on the surrounding terrain. This type of sensitivity analysis should be performed in future applications of the trajectory method.

- Trajectories begun two to three hours apart typically follow similar paths; however, there are cases in which the trajectories begun two hours apart travel to different air basins. This type of sensitivity analysis should also be performed in future applications of the trajectory method.

- Trajectory analyses are probably inadequate to properly characterize bay outflow conditions because of the low wind speeds and localized wind conditions under this regime. Changes in wind direction and speed may occur on a scale much smaller than the grid size of the wind model. In any event, sufficient data were not available with which to calculate trajectories under bay outflow (or northeast) conditions.

- Analysis of wind fields under bay outflow and northeast patterns associated with ozone episodes indicate that transport to the NCC is likely, transport to BSAC and NSJV is unlikely, and transport to Livermore is possible, depending on the strength of winds. Northeasterly flow regimes were found to actually be a combination of northerly to northeasterly winds in the Central Valley and bay outflow winds in the Bay Area. This pattern is unlikely to produce transport into the BSAC or NSJV.

Finally, although not evident in any of the days analyzed here, we believe that ozone or precursors could be transported from the Bay Area to the NCC via an offshore route or possibly over the Santa Cruz Mountains.

RELATIONSHIP OF METEOROLOGICAL CONDITIONS TO FLOW PATTERNS AND OZONE CONCENTRATIONS

Flow patterns identified in the previous section may be associated with a variety of meteorological conditions that control the magnitude of ozone concentrations in each subregion. In addition, it is likely that each flow pattern is associated with certain key meteorological conditions that are indicative of that pattern. In the following subsections, the meteorological conditions associated with ozone episode days, and the variations in meteorological conditions between episodes associated with different flow pattern, are explored.

A group of key daily meteorological variables was identified for use in this analysis (Table 3-6). Variables were selected primarily on the basis of results of previous studies of meteorological influences on ozone concentrations and transport routes in the study region (Zeldin and Meisel, 1978; Douglas et al., 1989). In particular, variables

identified in the study of Bay Area and NCC ozone episodes recently completed by the BAAQMD were considered in constructing the list (BAAQMD, 1993). Surface gradients in barometric pressure are a key element in the present analysis, as these gradients represent the forcing function driving the local circulation. Similarly, temperature gradients are indicators of thermal forcing factors and the influence of the marine layer.[3] Conditions aloft within the study region are represented by the inversion characteristics as estimated from the twice-daily (04:00 and 16:00 PST) upper-air soundings taken at Oakland. The upper-air circulation pattern is indicated by the 700 mb and 500 mb height gradients to the east (Winnemucca), north (Medford), and south (LMU) of Oakland.

Meteorological Characteristics of Episode Days

Table 3-7 compares means, standard deviations, and 90-percent confidence intervals for the means of the key meteorological variables for the episode days listed in Table 3-5 to values over all days in the study period. Episode days exhibit several unique characteristics, including higher than average 850 mb temperatures, lower morning inversion base heights, greater inversion strength, warmer temperatures in Sacramento and Fresno, larger negative San Francisco-to-Sacramento temperature gradients, negative San Francisco-to-Reno pressure gradients, and generally flat 500 mb height gradients. These conditions are indicative of days with strong subsidence inversions and thermally driven circulations. Higher sea level pressure in Reno appears to be an indication of a strong, low subsidence inversion that flattens the marine layer and limits the extent to which fog and low clouds penetrate inland. As indicated by the continued cool temperatures along the coast, however, the pressure gradient is not so severe as to completely eliminate the spreading of the marine layer into the Bay. Thus, a weak sea breeze sufficient to transport ozone and precursors from the primary source regions around the Bay to the inland areas is still present.

Meteorological Features of Selected Flow Patterns

Although most ozone episodes in the study region are associated with the general meteorological conditions described above, there is considerable variation in conditions between episodes as indicated by the different flow patterns discussed above. To assist in identifying the principal meteorological features associated with each flow pattern, values of the key meteorological variables in Table 3-6 were examined for each flow type. This comparison is facilitated by the side-by-side box plots in Figure 3-32, which compare the distributions of each key variable on episode days corresponding to each flow type. In examining these figures, it is important to keep in mind the small number of days associated with some of the flow patterns. For example, the box plots for the southerly

[3] Cloud cover is not included here as observations are only available at a handful of airport sites, and the inland intrusion of marine stratus is a highly localized phenomenon which is unlikely to be related to region-wide flow patterns in ways that are not more appropriately represented by the temperature, and temperature and pressure gradient variables.

and calm flow patterns are based on just two days of data, with values on these two days corresponding to the top and bottom of the boxes. Examination of Figure 3-32 reveals the following features:

- NW Days: Since this is the most frequent category of episode days, conditions on these days are representative of the typical episode conditions described above. A salient characteristic of this group is the relatively small negative San Francisco-to-Reno pressure gradient.

- S Days: Only two episode days correspond to this category, and ozone concentrations in the Bay Area and the NCC did not exceed 9 pphm on either day. The days are quite different from one another in that the San Francisco-to-Reno pressure gradient is moderately negative on one of the days and positive on the other. The San Francisco-to-Redding pressure gradient also has opposite signs on these two days, suggesting that these days do not represent an identifiable meteorological pattern.

- C Days: Only two days fall in this category, making it difficult to draw conclusions concerning the general meteorological conditions associated with this flow pattern. San Francisco-to-Redding and San Francisco-to-Fresno pressure gradients are small on both days and coastal to inland temperature gradients are moderate. The 500 mb height gradients between Oakland, Medford, Winnemucca and LMU (not shown) are also moderate on these two days. These conditions are consistent with the weak, unorganized flow characteristic of these days.

- NE Days: The four northeast days are quite distinct from the other episode days. The most significant distinction is the large negative San Francisco-to-Redding pressure gradient which coupled with large negative San Francisco-to-Reno pressure gradients results in a northeasterly flow through much of the region. San Francisco-to-Fresno pressure gradients are weak, in contrast to the larger positive values generally found under most of the other flow patterns. Another key feature of this flow pattern are the small San Francisco-to-Sacramento temperature gradients which reflect the unusually warm weather along the coast. The 850 mb temperatures under this flow pattern are generally cooler than on other episode days and the morning inversion base height is lower. Maximum temperatures in Sacramento and Fresno are also relatively cool. Thus, NE days are indicated by higher pressure to the north and east of San Francisco with a strong, low subsidence inversion which acts to hold back the marine layer. Northerly winds in the Sacramento Valley act to reduce daily maximum temperatures there below the levels reached on more stagnant days. Note that ozone exceedances can only occur if the offshore push is moderate and not strong enough to actually penetrate westward through the Bay Area and out to sea. Thus, as indicated in the wind field analyses described above, the circulation in the Bay Area under this pattern is weak and driven primarily by local surface heating differentials (i.e., similar in most respects to the bay outflow pattern).

- BO Days: This pattern is not particularly well differentiated from the NW pattern, most likely because there can be considerable overlap between the two, making them difficult to distinguish from one another when analyzing wind fields.

  The principal distinguishing features of bay outflow days appear to be higher 850 mb temperatures and maximum temperatures in the Sacramento and Northern San Joaquin valleys (average temperatures on bay outflow days are exceeded only by those on the four NW-S days) coupled with average Oakland-to-Medford 700 and 500 mb height differences that are lower than on northwest days. These features are indicative of a broad, flat high pressure system with strong subsidence and associated adiabatic heating, which results in a weak circulation pattern primarily driven by thermal effects (as indicated by the surface pressure gradients and San Francisco-to-Sacramento temperature gradients) with little or no synoptic-scale forcing.

- NW-S Days: These four days appear to be represented by a variety of conditions which are similar in most respects to NW or BO days although they exhibit some of the warmest 850 mb temperatures and Sacramento and Fresno temperatures, and some of the strongest negative San Francisco-to-Reno pressure gradients. Average San Francisco-to-Redding and San Francisco-to-Fresno pressure gradients are lower than on BO or NW days, but the values have a wide range.

Cluster Analysis

The results described above indicate that some days included in each flow type do not match the overall pattern of meteorological conditions for that type. This suggests that it may be possible to improve on the classifications by reshuffling days between groups. We attempted to do this through a directed clustering procedure in which six cluster seeds corresponding to the NW, S, NW-S, NE, C, and BO flow types were defined using mean values of seven of the key meteorological variables for the days assigned to each flow type: Oakland 04:00 PST 850 mb temperature, Sacramento daily maximum temperature, daily maximum temperature gradient San Francisco-to-Sacramento, sea level pressure gradients for San Francisco to Reno, Redding, and Fresno, and the Oakland-to-LMU 500 mb height gradient. A seventh seed was defined using the mean values on non-episode days. All observations and mean values were divided by their standard deviations. The SAS FASTCLUS procedure was then used to assign each day to a cluster based on the Euclidean distance between the observation and the cluster seed. By using observations and cluster seeds that have been divided by their standard deviations, this procedure amounted to assigning days to the cluster with the minimum sum of squared standardized differences between the observation and the cluster seed. Thus, the contribution of each variable to the total distance was determined by its normalized deviation from the mean.

Table 3-8 summarizes the results of the initial cluster assignment procedure. All but one of the 79 ozone episode days were assigned to one of the "high ozone" clusters (1 - 6); however, 164 of the 563 non-episode days (29%) were assigned to one of these clusters. This suggests that it is very difficult to identify an episode day solely on the basis of the

meteorological variables included in the cluster analysis, although these variables do identify conditions ripe for ozone formation. Additional analysis may identify other factors that intervene to prevent the occurrence of a peak concentration event.

Seven of the 17 bay outflow days are similar enough to one another to be assigned to the same cluster; the remaining 10 are spread evenly across three other clusters. Both calm days are more similar to each other than to any other group, as are three of the four northeast days. The two southerly flow cases are quite different and are assigned to different clusters. The 29 northwest and 4 NW-S days do not appear to form coherent groups in this scheme, although nearly twice as many of these days are assigned to the northwest cluster than would be expected based simply on the proportion of all episode days assigned to this cluster (17 out of 79).

After the initial assignment of days to each cluster, the initial cluster seeds were replaced with the centroids of the new clusters and the assignment of days to clusters repeated. This sequence of steps was repeated until the differences between the seeds from one iteration to the next became less than 0.2 times the minimum distance between cluster centroids. Results of the final clusters (Table 3-9) are similar to those from the initial cluster assignments, with the exception that the northwest and bay outflow days are reassigned to a broader array of final clusters.

Side-by-side box plots summarizing the distributions of key meteorological variables within each of the new clusters formed via this iterative clustering procedure were prepared (Figure 3-33). These plots can be compared to those shown in Figure 3-32 for the classification of days by flow pattern. To aid in this comparison, the flow pattern originally assigned to each cluster is indicated along the bottom of each page, but it must be kept in mind that these flow patterns may no longer be relevant based on the final assignment of days to each cluster. The reshuffling of days between categories seems to have resulted in clusters that are primarily distinguished by differences in 850 mb temperature, pressure gradients from San Francisco to Reno, Redding and Fresno, and San Francisco-to-Sacramento temperature gradients. Northeast days (cluster 4) have the distinguishing features noted previously with the one "outlier" day out of the original four northeast days moved to cluster 5. A number of the days originally assigned to the NW flow pattern were moved into this category.

Table 3-10 lists the median values of the key distinguishing meteorological conditions on days assigned to each cluster by the iterative procedure. The clusters with initial seeds corresponding to NW, NE, C, and BO flow patterns appear to be good representations of the key characteristics of these days. The NW-S cluster represents days that have the large negative San Francisco-to-Reno pressure gradient characteristic of BO days, but with slightly higher temperatures along the coast, a slight negative San Francisco-Redding pressure gradient, and a more moderate positive San Francisco-Fresno pressure gradient. It is not clear if the cluster is a statistical oddity of the particular set of episode days examined or if it represents a unique source-receptor scenario.

An interesting feature of Table 3-9 is that the number of days in each final cluster is approximately equal. This appears to be a result of the tendency of the iterative

clustering procedure to produce clusters of roughly equal size and is undesirable in that we would expect certain episode patterns to occur much less frequently than others. Thus, forcing the clusters to be of equal size may result in groupings that are not physically meaningful. Another caveat to be considered when interpreting these results is that the final cluster assignments from an iterative application of the FASTCLUS procedure may be sensitive to the initial ordering of days read into the program for sample sizes of less than about 100.

Discriminant Analysis

A linear discriminant analysis was performed on the high ozone days to further explore the key relationships between meteorological conditions and flow patterns. This analysis was conducted with the eventual goal of developing a simple objective procedure for identifying source-receptor scenarios on the basis of routine meteorological observations. The assigned flow categories listed in Table 3-3 were used as the classifications to be predicted by the discriminant procedure; the key meteorological variables listed in Table 3-6, with the exception of the Oakland inversion variables (OAK4AIBH, OAK4ADELT, OK4PIBH), and the change in SFO-to-Sacramento temperature gradient (TMDFSFSC), were used as predictors. The inversion base height and strength variables exhibit somewhat erratic behavior, have large within-group variations, and are not likely to be even approximately normally distributed, making them unsuitable for use with the discriminant procedure. In any event, the inversion height and strength are expected to be closely related to the 850 mb temperature, which is included among the 13 remaining variables. TMDFSFSC is a linear function of the daily maximum and 16:00 LST temperature gradients and is therefore redundant in this analysis.

The SAS DISCRIM procedure (SAS, 1985) was used to derive a set of linear combinations of the meteorological variables that best describe the conditions associated with each flow category. These linear combinations or discriminant functions form a decision rule which can be used to identify the most likely flow category for any given day based on values taken on by the key meteorological variables. To keep the resulting classification procedure reasonably simple, the discriminant analysis was performed using the pooled variance-covariance matrix. In other words, it was assumed that the variances of each meteorological variable and the covariances between variables were equal between groups. This results in a set of linear discriminant functions.

Results of the discriminant analysis are summarized in Table 3-11, which indicates the category assignments obtained by applying the derived discriminant functions to each high ozone day included in the analysis and identifying the most likely category. As one might expect, these resubstitution results are somewhat similar to those of the non-iterative cluster assignment procedure described in the previous subsection but with fewer reassignments of NW days.[4] The two South days are dissimilar, and one is assigned by

[4] Note that the total number of days in each category in Table 3-11 differs from that in Table 3-8 since days with one or more missing variables are not included in Table 3-8.

the discriminant function to the Northwest category. Bay Outflow days are split evenly among the BO and NW categories while 20 percent of the Northwest days are assigned to the BO category. Three of the four NE days are assigned to the NE category while the fourth is assigned to NW. The NW-S days are split across the BO, NW, and NW-S categories.

Source-Receptor Scenario Assignments

Based on the results of the cluster and discriminant analyses described above, it appears that some of the days initially assigned to each category on the basis of the onshore and offshore flow types do not match the meteorological conditions exhibited by a majority of days in the category. For example, one of the days initially assigned to the NE category (9/2/91) was identified by both the clustering and discriminant analysis procedures as being quite different from the other three NE days. Although the snapshot of winds at 10:00 on this day are similar to the usual NE pattern (although with very light winds), the meteorological conditions on this day differ from those of the other NE days primarily in the lack of a strong negative SFO-to-Redding pressure gradient and a larger difference in daily maximum temperatures between SFO and Sacramento. These features indicate a better fit with the Bay Outflow pattern. In the very heterogeneous NW category, a review of the meteorological conditions on days put into other categories by these procedures reveals that conditions on at least some of these days are indeed much more indicative of Bay Outflow (and in a few cases Northeast) events than Northwest events. Conversely, some of the days initially classified as Bay Outflow do not exhibit the primary characteristics of Bay Outflow events (i.e., high 850 mb temperatures and high temperatures inland, large negative SFO-to-Reno pressure gradients, and large negative SFO-to-Sacramento temperature gradients).

A full examination of meteorological conditions on days for which alternative classifications were suggested by the clustering and discriminant analysis procedures resulted in revisions to category assignments on 14 days as shown in Table 3-12. Only days for which alternate category assignments were clearly indicated by the meteorological conditions were switched—no changes were made in borderline situations. The primary effects of these changes were to limit the range of conditions included in the Bay Outflow category, move some of the days originally assigned to the Northwest category into categories with a much better fit, and move the one day originally assigned to the Northeast category to the Bay Outflow category as described above. No attempt was made to deal with the two episode days classified as South since the available data did not allow for an adequate characterization of this category.

The discriminant analysis procedure was rerun using the revised category memberships to determine the effect of the reclassification; results are summarized in Table 3-13. Clearly, the reassignment of a few days resulted in a much improved agreement between the revised 10:00 a.m. flow patterns and the categories assigned by the discriminant analysis. The overall resubstitution "error" rate (i.e., the fraction of days that are moved to a different category by the discriminant procedure) is only 7 percent. This indicates that the revised groups are reasonably well defined, although there may be some

disagreement on a few days about which category best fits the 10:00 PST flow charts. It should be noted that the "true" category for a given day is unknown; Table 3-13 only compares the assignment of categories based on meteorological conditions with categories assigned on the basis of a subjective analysis of 10:00 a.m. flow charts.

OBJECTIVE CLASSIFICATION PROCEDURE

Results of the discriminant analysis described above performed with the revised category assignments form the basis of an objective procedure for classifying any given day into one of the six flow categories given values for the meteorological variables used in the analysis. This procedure consists of calculating the value of the discriminant function for each class, j = 1, ... , 6:

$$D_j = K_j + \text{sum}_i[C_{ij}M_i]$$

where D_j is the value of the discriminant function for the jth class, M_i is the ith meteorological variable, and values for the constant K_j and the coefficients C_{ij} are listed in Table 3-14. The assigned category for the day is the one for which D_j is a maximum. For routine applications, it may be desirable to develop a modified set of discriminant functions based on a subset of the 13 meteorological variables used here.

Evaluation of the Objective Classification Procedure

The resubstitution error rate noted above resulting from application of the objective classification procedure to the source-receptor categories is most likely an underestimate of the true error rate that would be obtained by applying the procedure to an independent set of days and comparing the resulting classifications to the "true" categories. The degree to which the true error rate is greater than the resubstitution error rate indicates the degree to which the discriminant function coefficients have been "tuned" or overfit to the peculiarities of the particular data set from which they were derived.

Since all the available data were used to develop the discriminant function, such an independent data set is not available. However, an estimate of the true error rate can be obtained via crossvalidation. Crossvalidation consists of removing a single day from the data set, repeating the discriminant analysis, applying the resulting discriminant function to the day which was removed, and comparing the category assigned by the discriminant function with the "true" category. This process is repeated, removing a different day from the data set each time. A summary of the resulting "independent" classifications is provided in Table 3-15. As one would expect, the misclassification rates are higher than in the case of resubstitution. This is particularly true for the C, BO, NE, and NWS categories. However, crossvalidation error rates for the C, NE, and NWS categories are most likely not representative of the true error rates due to the small number of days in each of these categories. With only a few observations to work with, elimination of one day from the category during the crossvalidation can radically alter the discriminant function, resulting in the subsequent misclassification of the day which was removed. If

more were available, this problem could be overcome and a better estimate of the true error rate obtained. Predictions of NE pattern by the discriminant analysis are likely to be reliable given the unique nature of these days. Meteorological conditions on C, S, and NW-S days appear to be less distinct than on NE days, making accurate prediction of these days less certain.

Crossvalidation results shown in Table 3-15 for the BO category indicate that the difference between NW and BO days are subtle and difficult to determine accurately from the meteorological variables used in this study. However, only minimal misclassification of NW days are seen in these results.

The crossvalidation results described above suggest that the discriminant function classification procedure provides a reliable prediction for NW days and identifies a set of conditions distinct from those on NW days which are frequently associated with a determination of Bay Outflow wind pattern based on a visual examination of the 10:00 PST ARB flow charts.

Application of the Objective Classification Procedure

Screening Procedure

The discriminant analysis procedure described above was developed on the basis of meteorological conditions during ozone episodes and is not, strictly speaking, suitable for use under non-episode conditions. The flow patterns described by Hayes et al. (1984) may include all of the flow types that occur on both high and low ozone days; however, there is no guarantee that the relationships between these patterns and the key meteorological variables considered here hold under conditions radically different from those that favor high ozone concentrations. Therefore, an additional component of the objective classification procedure is needed in which most of the low ozone events are eliminated on the basis of meteorological conditions before application of the discriminant functions.

As indicated above, previous attempts to eliminate low ozone days on the basis of the key meteorological variables via CART and cluster analysis were largely unsuccessful because so many episode days were categorized as non-episodes. Similar results were obtained from an attempt to generalize the discriminant analysis to include a low ozone category. Therefore, a simple screening procedure was devised that retains nearly all of the episode days while eliminating a large proportion of the non-episode days. This procedure is based on the observation that nearly all high ozone events occurred in conjunction with high 850 mb temperature, high Sacramento and Fresno surface temperatures, and SFO-to-Reno pressure gradients that were near zero or negative. Thus, any day not meeting the following criteria was classified as a low ozone day:

Oakland 850 mb temperature $\geq$ 17.5° C

Sacramento max temperature $\geq$ 85° F

Fresno max temperature $\geq$ 85° F

SFO-to-Reno pressure difference $\leq$ 10 mb.

Of the 642 days examined, 476 were eliminated by this screening procedure, leaving 70 of the 81 ozone episode days as listed in Table 3-3 and 96 additional non-episode days. We refer to the days that meet the above criteria as "potential ozone days." Use of the screening procedure to identify potential ozone days should help to ensure the applicability of the discriminant function classification procedure.

Results

The discriminant functions developed on the basis of the episode days were applied to the set of 166 "potential ozone days," resulting in the assignment of a flow category for each day. Daily maximum ozone concentrations within each category were examined to evaluate differences in the distribution of ozone between each source-receptor category as defined by the combination screening and linear discriminant function objective classification procedure. Side-by-side box plots of daily maximum ozone concentrations prepared for key subregions and individual monitoring sites are presented in Appendix A. In addition, the percent of days in each category with concentrations $\geq$ 9.5 pphm (12.5 pphm in the Central San Joaquin) was calculated for each subregion (Table 3-16). Finally, as an aid to understanding the potential for transport impacts under each category, average diurnal profiles of hourly ozone concentrations were computed for key monitoring sites (ozone episode days only). A complete set of profiles is presented in Appendix B. Except as noted below, the profiles are quite similar for each category. Profiles for NE days may not be representative of that category, since only three days were available from which to calculate an average profile.

The daily maximum ozone distributions, exceedance summaries, and diurnal profiles can be summarized as follows:

North Bay: Concentrations tend to be lowest under the NW category when the influence of clean marine air is most prevalent, except for a few extreme events. Maximum concentrations occur under NE and BO conditions in the absence of northwest winds.

Western Alameda: Concentrations follow a pattern similar to that of the North Bay but with some high concentrations occurring under Calm conditions when transport out of the immediate source area is minimal.

Contra Costa: Concentrations show relatively little variation between categories. The abundant NW days include the most extreme high and low events; however, concentrations above 9.5 pphm are more common under BO and NE conditions.

South Bay: Average, median, and higher percentile concentrations are largest and exceedances of 9 pphm are most prevalent at San Jose and Gilroy under the Calm and

Northeast categories when there is little transport out of the area. Some Northeast days may be associated with transport of high concentrations from the primary Bay Area source regions into the South Bay.

Southern Santa Clara Valley: Concentrations at Hollister are low in most cases with the highest average and median values under Calm conditions but without any exceedances of 9 pphm. Exceedances were only observed under the BO and NW patterns. Concentrations at Pinnacles significantly above 10 pphm only occurred under the BO and NW categories. Only one non-missing daily maximum concentration was available under the South category at this site.

Livermore: 75th percentile concentrations are nearly identical under all categories. Highest concentrations are observed under the BO and NW categories. Exceedances of 9 pphm are most common under the BO conditions.

Sacramento: Concentrations are lowest under the NE category when transport from the west and south is cut off. Northwest days and especially the more stagnant Bay Outflow days lead to much higher concentrations and frequencies of exceedances. Diurnal profiles show no delay in or lengthening of the afternoon ozone peak under BO days as opposed to NW days. Thus, the higher concentrations under BO conditions appear to be related to increased stagnation with reduced vertical mixing rather than transport.

Northern San Joaquin: Concentration patterns are like that for Livermore, with exceedances of 9 pphm most common under BO conditions and least common under NWS.

Central San Joaquin: Concentrations tend to be highest under BO conditions, as in the Northern San Joaquin.

TABLE 3-1. Joint frequencies of occurrence of 10:00 PST onshore and nearshore flow patterns (onshore patterns are defined in Figure 3-2; nearshore patterns are defined in the text).

Onshore Pattern	Nearshore Pattern																
	C	C-NW	E	M	NE	NW	NW-C	NW-S	NW-U	S	S-C	S-NW	U	W	W-NW	W-S	Total
2	0	0	0	1	0	4	0	1	0	26	0	0	0	0	0	0	32
3	0	0	0	0	0	0	0	0	0	1	0	0	0	0	0	0	1
4	0	0	1	0	3	7	0	0	0	0	0	0	0	0	0	0	11
5	0	0	0	0	0	0	0	0	1	0	0	0	0	0	0	0	1
6	4	2	0	0	1	19	0	2	0	12	0	3	4	0	0	0	47
7	1	0	0	0	1	5	0	1	0	3	1	1	1	0	0	0	14
1A	3	2	0	4	0	124	1	5	0	16	0	6	6	7	3	1	178
1B	0	0	0	4	0	21	0	3	0	6	0	0	2	3	4	0	43
Total	8	4	1	9	5	180	1	12	1	64	1	10	13	10	7	1	327

TABLE 3-2. Distribution of ozone episode and non-episode days by onshore flow category (numbers do not sum to 100% due to rounding).

Onshore Flow Type	Percent of All Days[1]	Percent of Episode Days
1 A/B (NW)	68	58
2 (S)	10	3
4 (NE)	4	6
6 (BO)	14	27
7 (C)	4	5

[1] Based on analysis of weekdays during the study period.

TABLE 3-3. Maximum hourly ozone concentration (pphm) in subregions on episode days. Only values above 9 pphm (12 pphm in SAC) are shown; subregions defined in Table 2-3.

Year	Month	Day	Onshore Category	Nearshore Category	Assigned Category	Subregion Max Hourly Ozone Concentration (pphm)								
						SAC	CONT	NBAY	IBAY	WALA	LVRM	SBAY[1]	SSAN[2]	MBAY
89	4	7										12		
89	4	8										10[3]		
89	4	9				13	11	12	10	11	10	13		10
89	6	1	Ia	NW	NW					11		10[3]		
89	6	2	Ib	NW	NW								11	
89	6	21	V	NW-U	NE							10		11
89	6	22	Ia	NW-S	NW-S		10	10		10	11	10[3]		
89	6	23	II	S	S	13								
89	7	5	Ib	M									10	
89	7	6	Ia	M			11	11		12	13	13	14	13
89	7	10	Ib	U		13								
89	7	19	Ia	NW	NW								10	
89	7	20	Ib	NW	NW	13							11	
89	7	21	Ib	NW	NW		10							
89	7	22					10				10			
89	7	27	Ia	NW	NW	17								
89	8	4	II	S	S	13								
89	8	7	Ib	W	NW	13								
89	8	13								11	11	11[3]		
89	8	14	Ia	NW	NW		10				14			
89	8	15	VI	U	BO	13	11							
89	9	3					11				10	10[3]		

TABLE 3-3. Continued.

Year	Month	Day	Onshore Category	Nearshore Category	Assigned Category	Subregion Max Hourly Ozone Concentration (pphm)								
						SAC	CONT	NBAY	IBAY	WALA	LVRM	SBAY[1]	SSAN[2]	MBAY
89	9	4	VI	S	BO						10			
89	9	12	VI	NW	BO							10		
89	9	13	Ib	NW	NW		11			11				
89	9	14	Ia	NW-C	NW		11	10		10	11	13	10	
89	9	21	Ia	NW	NW			10				11		
89	9	22	Ia	M			10					12[3]		
89	10	8					11			11		11[3]		
89	10	10	VII	S-C	C								10	
89	10	18	IV	NW	NE			10	10	12		12[3]		
89	10	19	Ia	NW	NW					10		11[3]		
90	5	4					11			11		10		
90	5	8											10	
90	6	8	Ia	NW	NW							10	11[6]	
90	6	19	VI	U	BO							12	12	
90	6	20	VI	C	BO		11				11	10[4]		
90	6	21	VI	S	BO	13								
90	7	10	Ia	C	NW		12	11		13	12	12		
90	7	11	Ia	NW	NW	15						10	11	
90	7	12	Ia	NW	NW	15					10		10	
90	7	18	Ia	NW	NW								11	

TABLE 3-3. Continued.

Year	Month	Day	Onshore Category	Nearshore Category	Assigned Category	Subregion Max Hourly Ozone Concentration (pphm)								
						SAC	CONT	NBAY	IBAY	WALA	LVRM	SBAY[1]	SSAN[2]	MBAY
90	7	31	Ia	NW	NW	13								
90	8	4			NW	15								
90	8	5			NW	14					12	10	10[6]	
90	8	6	Ia	NW-S	NW		12							
90	8	8	VI	S	BO	15	10				13	10[4]		
90	8	9	Ia	NW-S	NW-S						12			
90	8	10	Ib	NW-S	NW-S								10	
90	9	9						10			12			
90	9	29					10					10		
90	9	30					10			10	11	11		
91	6	7	Ia	NW	NW						10			
91	6	10	Ia	NW	NW	15								
91	7	1	VII	U	C					11		13	10	
91	7	2	VI	NW-S	BO	16	11	10		10	14	11[4]		
91	7	3	VI	S	BO	13					10	10[4]	10	
91	7	4	Ia	NW	NW	15						11[4]		
91	7	11	Ia	S-NW	NW	14								
91	7	29	VI	S	BO	15					10			
91	7	30	VI	S	BO	19								
91	8	13	IV	NW	NE								10	

TABLE 3-3. Concluded.

Year	Month	Day	Onshore Category	Nearshore Category	Assigned Category	Subregion Max Hourly Ozone Concentration (pphm)								
						SAC	CONT	NBAY	IBAY	WALA	LVRM	SBAY[1]	SSAN[2]	MBAY
91	9	2	IV	NW	NE					12	10	10[3]		
91	9	4	VI	NW	BO						11			
91	9	16	VI	C-NW	BO	13		10			10			
91	9	17	VI	NW	BO	16					10	10		12
91	9	18	VI	NW	BO	14								
91	9	21									11			
91	9	22									10			
91	9	23	VI	NW	BO						12			
91	9	24	VI	NW	BO		11	11		11	11	12	10[6]	
91	9	28									10			
91	9	29					10	10		12		10[3]		
91	10	2	Ia	NW	NW	15						10		
91	10	3	Ia	NW	NW		11	11		12	12	12[5]		
91	10	10	VII	NW-S	NW-S							11[4]		
91	10	13						10			10			
91	10	14	Ia	NW	NW	14	10				10			
91	10	18	Ia	NW	NW						10			10

[1] Maximum concentration shown is at Gilroy unless otherwise indicated
[2] Maximum concentration shown is at Pinnacles unless otherwise indicated
[3] San Jose
[4] Los Gatos
[5] Mountain View
[6] Hollister

TABLE 3-4. Number of days in each subregion with peak ozone greater than 9 pphm (> 12 pphm for SAC) by onshore flow category.

Onshore Flow Type	No. Days	No. Days/Expected No. Days								
		SAC	CONT	NBAY	IBAY	WALA	LVRM	SBAY	SSAN	MBAY
1 A/B (NW)	36	14/15	11/9	6/6	0/1	8/8	12/14	14/16	12/10	2/2
2 (S)	2	2/1	0/1	0/0	0/0	0/0	0/1	0/1	0/1	0/0
4 (NE)	4	0/2	0/1	1/1	1/0	2/1	1/2	3/2	1/1	1/0
6 (BO)	17	10/7	5/4	3/3	0/0	2/4	11/6	8/7	3/5	1/1
7 (C)	3	0/1	0/1	0/0	0/0	1/1	0/1	2/1	2/1	0/0
Subtotal	62	26	16	10	1	13	24	27	18	4
Unknown	19	1	8	4	1	6	11	11	2	1

TABLE 3-5. Summary of peak ozone concentrations, onshore and offshore wind flow patterns in the San Francisco Bay Area, and classification of wind flow patterns based on trajectories for July 9-12 and August 3-7, 1990.

1990 Wind Field Dates	Onshore Wind Flow Pattern SFBA	Wind Flow Pattern Offshore	Trajectory Flow Pattern SFBA	Peak Ozone Concentrations pphm	Locations
July 9	1a	S	S	*	
July 10	1a	C	NW	10-12	Delta
				13	Fremont
				12	Livermore
				11-13	South Bay
				10-11	North Bay
				>9	N. San Joaquin Valley
July 11	1a	NW	NW	10	South Bay
				10	Hollister
				11	Pinnacles
				15	Broader Sacramento
				>9	N. San Joaquin Valley
July 12	1a	NW	NW	10	Livermore
				10	Pinnacles
				15	Broader Sacramento
				>9	N. San Joaquin Valley
August 3	7	S	S	*	
August 4	1a	NW	NW	15	Broader Sacramento
August 5	1a	NW	NW	12	Livermore
				10	Gilroy
				10	Hollister
				10	Pinnacles
				>9	N. San Joaquin Valley
August 6	1a	NW-S	NW	12	Bethel Island
				15	N. San Joaquin Valley
				>9	Broader Sacramento
August 7	1b	S	S	10	Pinnacles
				>9	Broader Sacramento
				>9	N. San Joaquin Valley

* No exceedances; used as a setup day

TABLE 3-6. Key meteorological variables.

OAK4A850T	04:00 PST Oakland 850 mb temperature
OAK4AIBH	04:00 PST Oakland inversion base height
OAK4ADELT	04:00 PST Oakland temperature difference, inversion top – inversion base
OK4PIBH	16:00 PST Oakland inversion base height
TMPDMXSC	Daily maximum temperature, Sacramento
TMPDMXFR	Daily maximum temperature Fresno
SLVPSFRN	Sea level pressure gradient, SFO–Reno
SLVPSFRD	Sea level pressure gradient, SFO–Redding
SLVPSFFS	Sea level pressure gradient, SFO–Fresno
TMMXSFSC	Daily maximum temperature at SFO – daily maximum temperature at Sacramento
TM4PSFSC	16:00 PST temperature at SFO – 16:00 PST temperature at Sacramento
TMDFSFSC	TMMXSFSC – TM4PSFSC
D500OKWN	04:00 PST 500 mb height gradient: Oakland–Winnemucca
D500OKMD	04:00 PST 500 mb height gradient: Oakland–Medford
D500OKLM	04:00 PST 500 mb height gradient: Oakland–LMU
D700OKWN	04:00 PST 700 mb height gradient: Oakland–Winnemucca
D700OKMD	04:00 PST 700 mb height gradient: Oakland–Medford

TABLE 3-7. Means (with 90% confidence intervals) and standard deviations of key meteorological variables for episode days and for all days.

		OAK4A850T	OAK4AIBH	OAK4ADELT	OK4PIBH	TMPDMXSC	TMPDMXFR
Episode Days	Mean	21.1	113	12	177	98	98
	St. Dev.	2.9	166	9	249	5.82	5
	No. Days	78	78	78	78	79	79
90% CI for mean:	Upper	21.7	144.3	13.7	224.4	98.7	99.3
	Lower	20.6	81.7	10.5	130.4	96.6	97.3
All Days	Mean	14.8	458	8.33	934	85	88
	St. Dev.	6.17	1125	7.33	2117	11	10
	No. Days	631	631	631	632	642	642
90% CI for mean:	Upper	15.2	531.7	8.8	1072.5	85.7	88.6
	Lower	14.4	384.3	7.9	795.5	84.3	87.4

		SLVPSFRN	SLVPSFRD	SLVPSFFS	TMMXSFSC	TM4PSFSC	TMDFSFSC
Episode Days	Mean	-31	5	12	-21	-25	4
	St. Dev.	25	15	10	9	9	3
	No. Days	79	79	79	79	79	79
90% CI for mean:	Upper	-26.1	7.4	14.1	-19.1	-23.0	4.4
	Lower	-35.6	1.8	10.3	-22.6	-26.4	3.3
All Days	Mean	11	13	14	-15	-17	2.11
	St. Dev.	37	17	12	8.3	8.9	3.15
	No. Days	642	642	642	642	642	642
90% CI for mean:	Upper	13.4	14.1	14.8	-14.5	-16.4	2.3
	Lower	8.6	11.9	13.2	-15.5	-17.6	1.9

		D500KWN	D500KMD	D500KLM	D700KWN	D700KMD
Episode Days	Mean	22	26	7	7	7
	St. Dev.	36	35	25	15	17
	No. Days	76	76	76	77	77
90% CI for mean:	Upper	28.7	33.1	12.2	9.9	9.9
	Lower	14.9	19.6	2.6	4.1	3.4
All Days	Mean	30	49	-16	15	21
	St. Dev.	47	51	34	22	28
	No. Days	619	626	623	617	623
90% CI for mean:	Upper	33.1	52.4	-13.8	16.5	22.8
	Lower	26.9	45.6	-18.2	13.5	19.2

TABLE 3-8. Assignment of episode days to clusters based on minimum sum of squared standardized differences between key meteorological variables and their mean values for each flow pattern (results from the SAS PROC FASTCLUS procedure with MAXITR=0).

	Cluster							
Flow Pattern	1 S	2 NW-S	3 NW	4 NE	5 C	6 BO	7 Low O_3	Total
S	1						1	2
NW-S		1		1		2		4
NW	3	2	11	3	4	6		29
NE				3	1			4
C					2			2
BO		2	6		2	7		17
Unknown	6	4		5	4	2		21
Total episode days	10	9	17	12	13	17	1	79
Low ozone days	25	3	54	44	26	12	399	563

TABLE 3-9. Results of iterative cluster assignment procedure for ozone episode days.

	Cluster							
Flow Type	1 S	2 NW-S	3 NW	4 NE	5 C	6 BO	7 Low O_3	Total
S	1						1	2
NW-S		1		1		2		4
NW	4	1	7	3	4	7	3	29
NE				3	1			4
C	1				1			2
BO	3	2	5		2	5		17
Unknown	6	5		4	2	1	3	21
Total	15	9	12	11	10	15	7	79

TABLE 3-10. Median values of selected meteorological variables for groups of days defined by the iterative clustering algorithm.

Cluster	DA44A8JOT	OAK4AIBH	TPDMXSC	SLVPSFRN	SLVPSFRD	SLVPSFFS	TMMXSFSC
1 S	20°C	0	96	−20	5	12	−23
2 NW-S	21	0	97	−60	−5	5	−20
3 NW	23	100	100	−10	20	25	−28
4 NE	18	0	90	−50	−10	−2	−5
5 C	19	0	98	−45	−5	5	−15
6 BO	24	125 m	105	−40	10	17	−33
7 Low O_3	20	450	95	5	20	18	−20

TABLE 3-11. Resubstitution results from linear discriminant analysis for ozone episode days.

Original Category	Assigned Category						Total
	C	S	BO	NE	NW	NWS	
C	2						2
S		1			1		2
BO			8		7	1	16
NE				3	1		4
NW			5		23		28
NWS			1		1	2	4
Unknown	3	—	2	2	13	—	20
Total	5	1	16	5	46	3	76

TABLE 3-12. Reassignment of ozone episode days to source-receptor scenarios based on exploratory cluster and discriminant analysis.

Date	Original Scenario	Revised Scenario
6/1/89	NW	NE
6/22/89	NW-S	NE
8/15/89	BO	NW
9/4/89	BO	NW
9/13/89	NW	BO
9/21/89	NW	NE
10/19/89	NW	NE
6/21/90	BO	NW
7/4/91	NW	BO
7/29/91	BO	NW
7/30/91	BO	NW
9/2/91	NE	BO
10/3/91	NW	BO
10/14/91	NW	BO

TABLE 3-13. Resubstitution results of linear discriminant analysis for ozone episode days with revised category assignments.

Original Category	Assigned Category						
	C	S	BO	NE	NW	NWS	Total
C	2						2
S		1			1		2
BO			14	1	1		16
NE				7			7
NW			1		25		26
NWS						3	3
Unknown	2	—	2	10	6	—	20
Total	4	1	17	18	33	3	76

TABLE 3-14. Discriminant function coefficients for objective classification procedure (meteorological variables are defined in Table 3-6).

Meteorological Variable	Source-Receptor Scenario					
	C	S	BO	NE	NW	NW-S
Constant	−601.67	−629.33	−637.18	−557.79	−628.27	−700.93
D500OKLM	−1.84	−1.92	−1.87	−1.55	−1.89	−2.06
D500OKMD	−1.84	−2.02	−1.82	−1.57	−1.85	−1.95
D500OKWN	0.43	0.60	0.37	0.34	0.40	0.32
D700OKMD	4.50	4.72	4.38	3.93	4.53	4.79
D700OKWN	−0.80	−1.06	−0.68	−0.68	−0.84	−0.86
OK4A850T	−20.63	−19.42	−20.20	−19.45	−20.12	−20.75
SLVPSFFS	2.88	2.55	2.76	2.49	2.78	3.06
SLVPSFRD	4.84	4.73	4.96	4.35	4.81	5.03
TM4PSFSC	3.96	5.86	5.18	4.87	5.25	5.46
TMMXSFSC	0.10	−1.97	−1.17	−0.80	−1.36	−1.55
TMPDMXFR	5.70	6.17	6.09	6.29	5.74	5.64
SLVPSFRN	−3.16	−2.95	−3.26	−2.88	−3.11	−3.46
TMPDMXSC	10.76	10.42	10.70	9.60	10.99	11.76

TABLE 3-15. Crossvalidation results for discriminant analysis on ozone episode days with revised category assignments.

Original Category	Assigned Category						Total
	C	S	BO	NE	NW	NWS	
C			1		1		2
S		1			1		2
BO			8	2	5	1	16
NE	2	1		3	1		7
NW	1		2		22	1	26
NWS			1		2		3
Total	3	2	12	5	32	2	56

TABLE 3-16. Percentage of potential high ozone days with concentrations greater than or equal to 9.5 pphm (12.5 pphm for Central San Joaquin Valley subregion) by source-receptor category and over all categories.

Subregion	Source-Receptor Category						
	BO	S	C	NE	NW	NW-S	All
North Bay (all site avg.)	6	0	0	6	1	0	3
Contra Costa Co. (all site avg.)	11	0	0	10	5	0	7
Western Alameda Co. (all site avg.)	6	0	17	13	3	0	6
Livermore	35	0	0	21	16	12	20
South Bay							
San Jose-4th St.	9	0	33	26	4	0	10
Gilroy	14	0	17	16	9	0	11
South Santa Clara Valley							
Hollister	3	0	0	0	4	0	3
Pinnacles	12	0	40	0	18	17	15
Sacramento (all site avg.)	43	0	0	6	34	12	28
North San Joaquin (all site avg.)	43	0	17	23	25	12	27
Central San Joaquin (all site avg.)	34	0	0	3	12	12	15

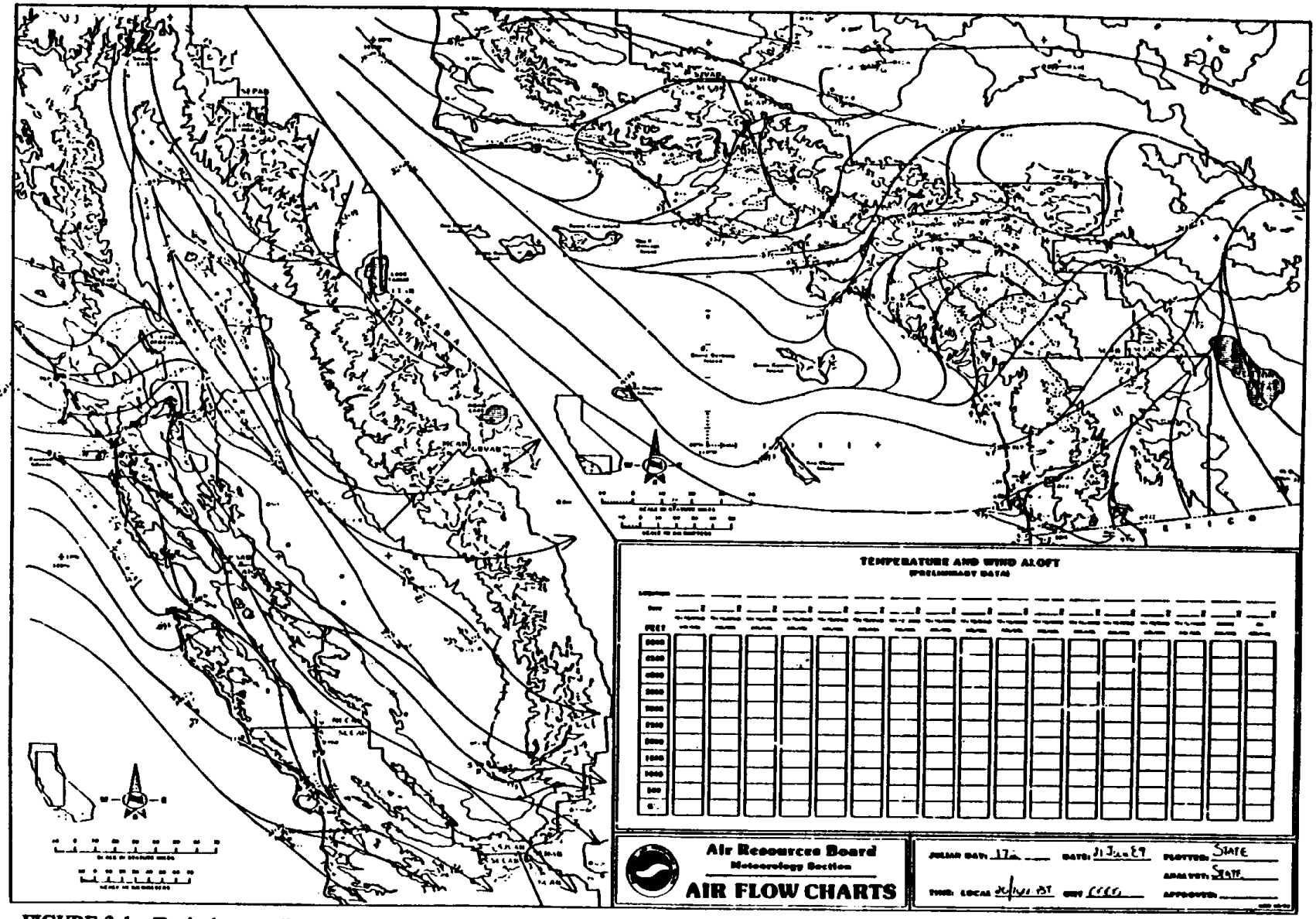

FIGURE 3-1. Typical streamline analysis prepared four times daily by the California Air Resources Board.

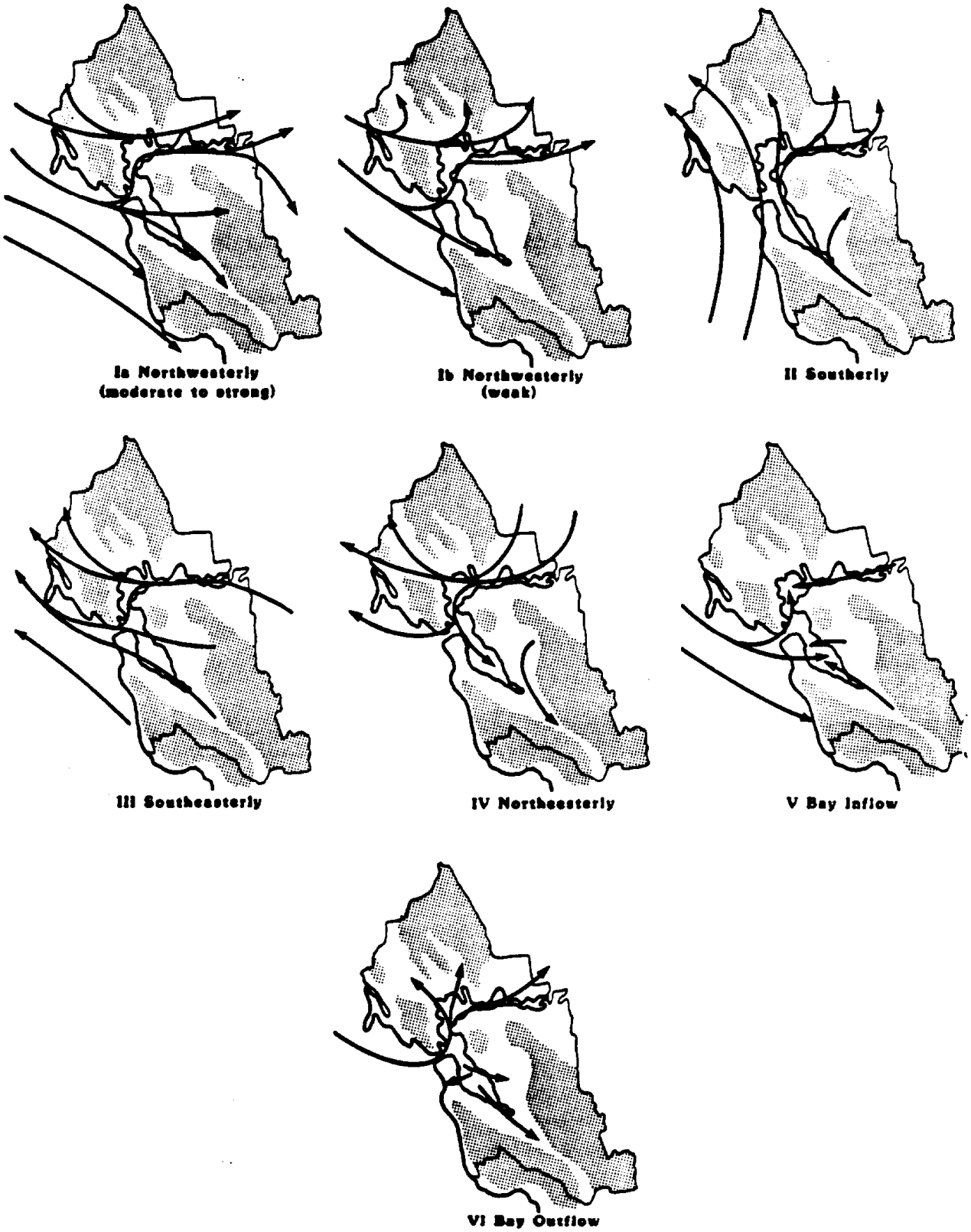

FIGURE 3-2. ARB Bay Area air flow patterns. (Source: Hayes et al., 1984)

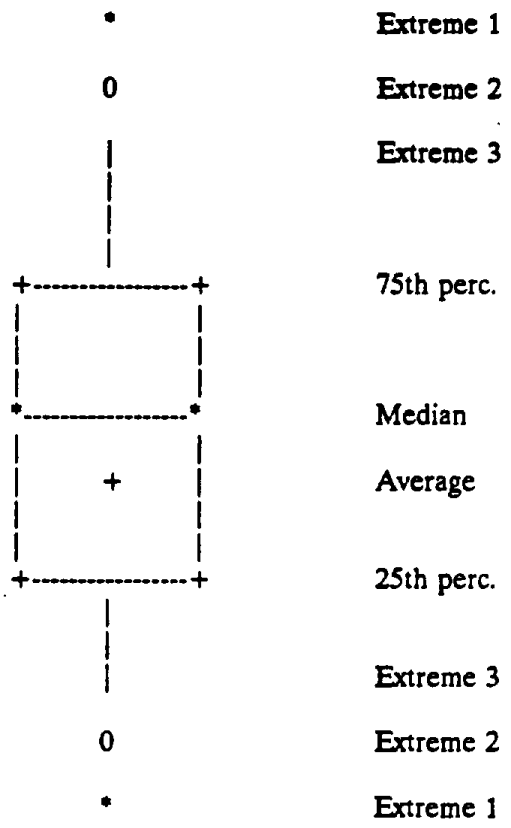

FIGURE 3-3. Key for boxplots in Figures 3-4 to 3-7; Extreme 1 = values more than 3 times interquartile range* above or below median. Extreme 2 = values between 1.5 and 3 times interquartile range above or below median. Extreme 3 = largest (smallest) value that is not more than 1.5 times interquartile range above (below) median.

*Interquartile range is the interval between the 75th and 25th percentiles.

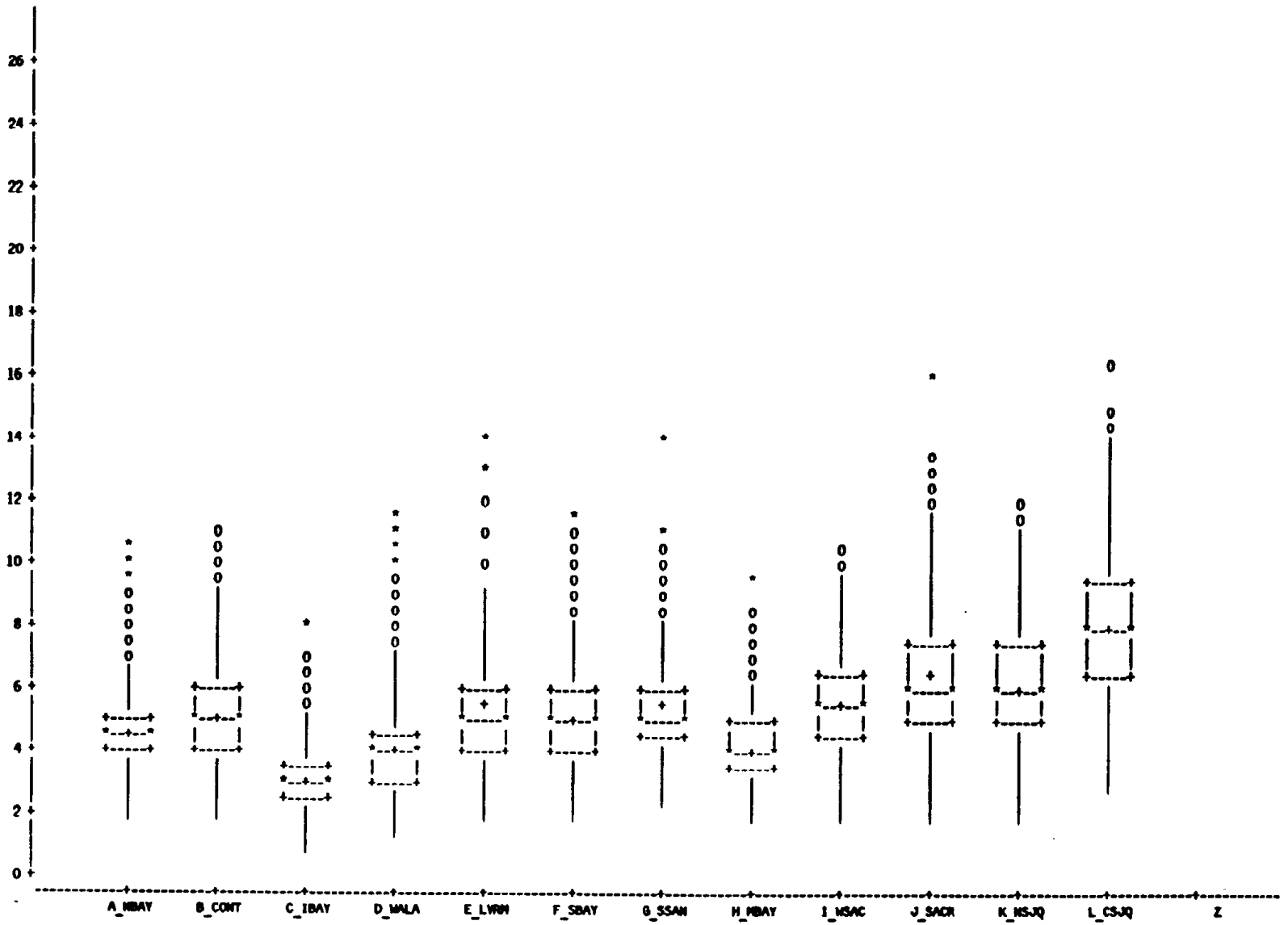

FIGURE 3-4. Boxplots of subregion average daily maximum ozone concentrations (pphm) for all days in the study period.

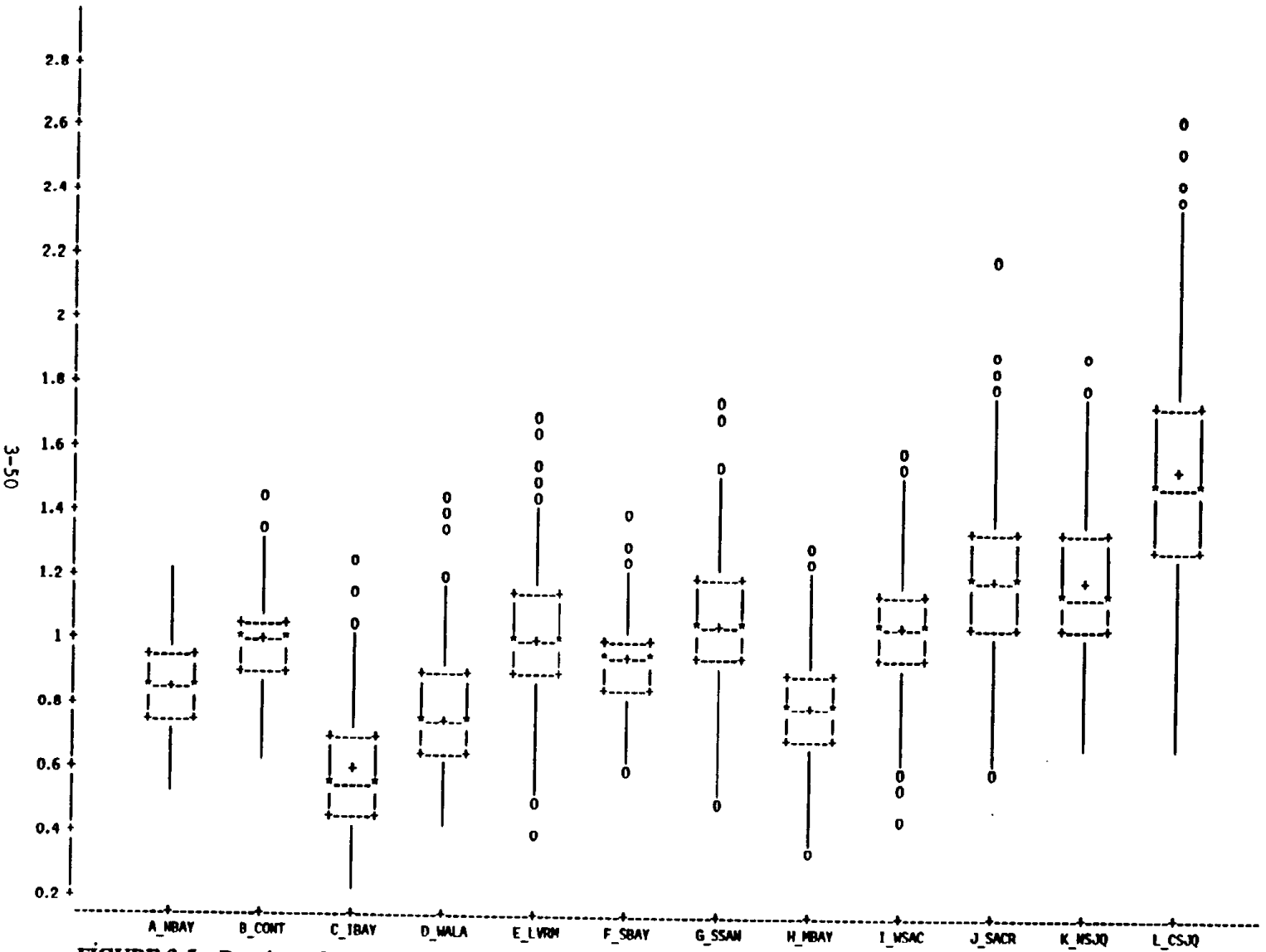

FIGURE 3-5. Boxplots of relative subregion average daily maximum ozone concentrations (pphm) for all days in the study period.

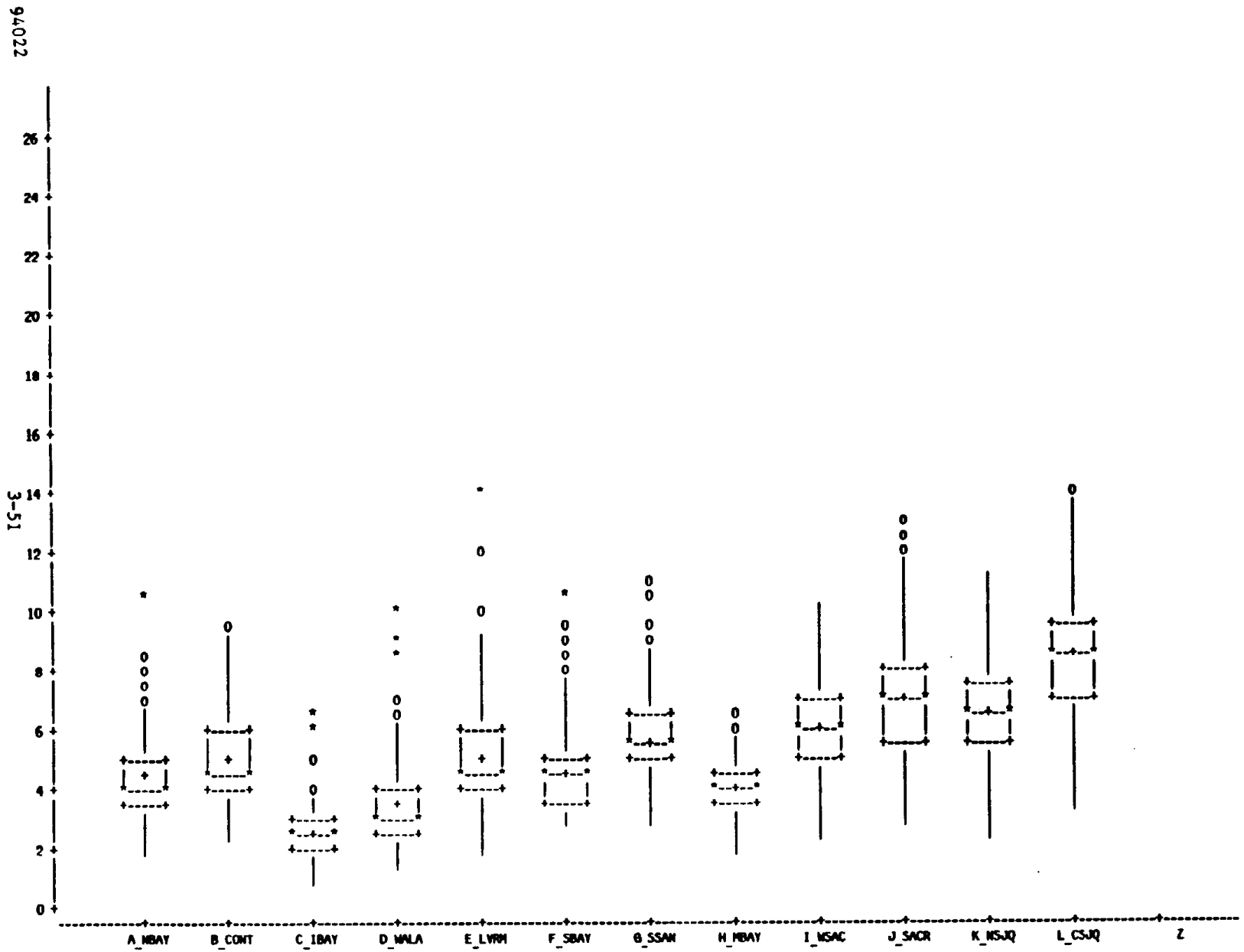

FIGURE 3-6a. Boxplots of subregion average daily maximum ozone concentrations: 1A-NW flow pattern.

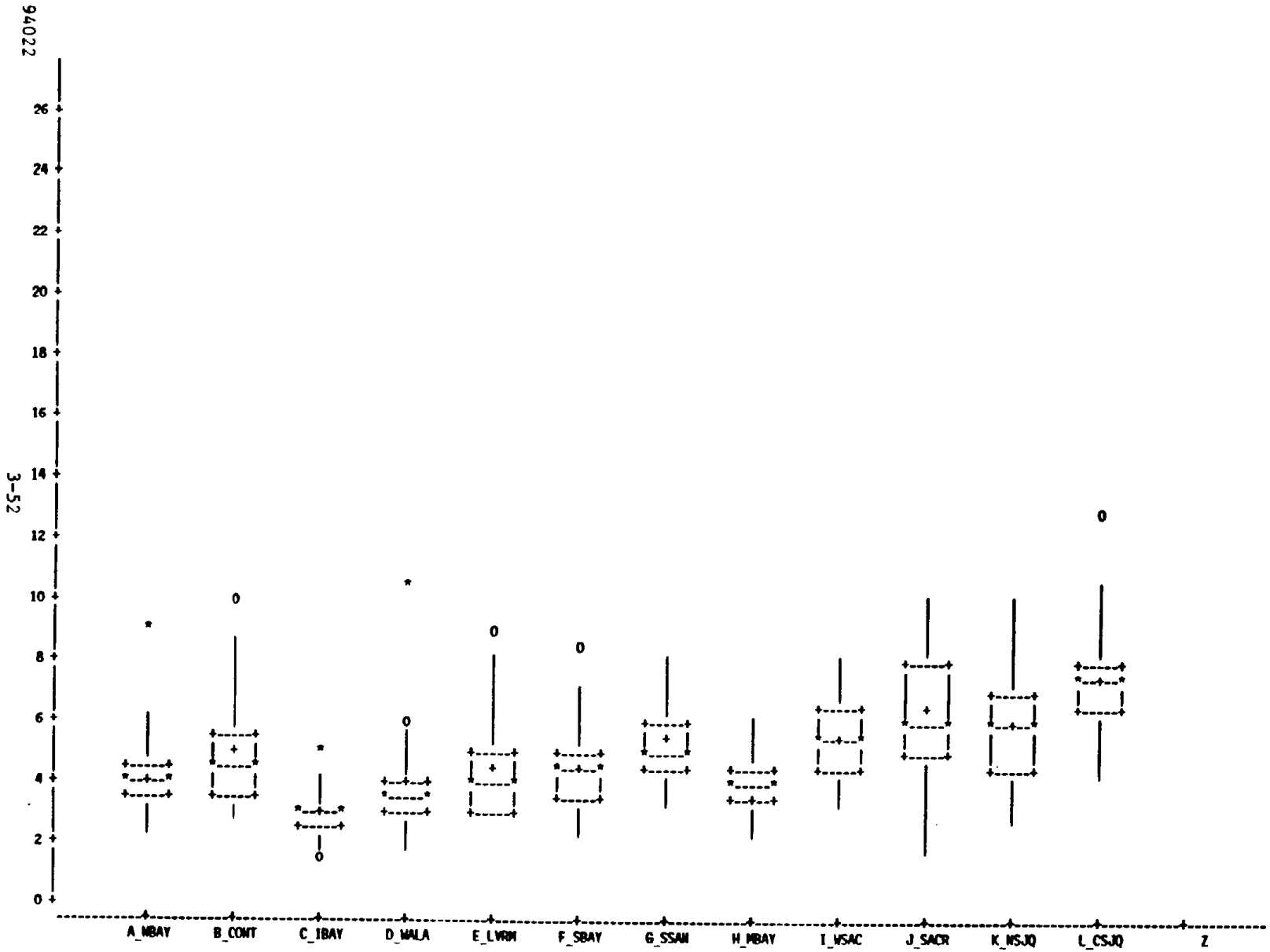

FIGURE 3-6b. Boxplots of subregion average daily maximum ozone concentrations: 1B-NW flow pattern.

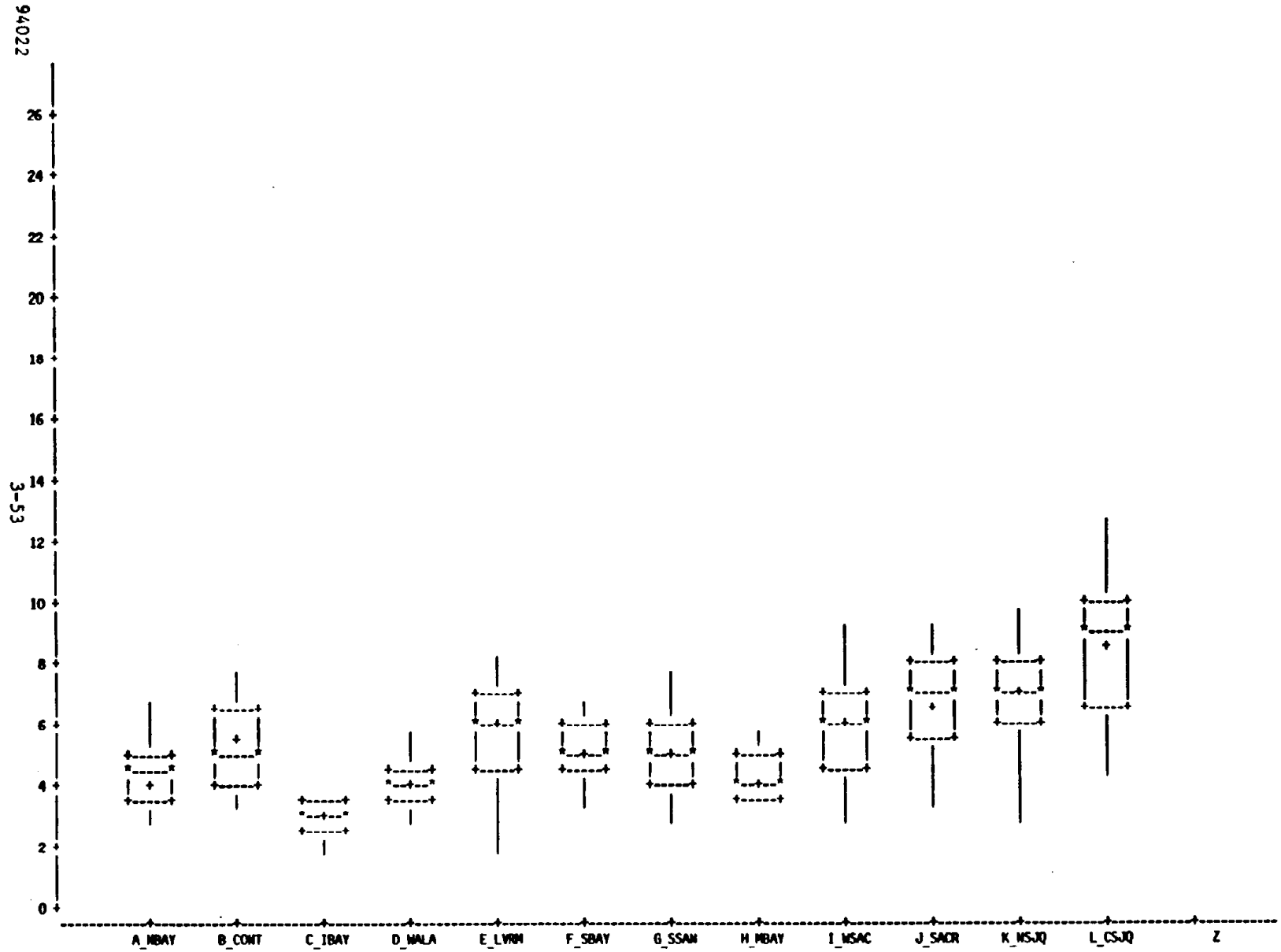

FIGURE 3-6c. Boxplots of subregion average daily maximum ozone concentrations: 1A-S flow pattern.

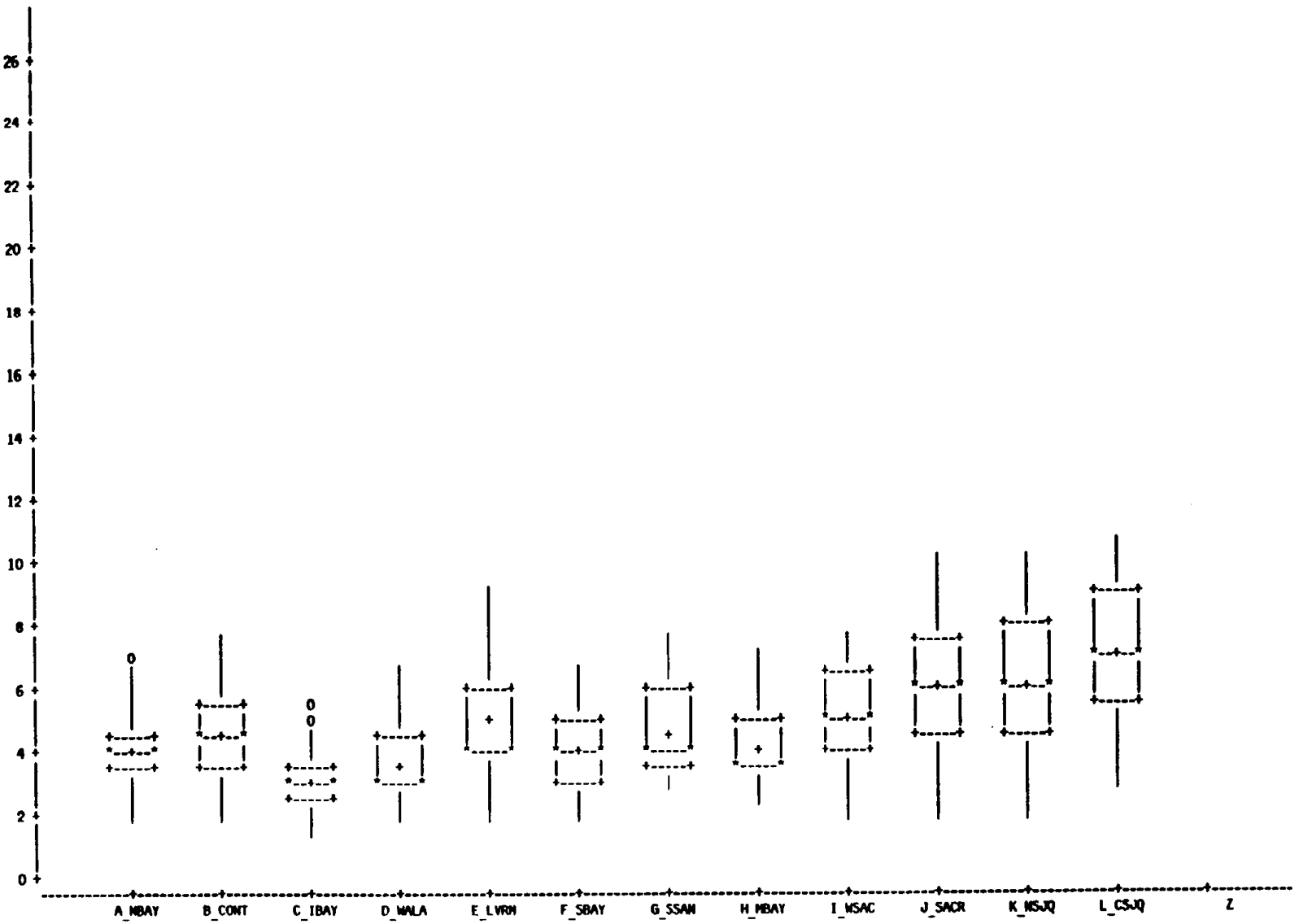

FIGURE 3-6d. Boxplots of subregion average daily maximum ozone concentrations: 2-S flow pattern.

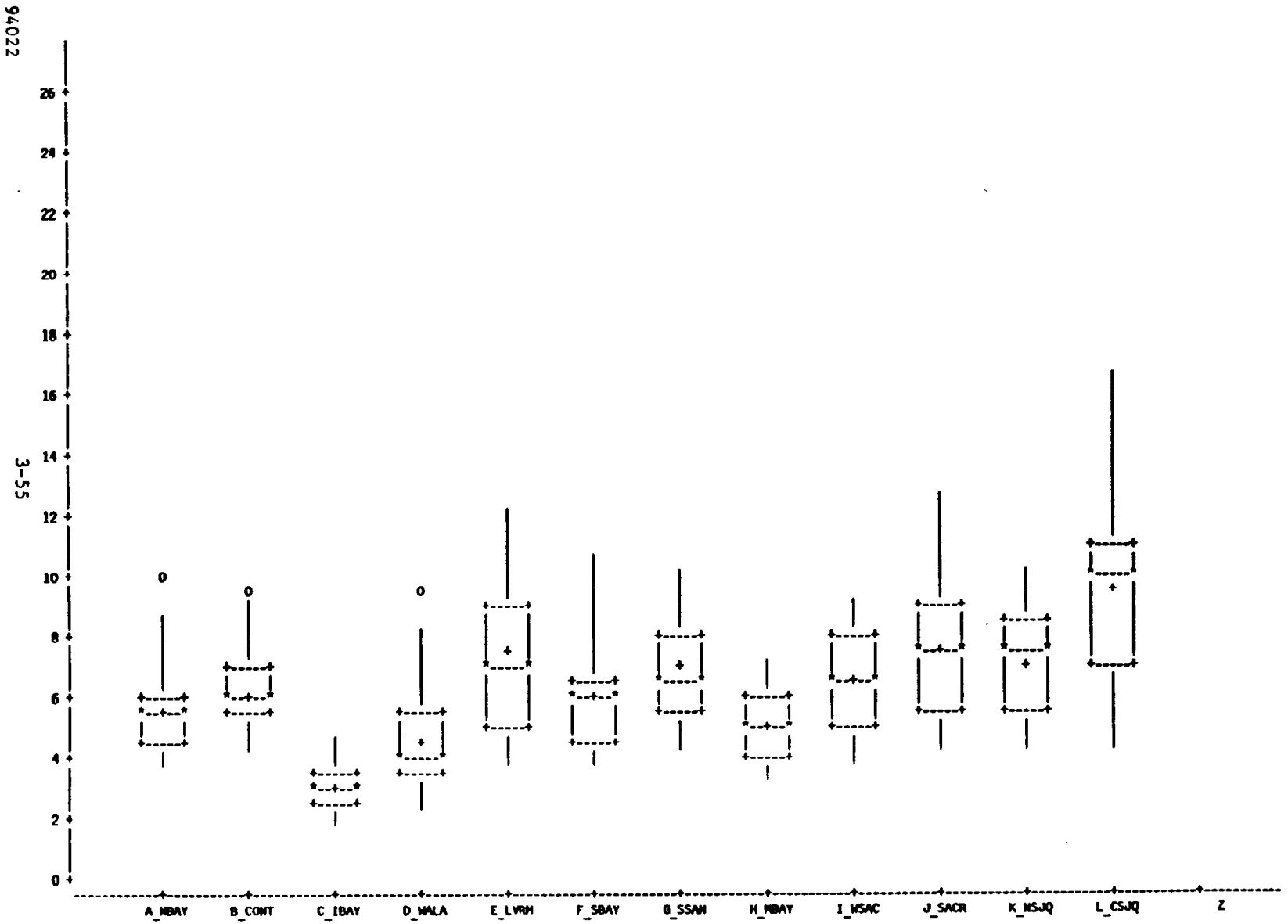

FIGURE 3-6e. Boxplots of subregion average daily maximum ozone concentrations: 6-NW flow pattern.

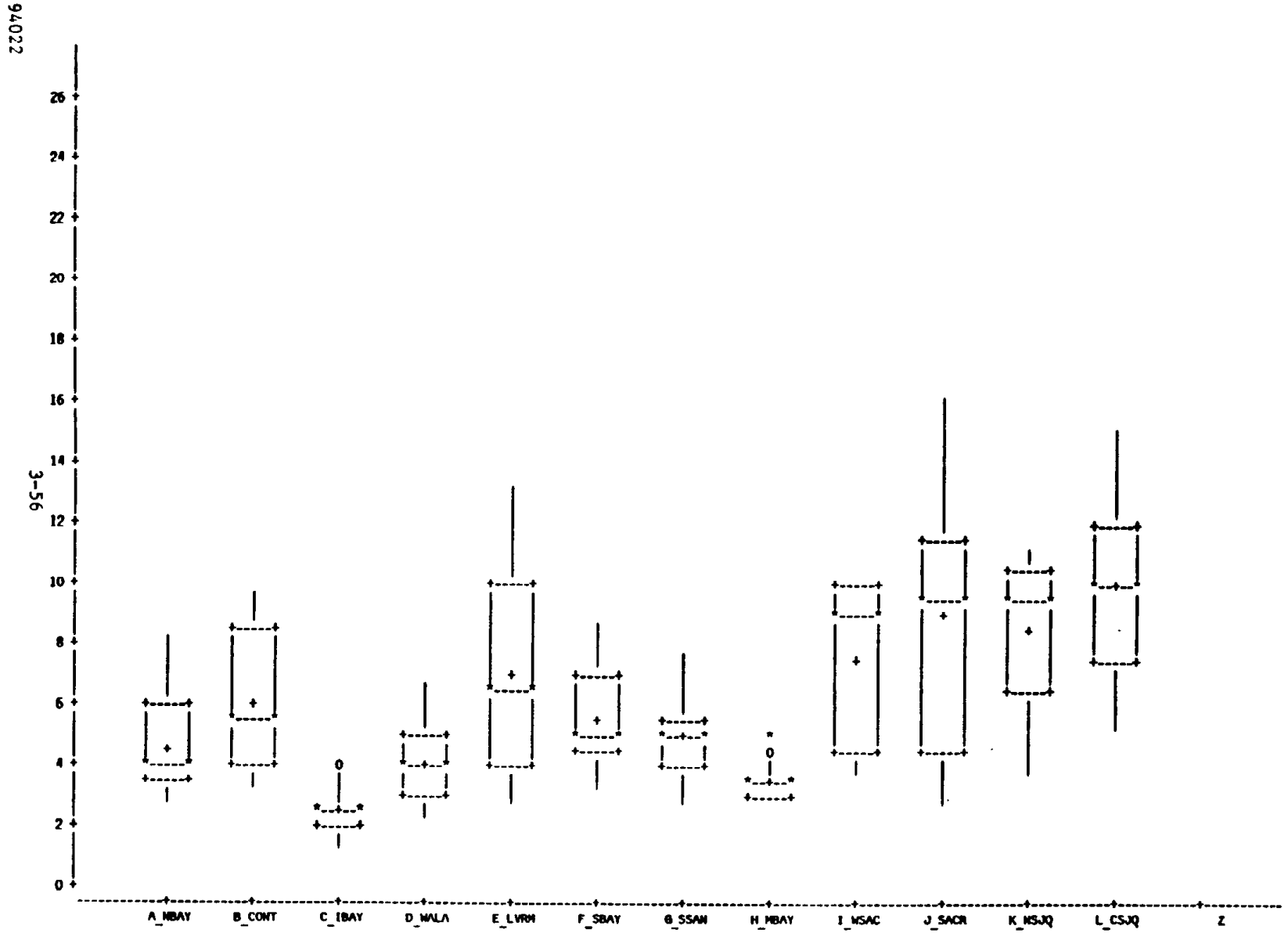

FIGURE 3-6f. Boxplots of subregion average daily maximum ozone concentrations: 6-S flow pattern.

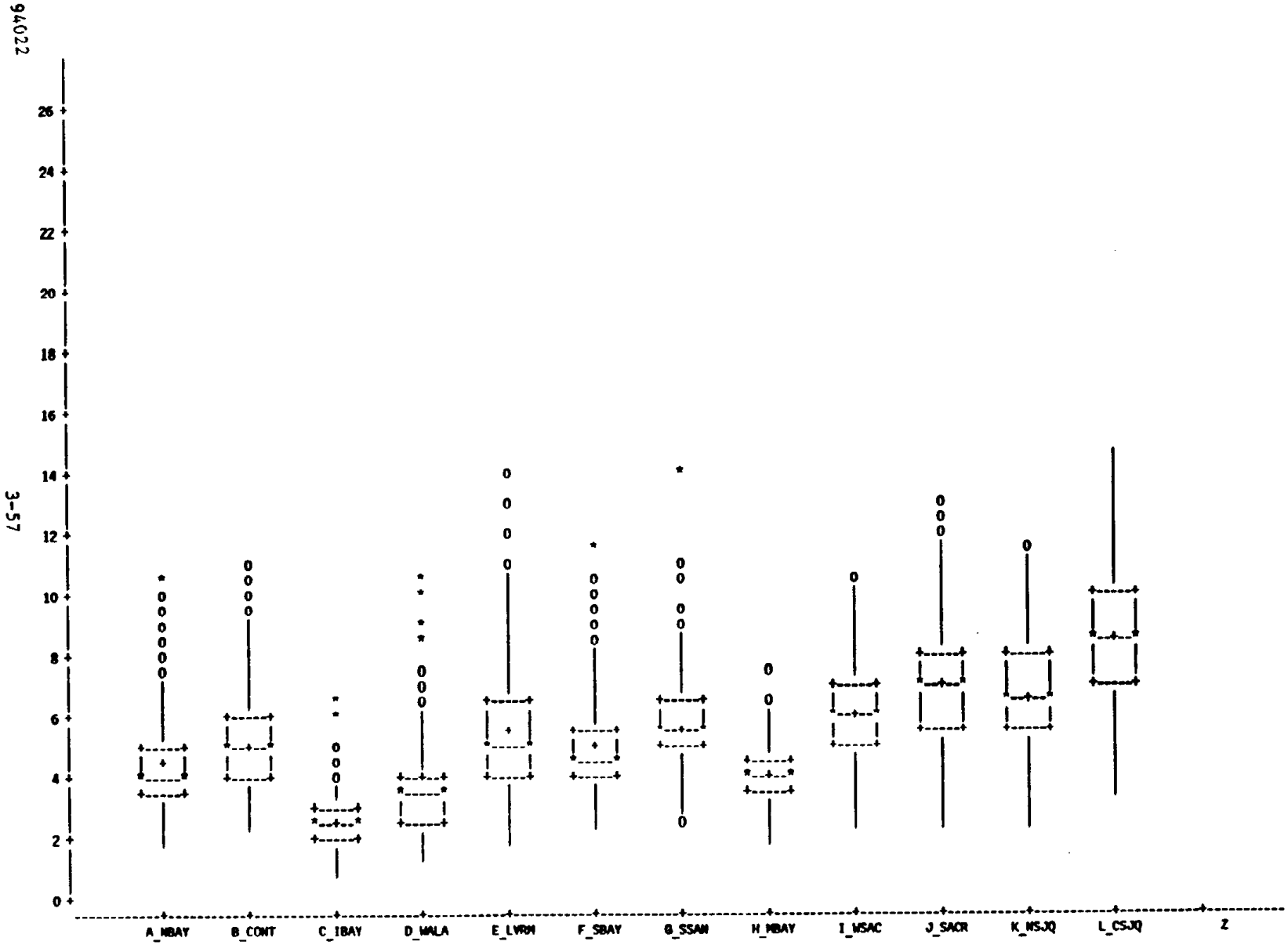

FIGURE 3-6g. Boxplots of subregion average daily maximum ozone concentrations: 1A flow pattern.

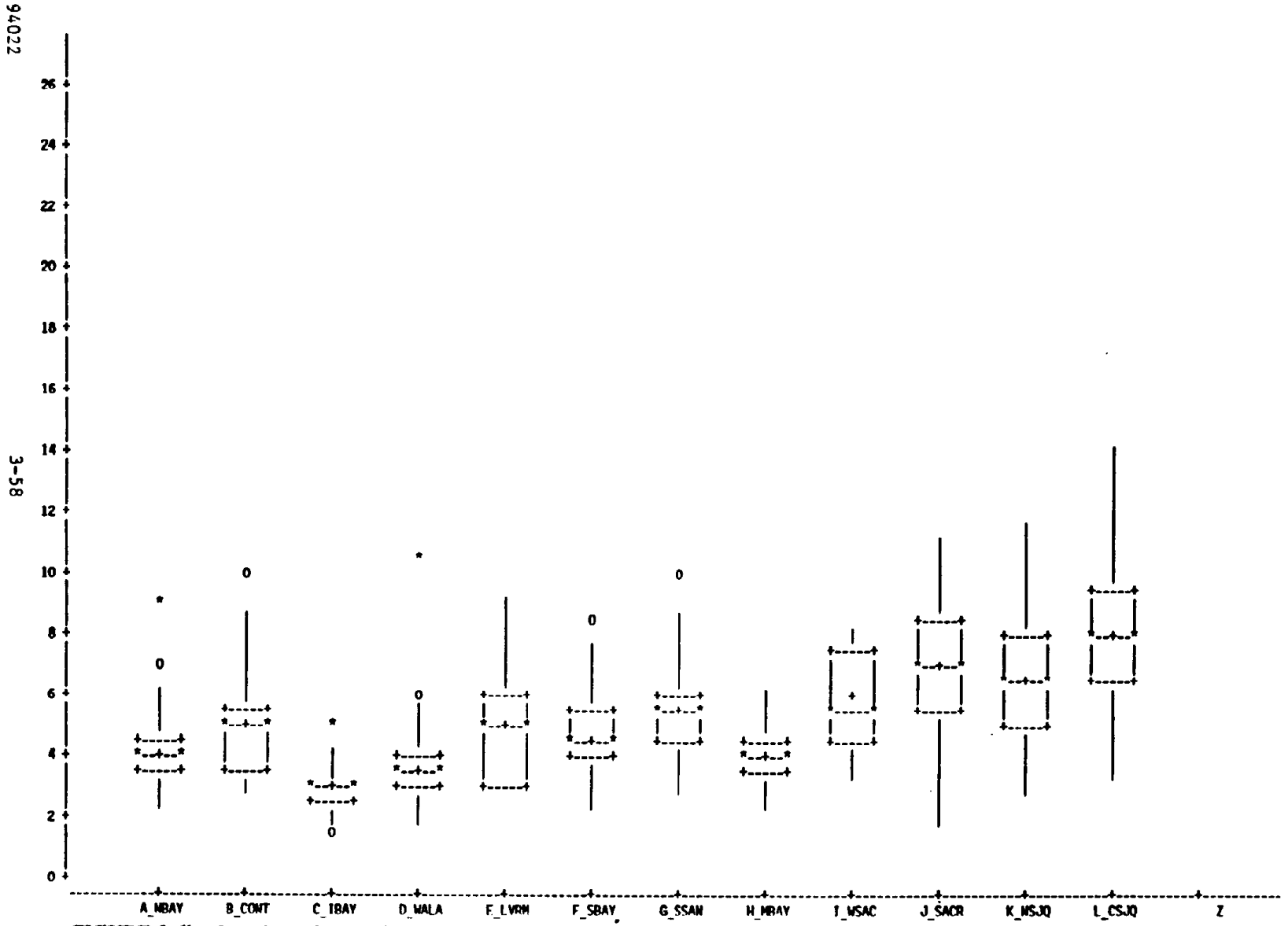

FIGURE 3-6h. Boxplots of subregion average daily maximum ozone concentrations: 1B flow pattern.

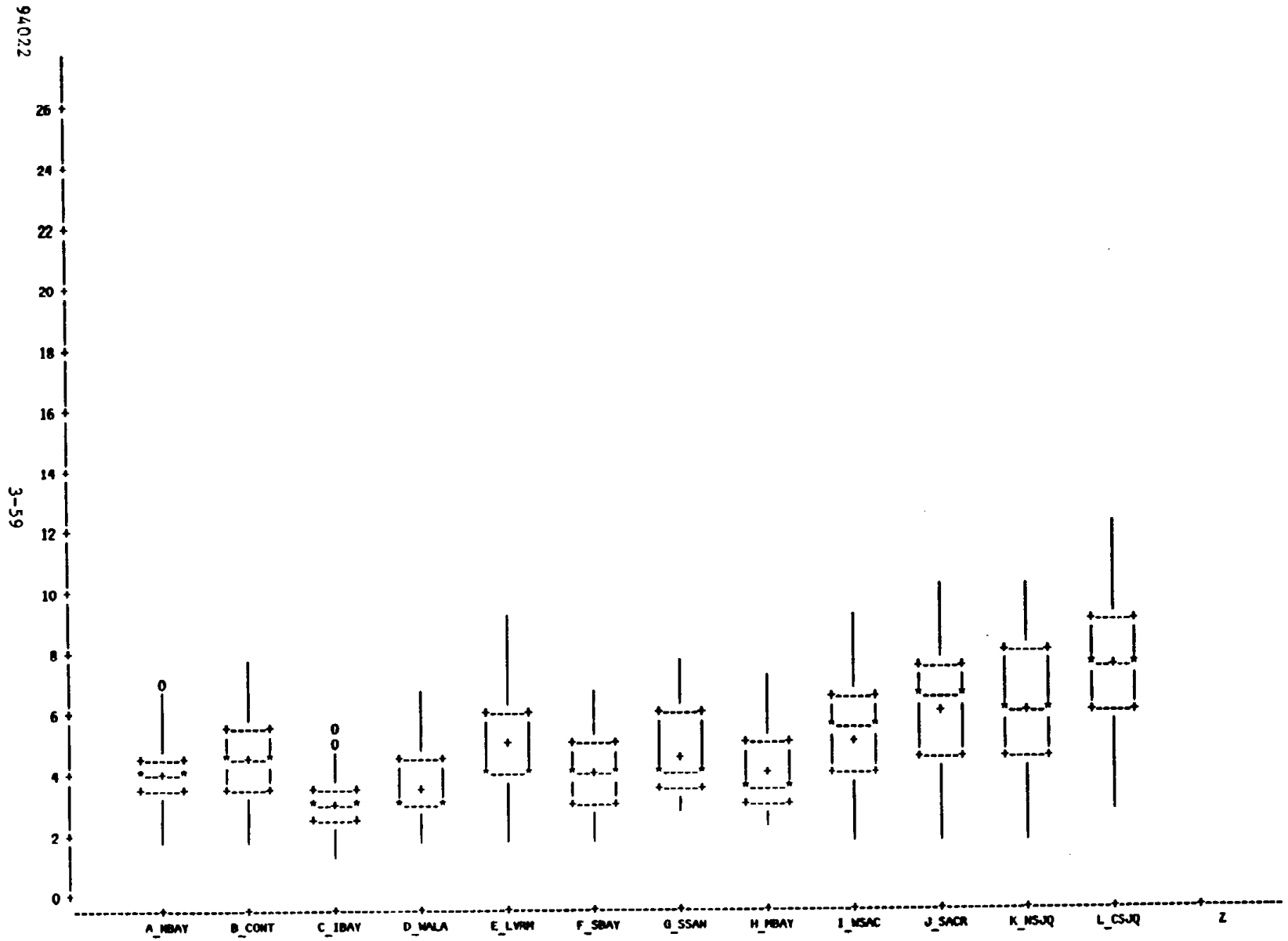

FIGURE 3-6i. Boxplots of subregion average daily maximum ozone concentrations: 2 flow pattern.

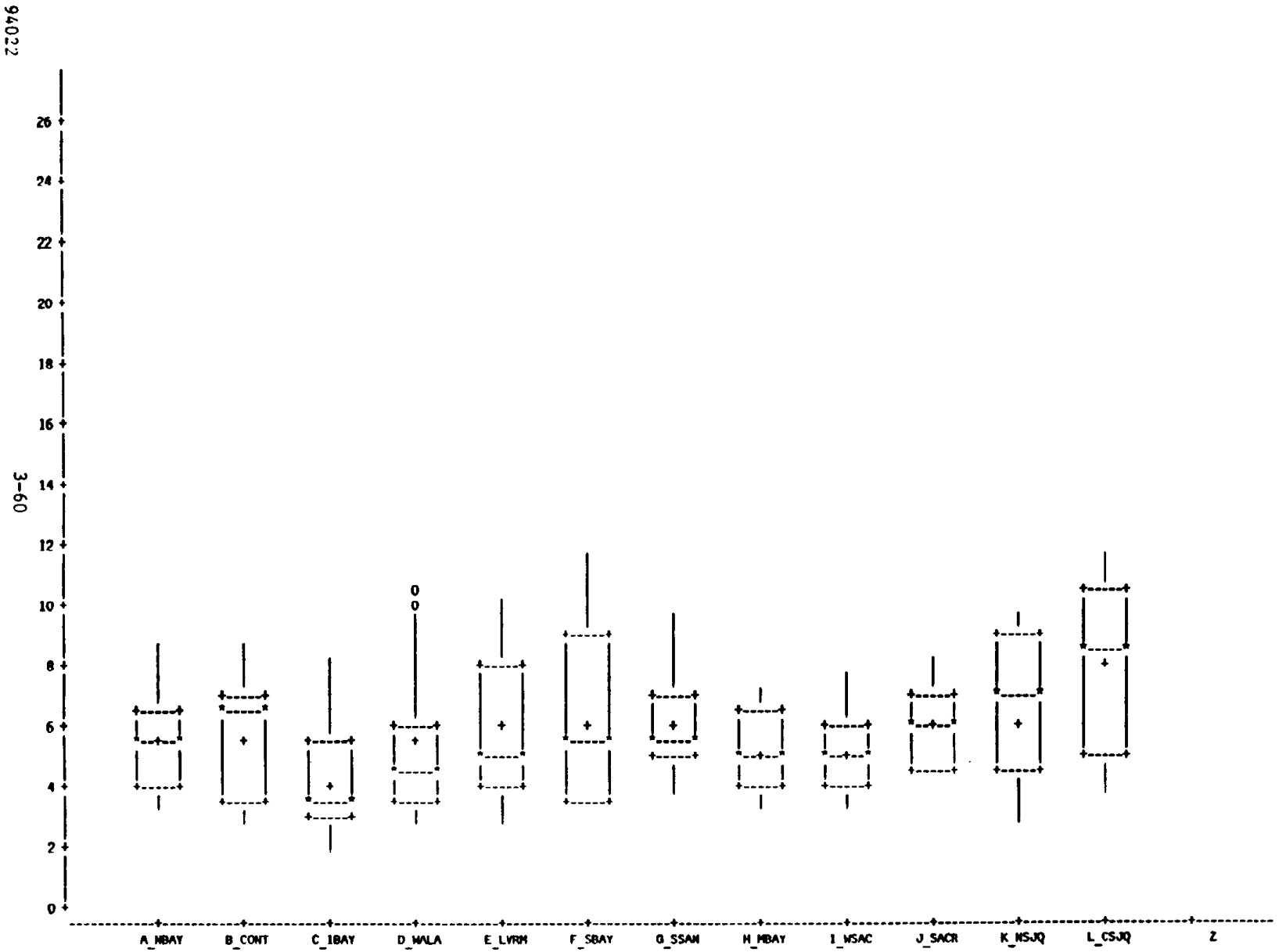

FIGURE 3-6j. Boxplots of subregion average daily maximum ozone concentrations: 4 flow pattern.

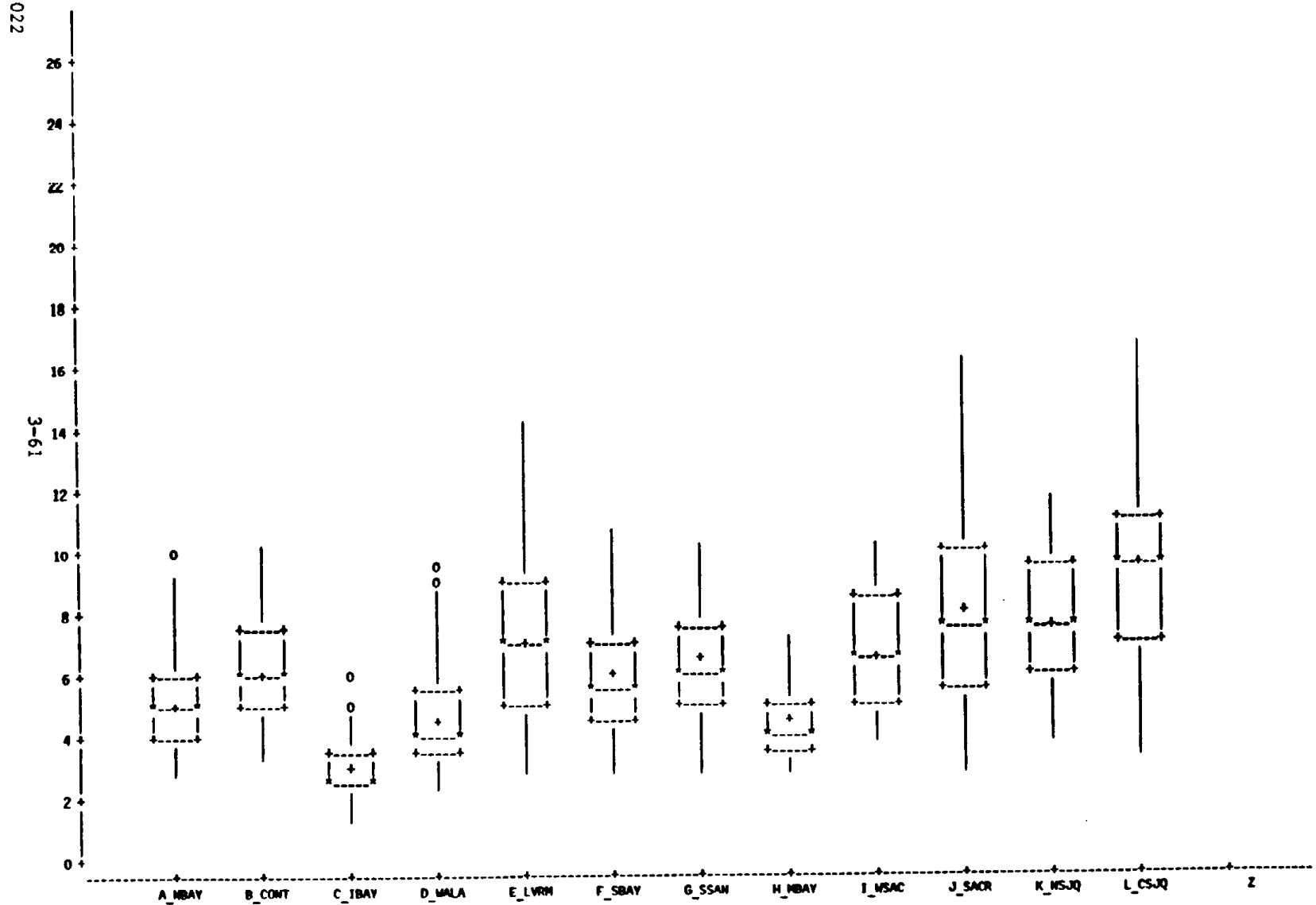

FIGURE 3-6k. Boxplots of subregion average daily maximum ozone concentrations: 6 flow pattern.

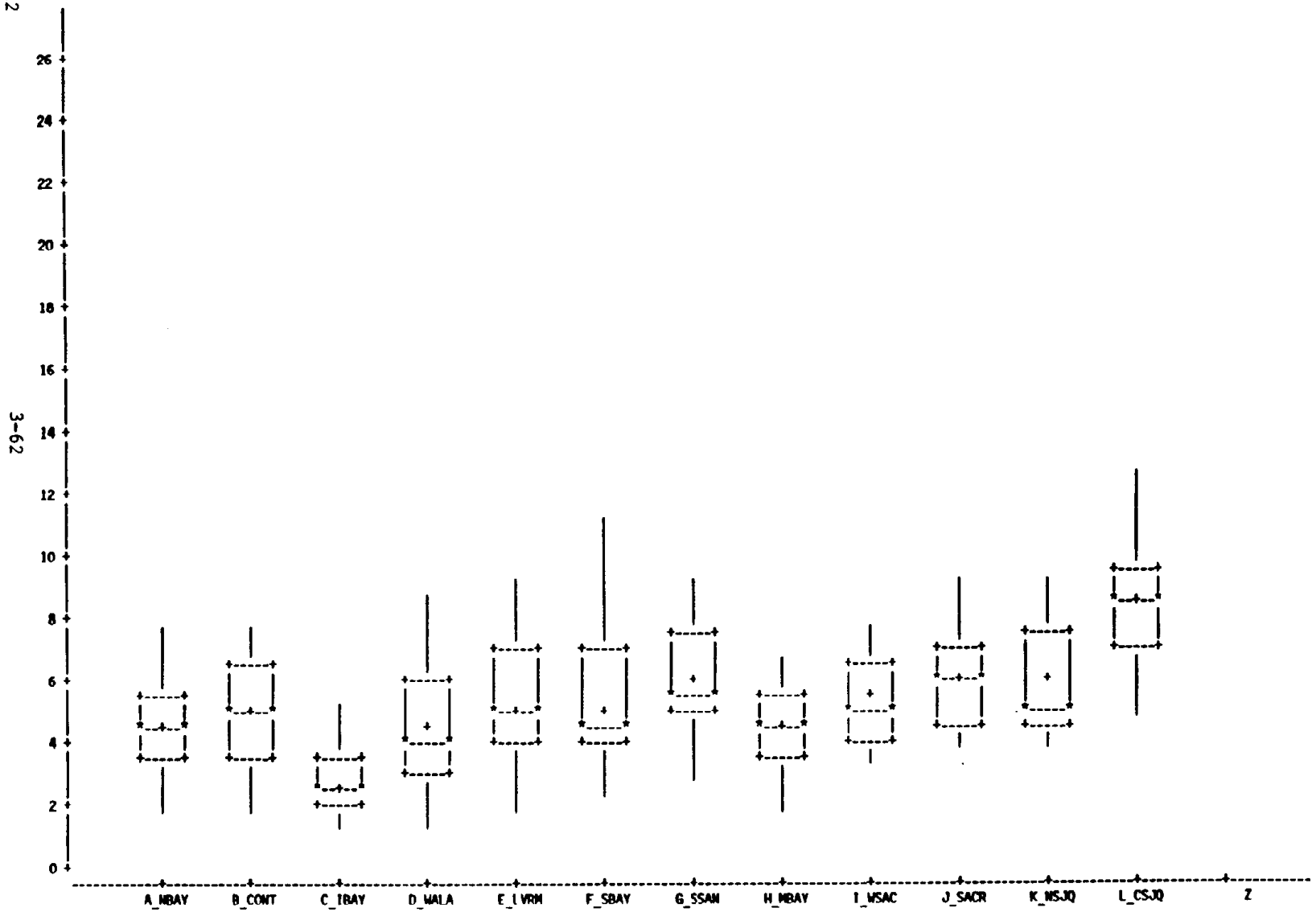

FIGURE 3-61. Boxplots of subregion average daily maximum ozone concentrations: 7 flow pattern.

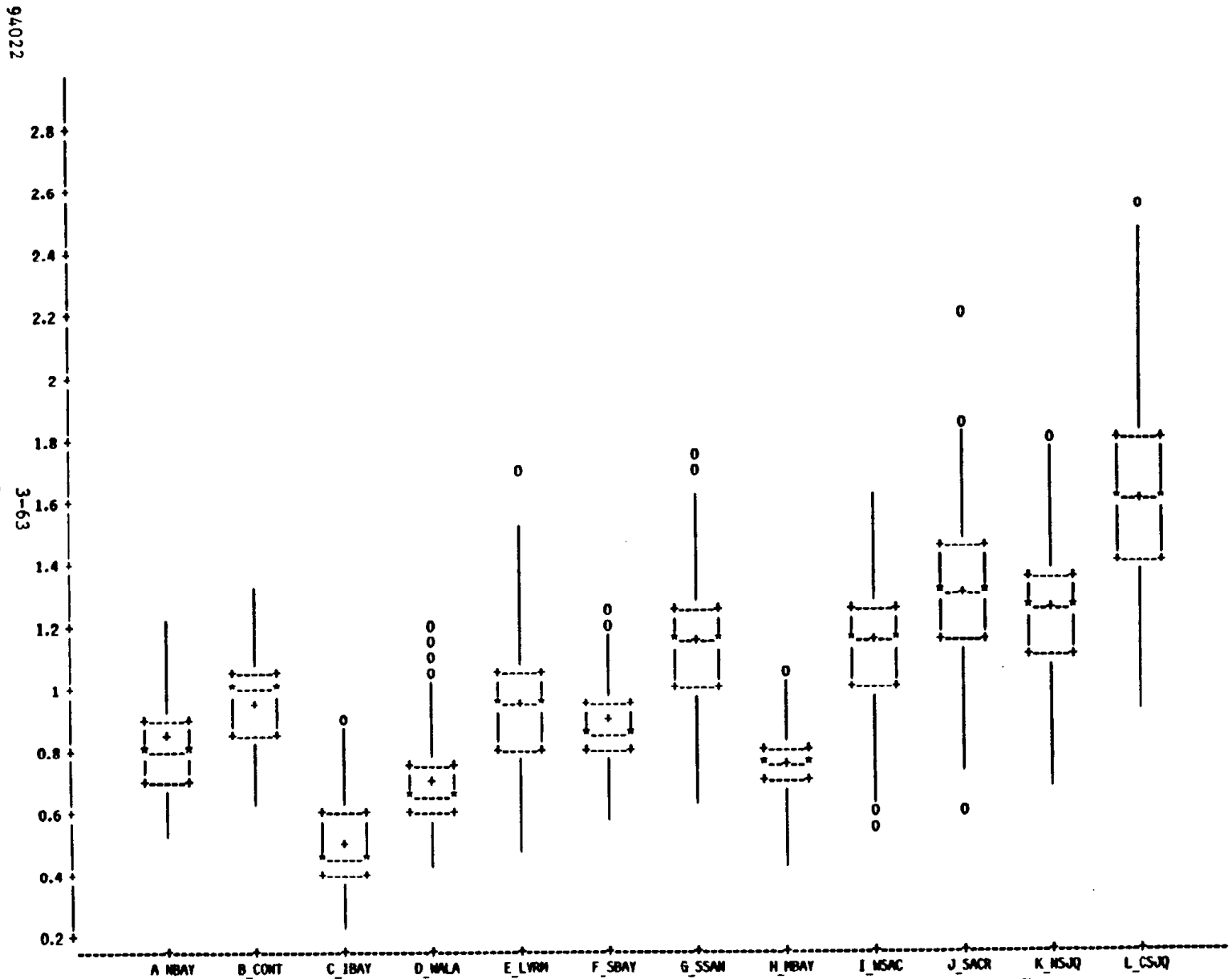

FIGURE 3-7a. Boxplots of subregion average relative daily maximum ozone concentrations: 1A-NW flow pattern.

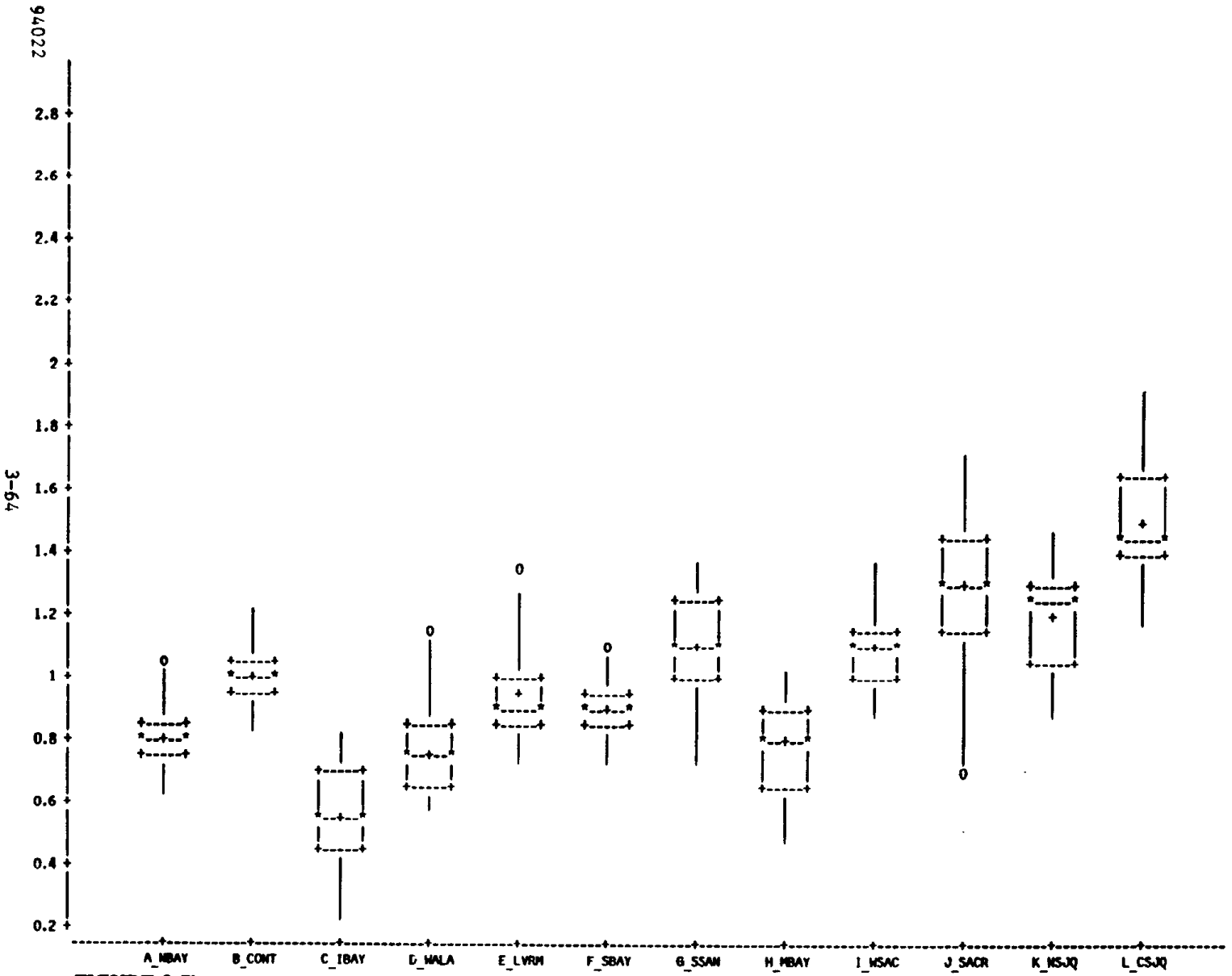

FIGURE 3-7b. Boxplots of subregion average relative daily maximum ozone concentrations: 1B-NW flow pattern.

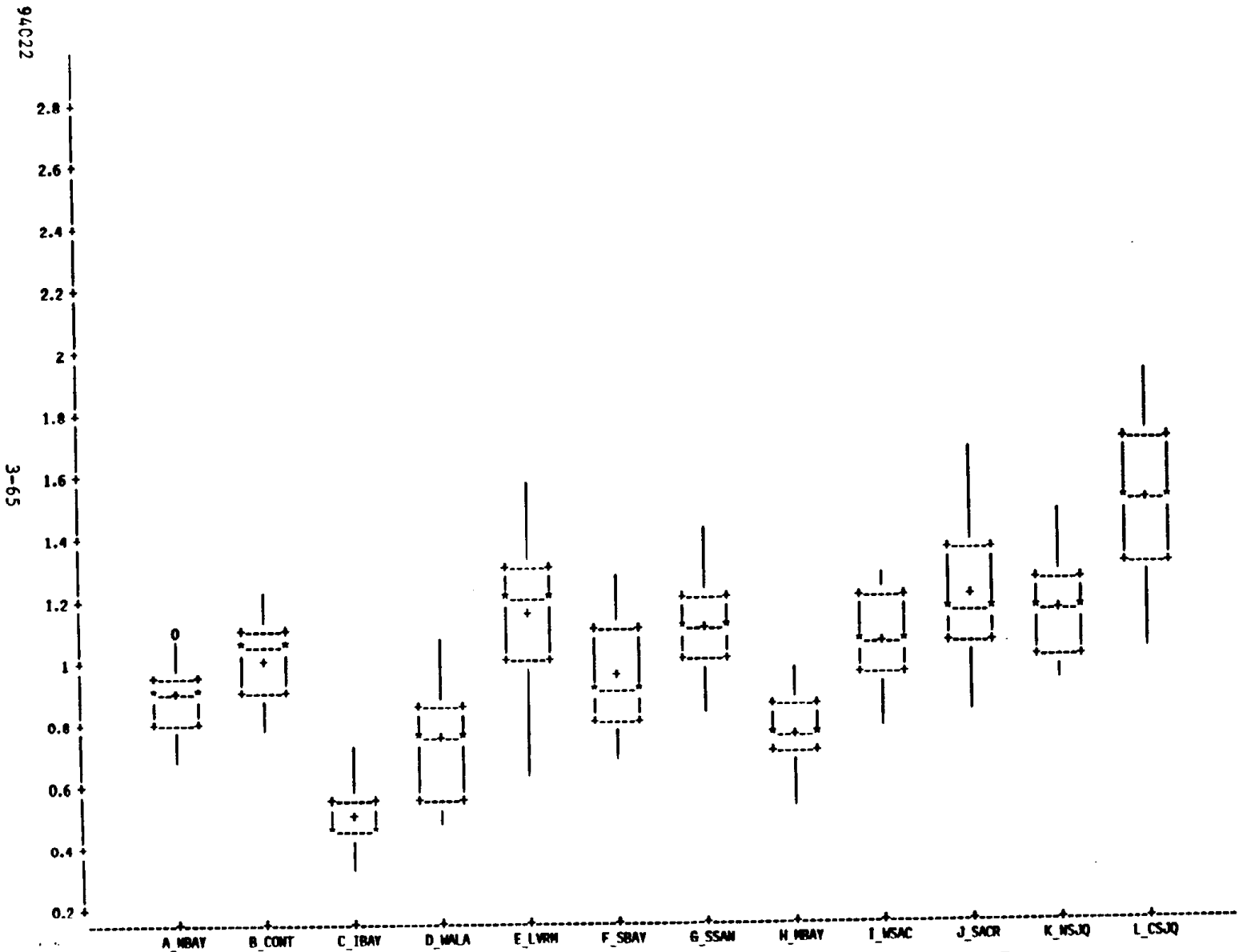

FIGURE 3-7c. Boxplots of subregion average relative daily maximum ozone concentrations: 6-NW flow pattern.

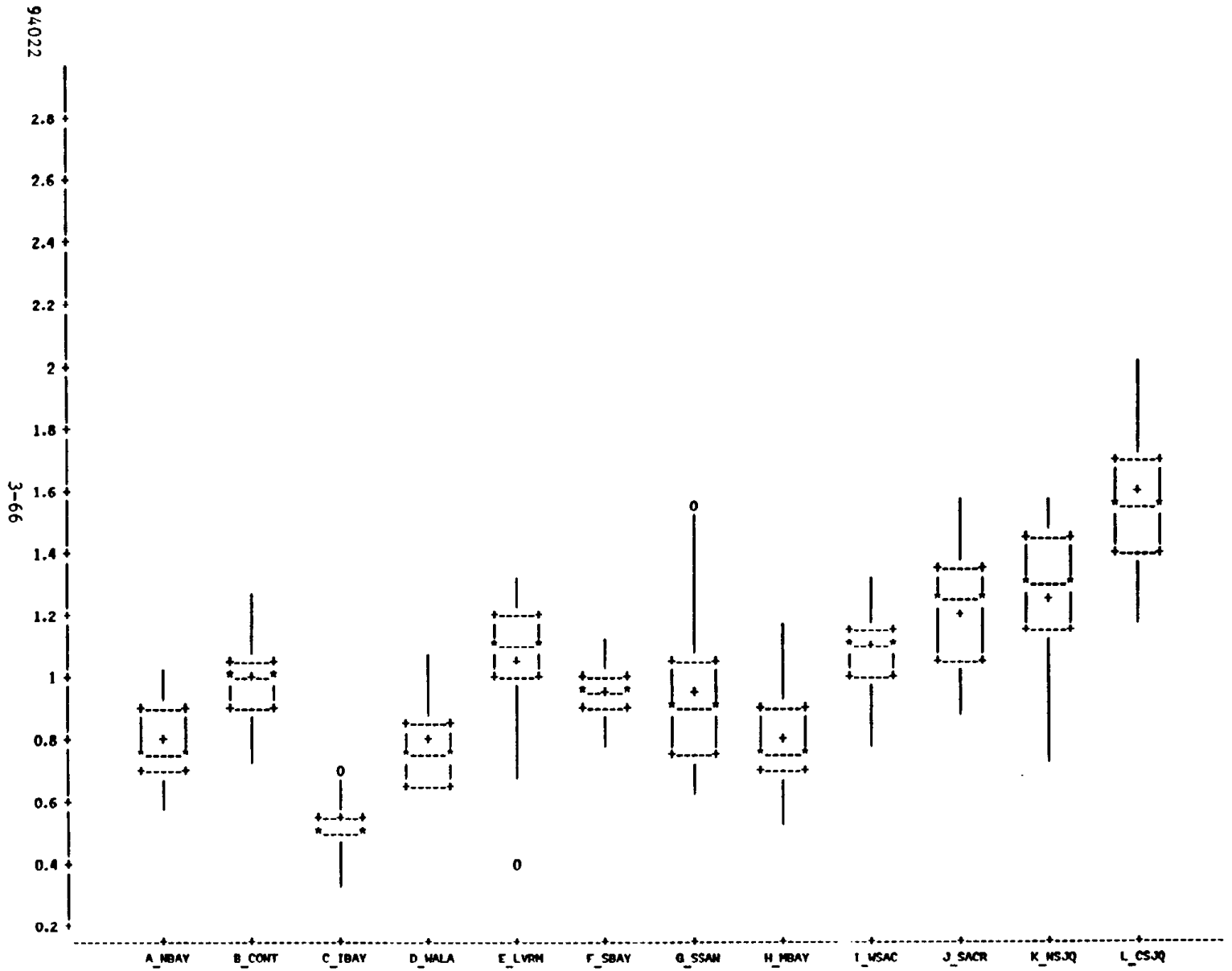

FIGURE 3-7d. Boxplots of subregion average relative daily maximum ozone concentrations: 1A-S flow pattern.

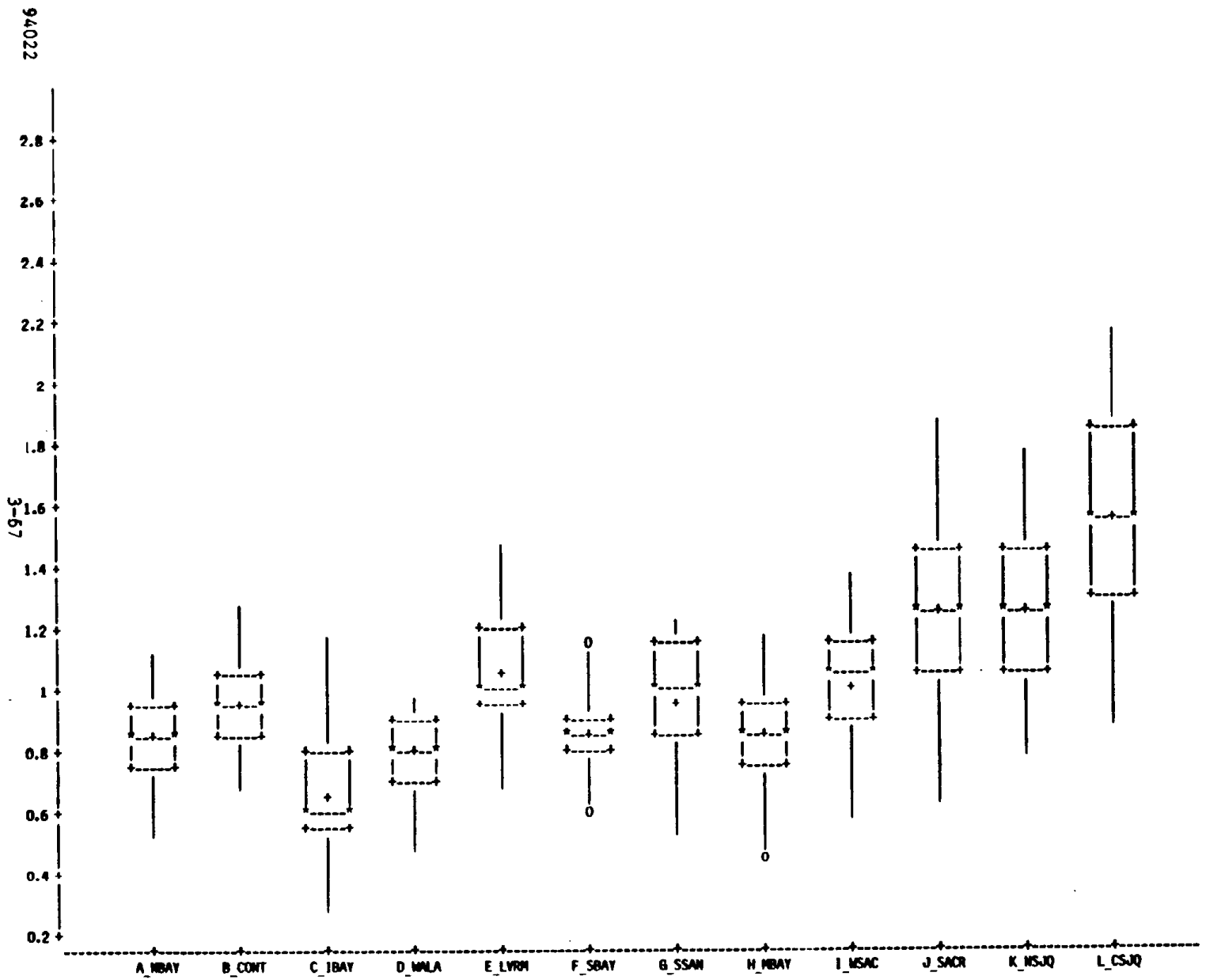

FIGURE 3-7e. Boxplots of subregion average relative daily maximum ozone concentrations: 2-S flow pattern.

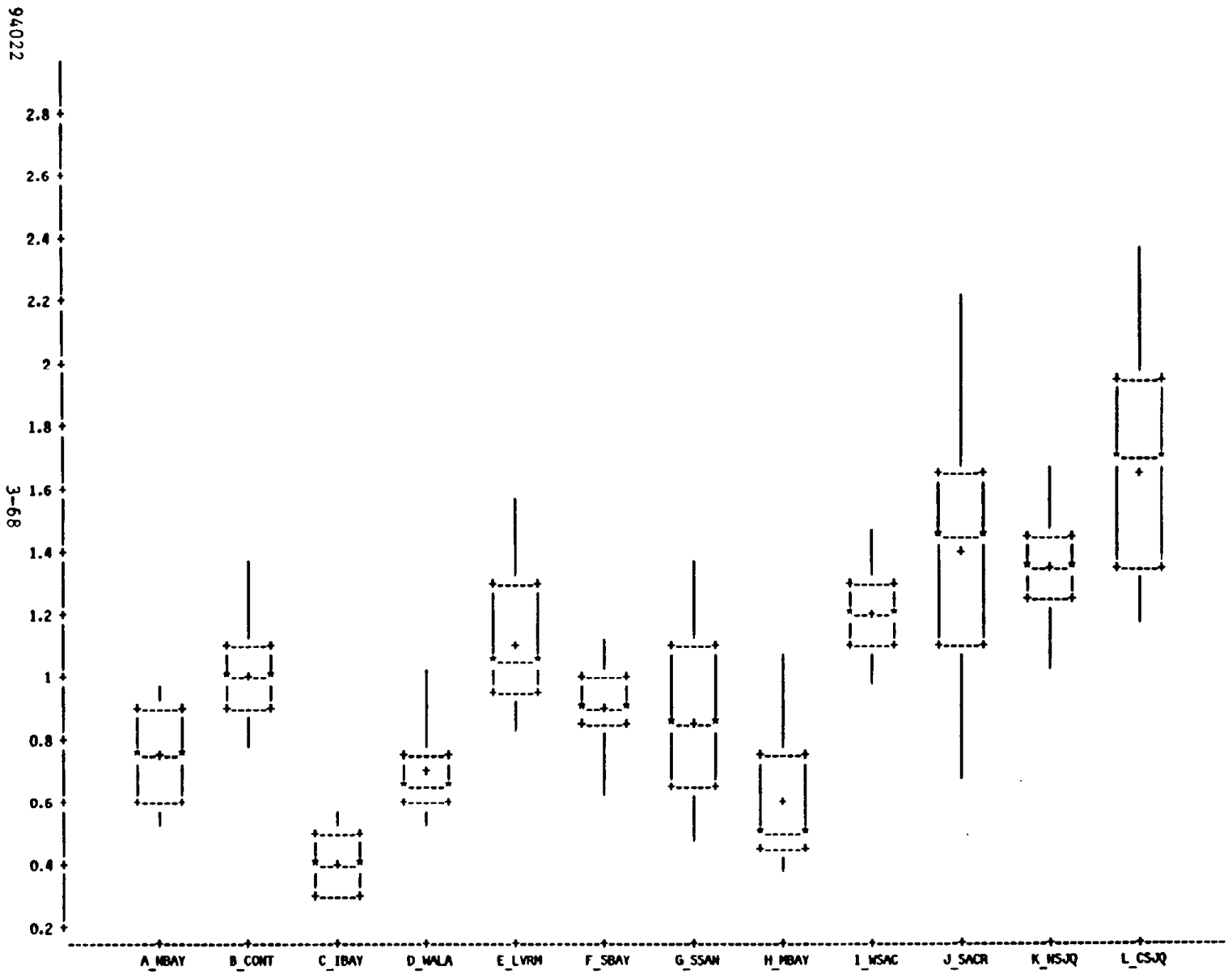

FIGURE 3-7f. Boxplots of subregion average relative daily maximum ozone concentrations: 6-S flow pattern.

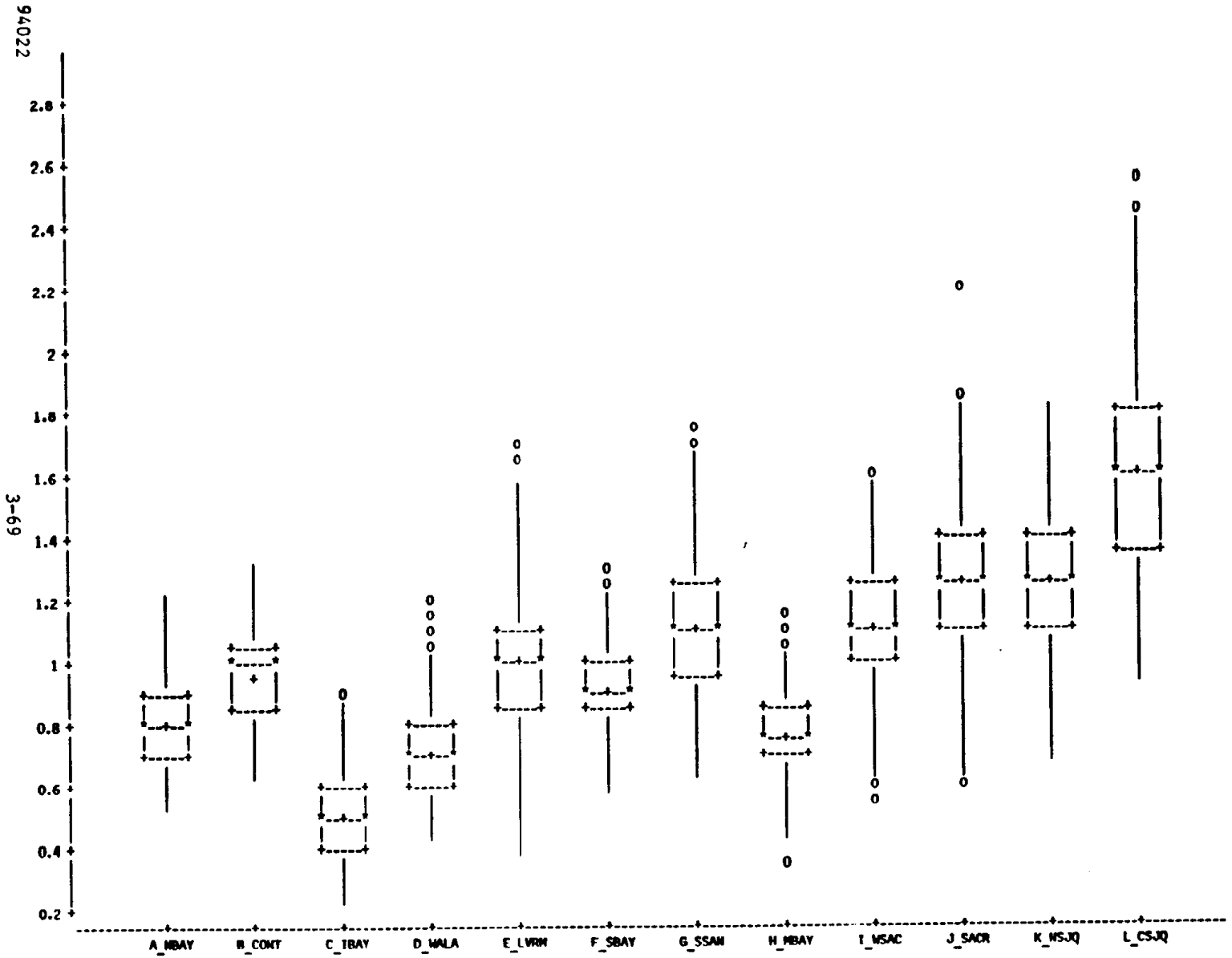

FIGURE 3-7g. Boxplots of subregion average relative daily maximum ozone concentrations: 1A flow pattern.

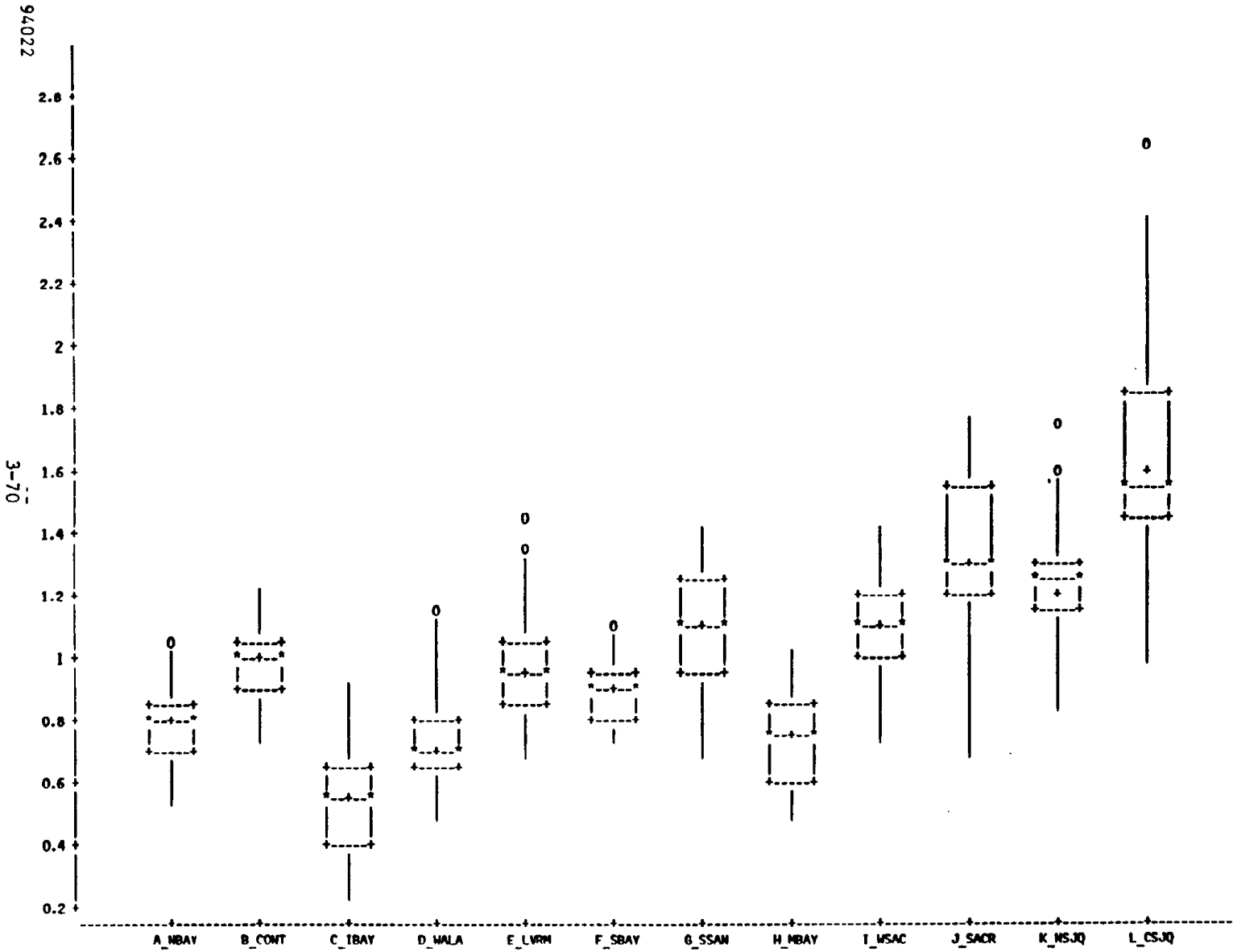

FIGURE 3-7h. Boxplots of subregion average relative daily maximum ozone concentrations: 1B flow pattern.

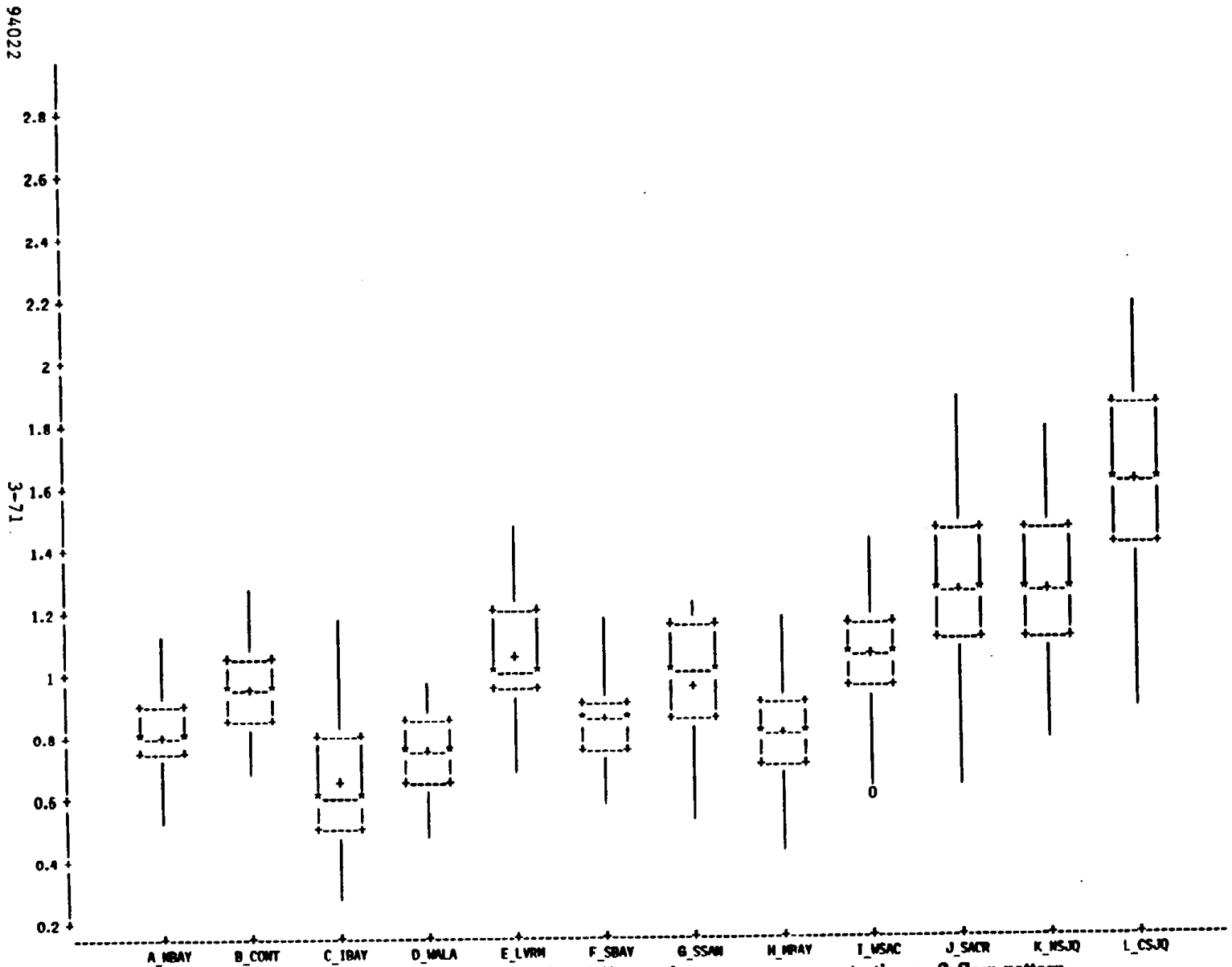

FIGURE 3-7i. Boxplots of subregion average relative daily maximum ozone concentrations: 2 flow pattern.

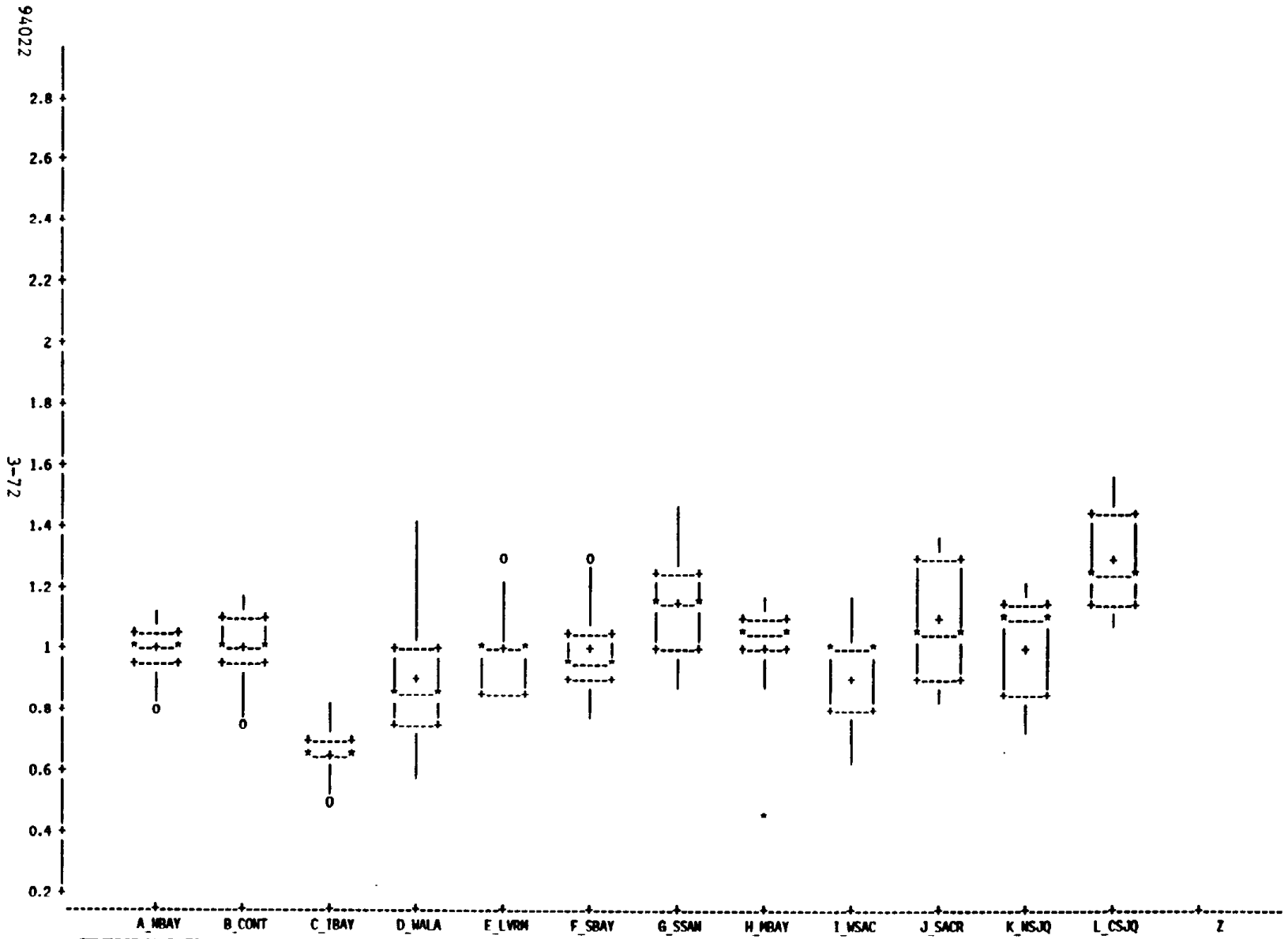

FIGURE 3-7j. Boxplots of subregion average relative daily maximum ozone concentrations: 4 flow pattern.

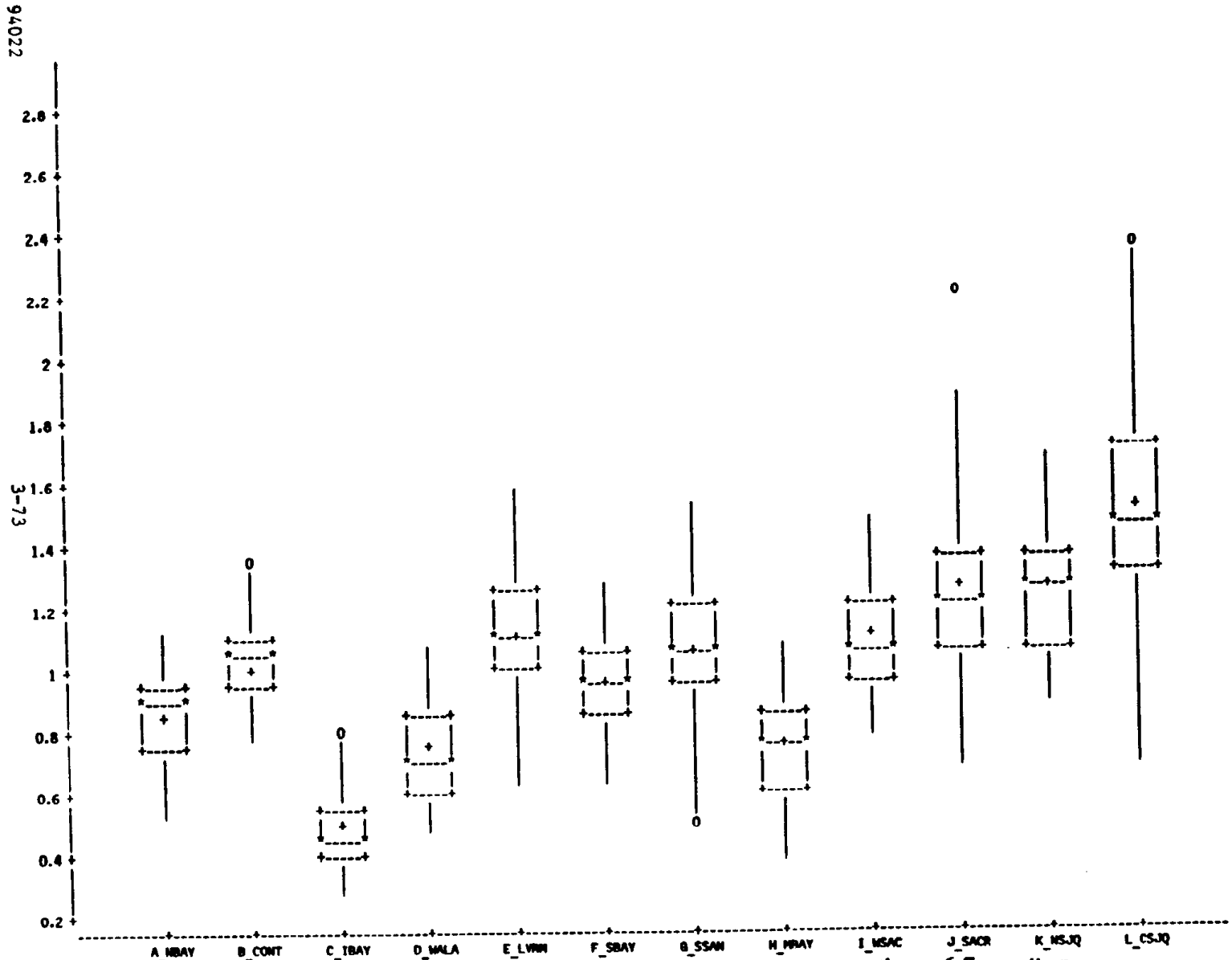

FIGURE 3-7k. Boxplots of subregion average relative daily maximum ozone concentrations: 6 flow pattern.

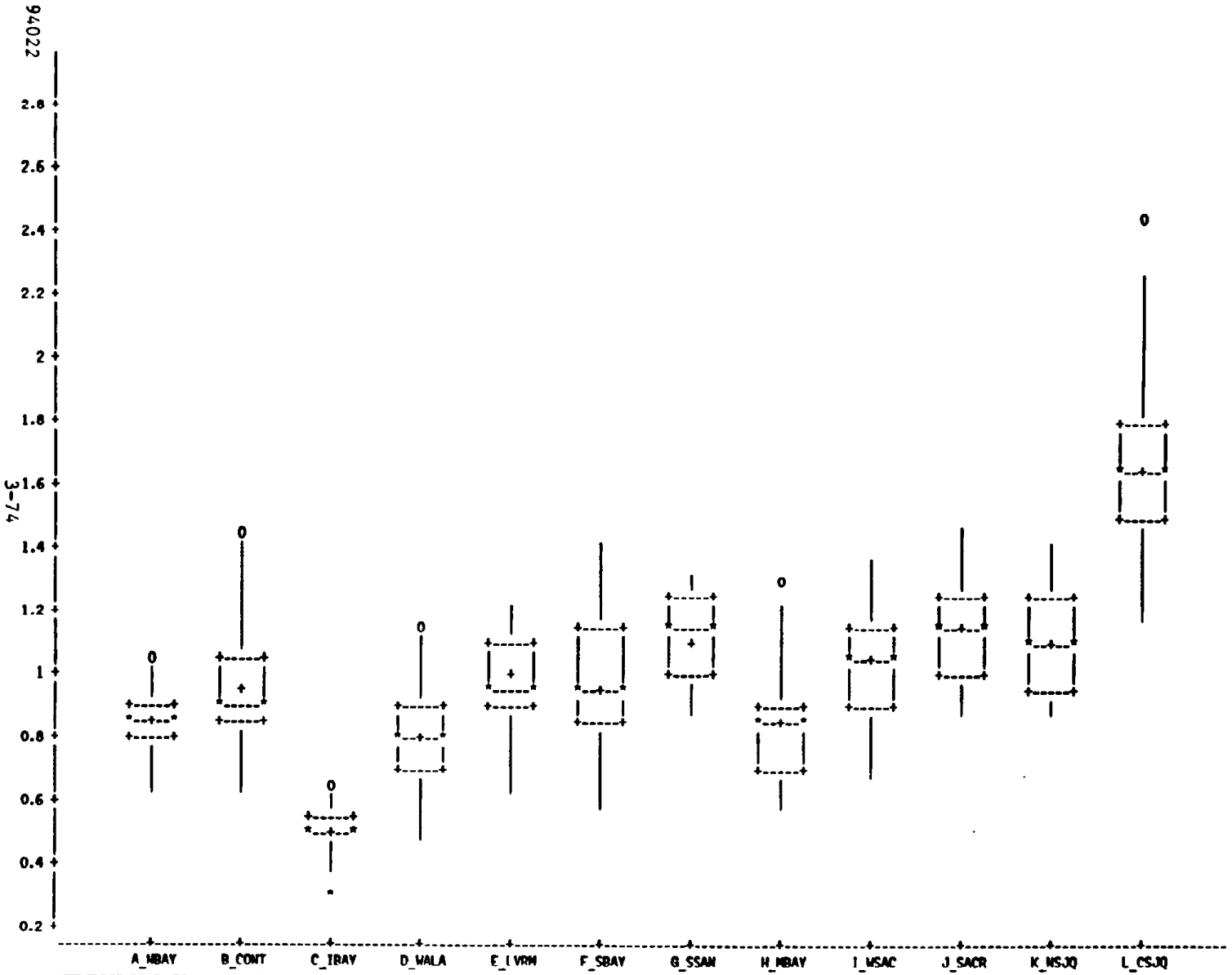

FIGURE 3-71. Boxplots of subregion average relative daily maximum ozone concentrations: 7 flow pattern.

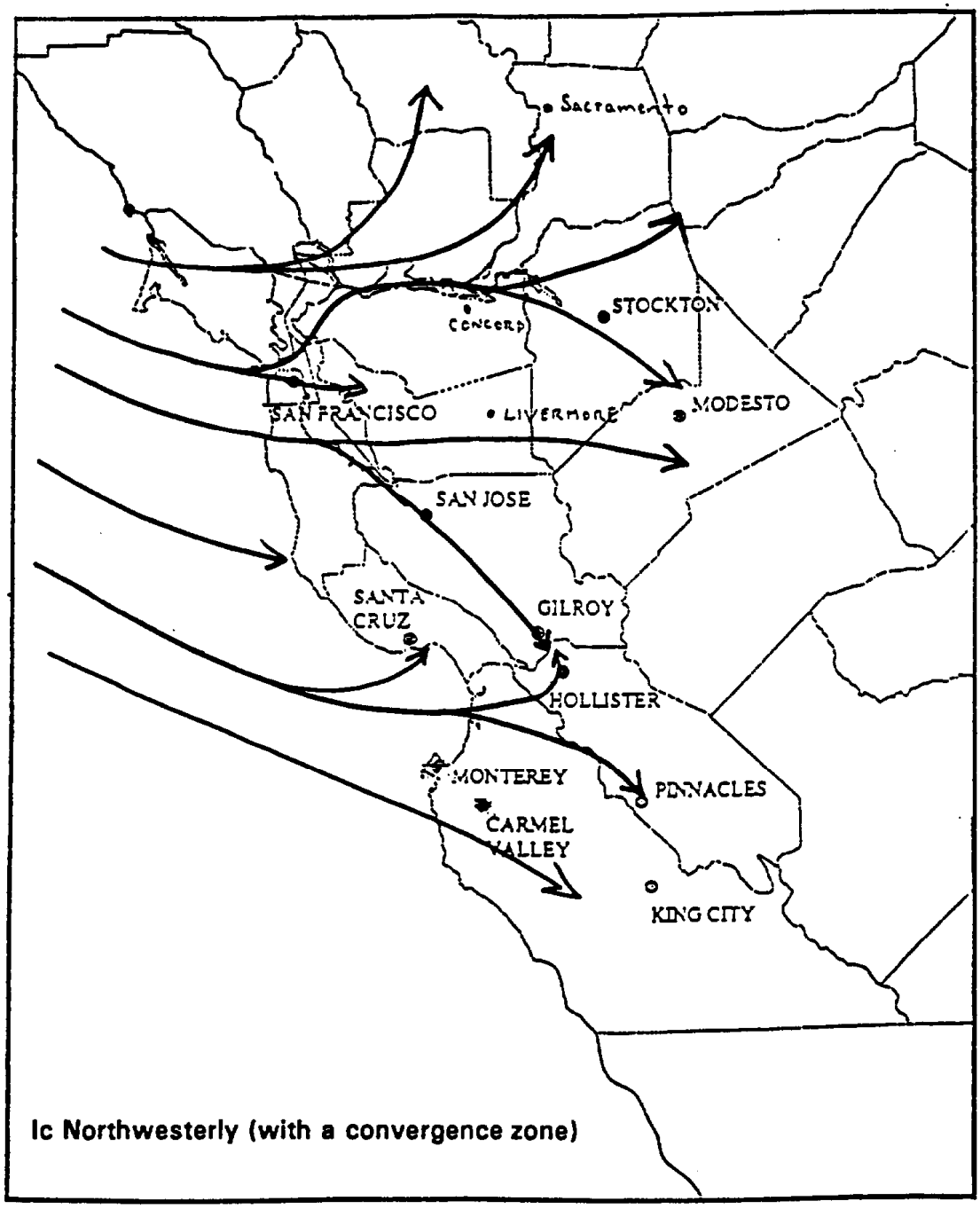

FIGURE 3-8a. Northwesterly flow with a convergence zone (Ic) - conceptual drawing.

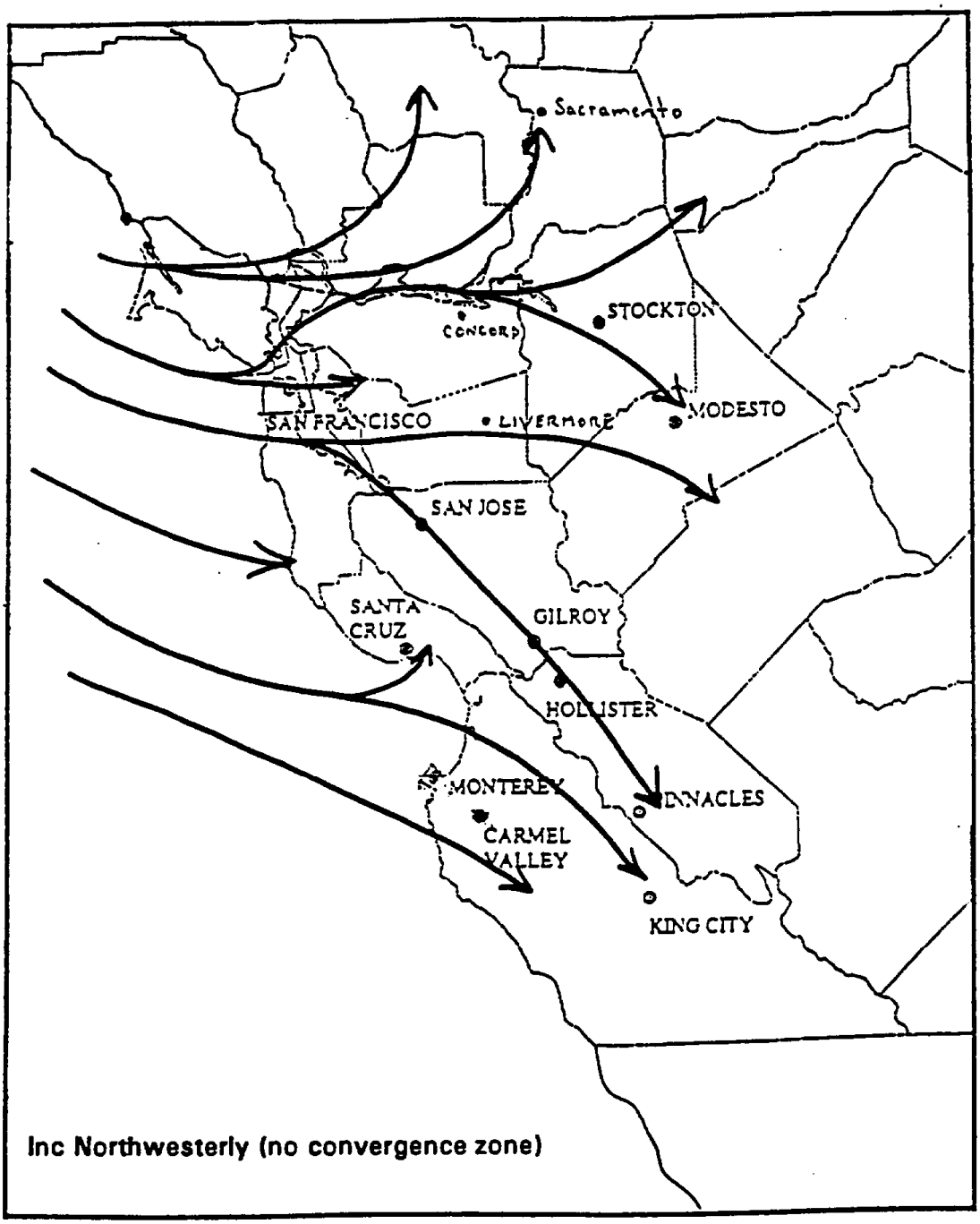

FIGURE 3-8b. Northwesterly flow without a convergence zone (Inc) - conceptual drawing.

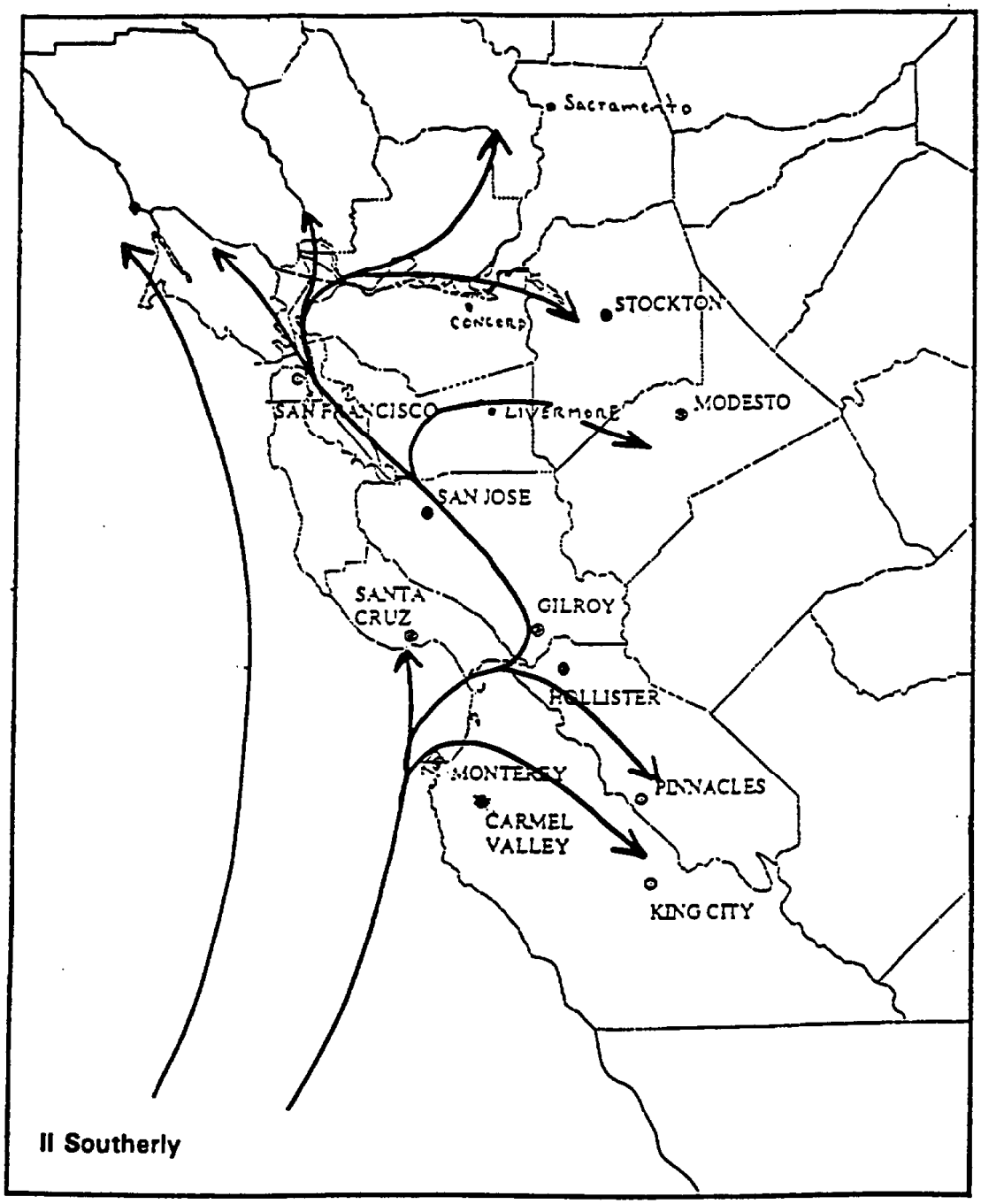

FIGURE 3-8c. Southerly flow (II) - conceptual drawing.

94022

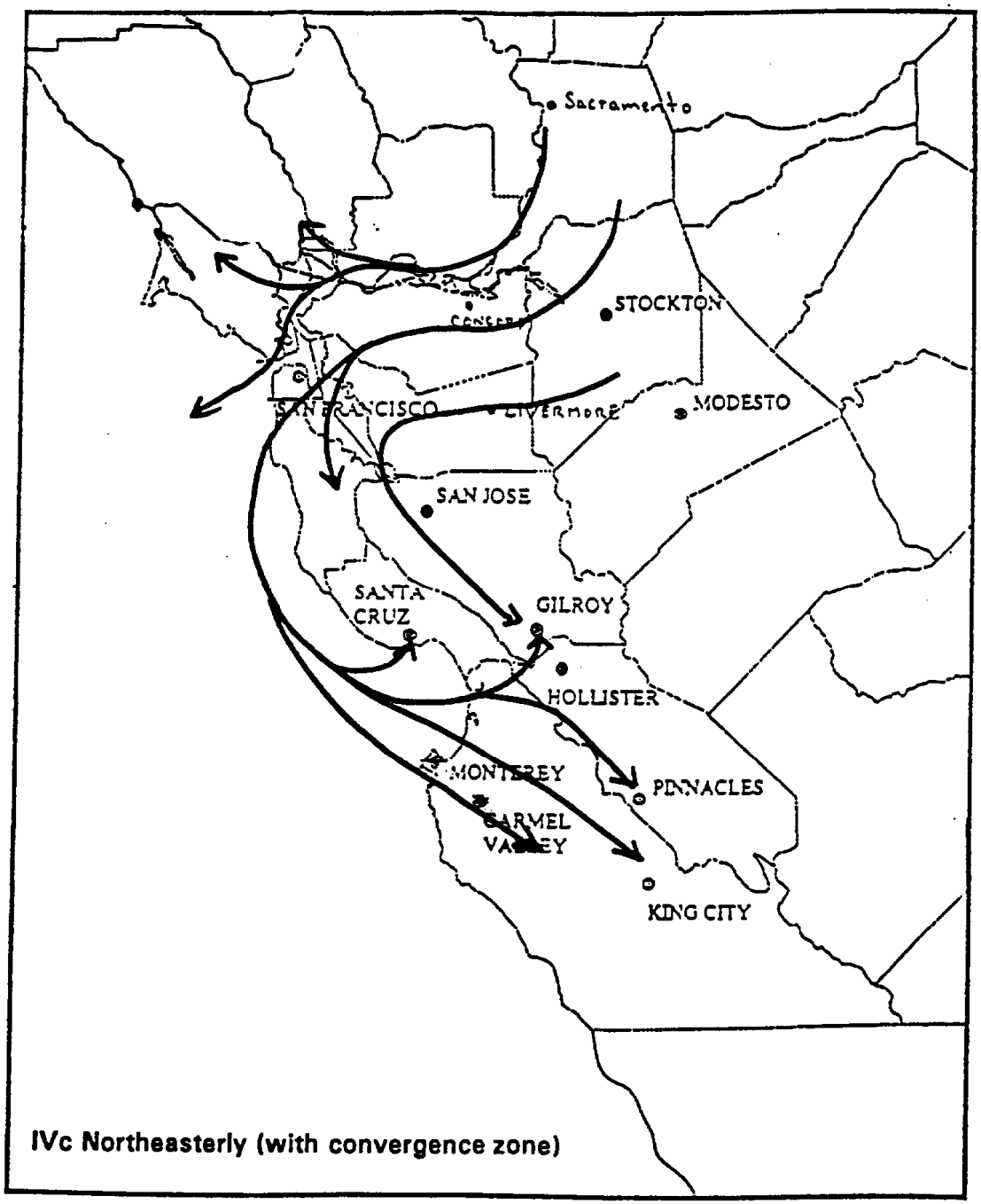

FIGURE 3-8d. Northeasterly flow with a convergence zone (IVc) - conceptual drawing.

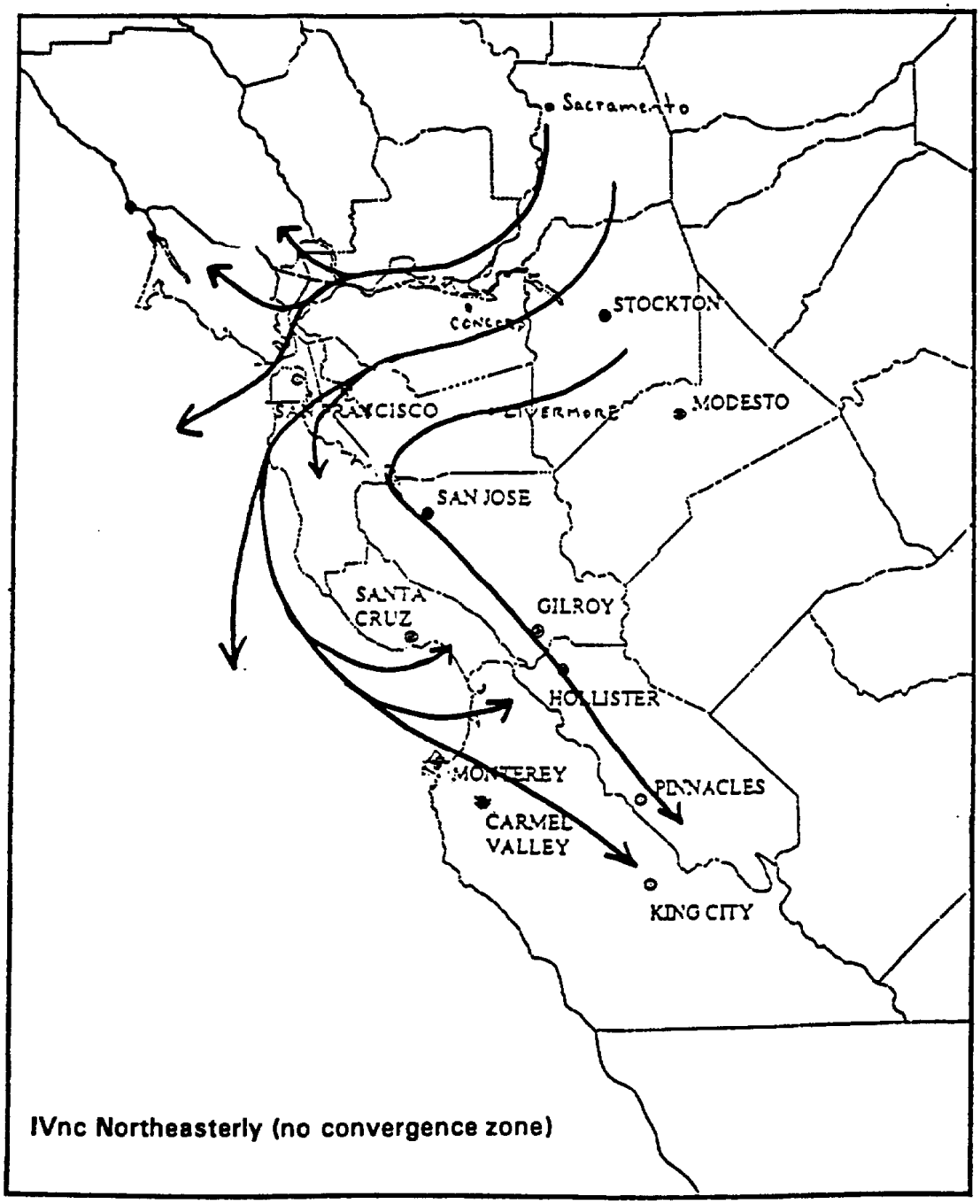

FIGURE 3-8e. Northeasterly flow without a convergence zone (IVnc) - conceptual drawing.

94022

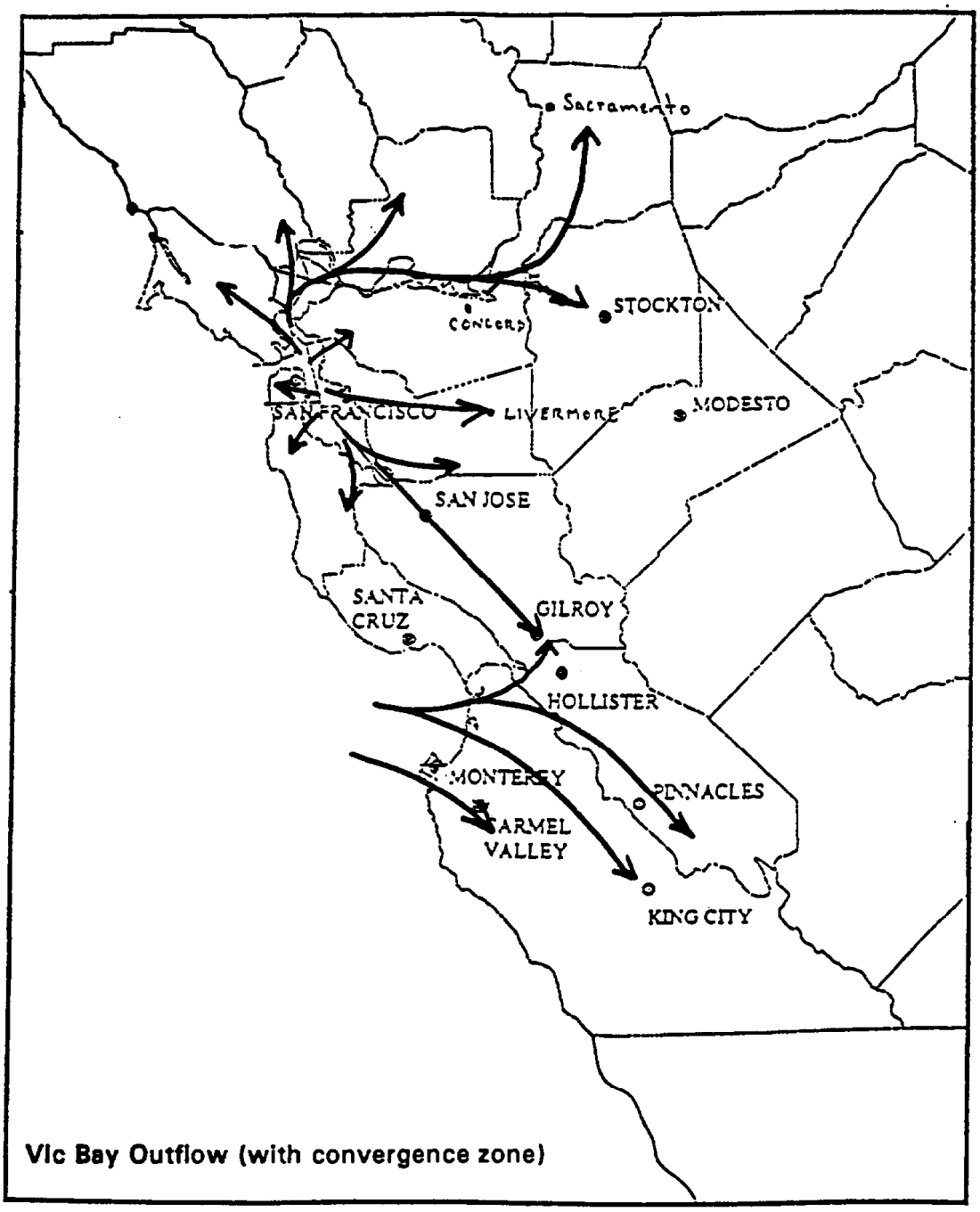

FIGURE 3-8f. Bay outflow with a convergence zone (VIc) - conceptual drawing.

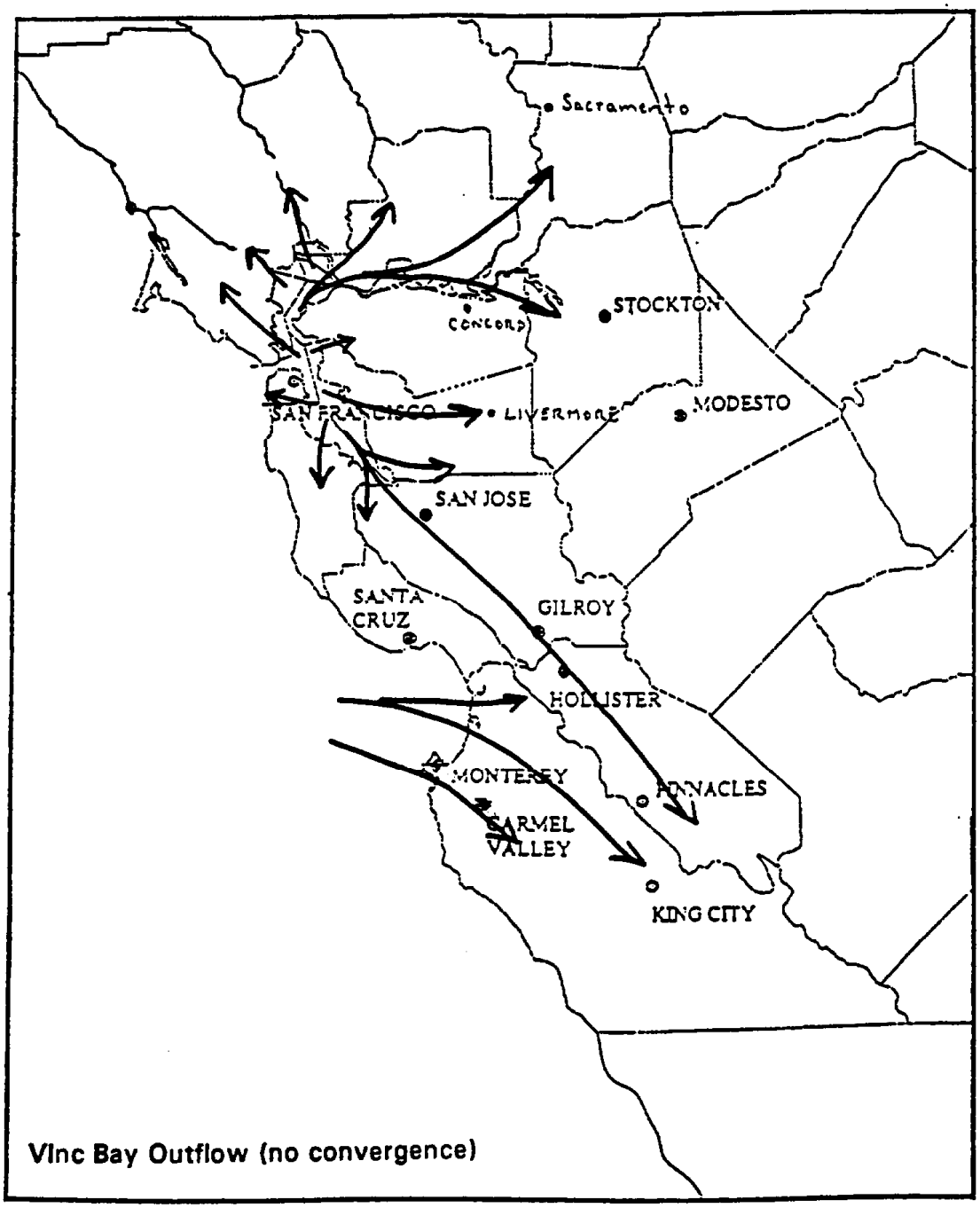

FIGURE 3-8g. Bay outflow without a convergence zone (VInc) - conceptual drawing.

94022

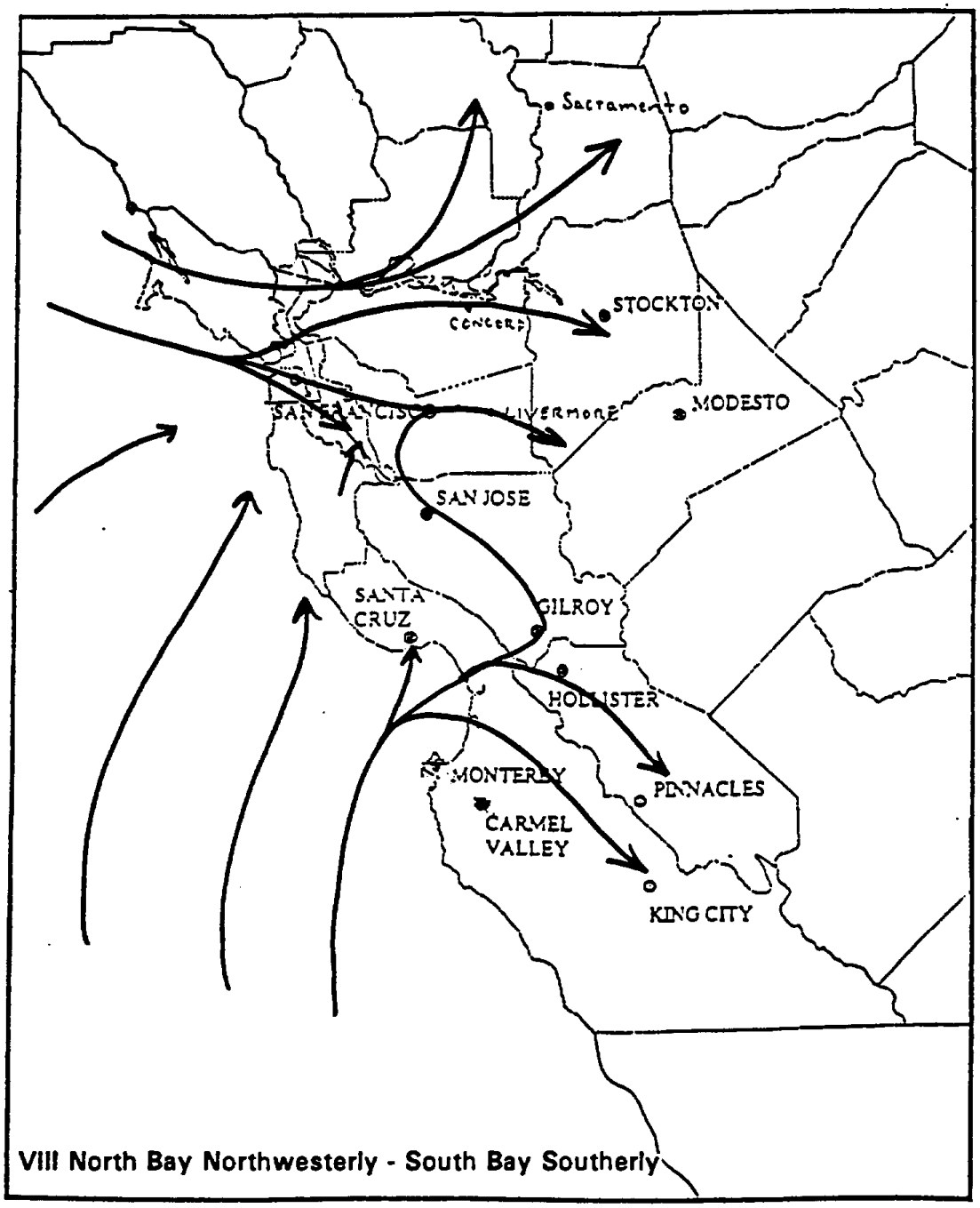

FIGURE 3-8h. North Bay Northwesterly - South Bay Southerly (VIII) - conceptual drawing.

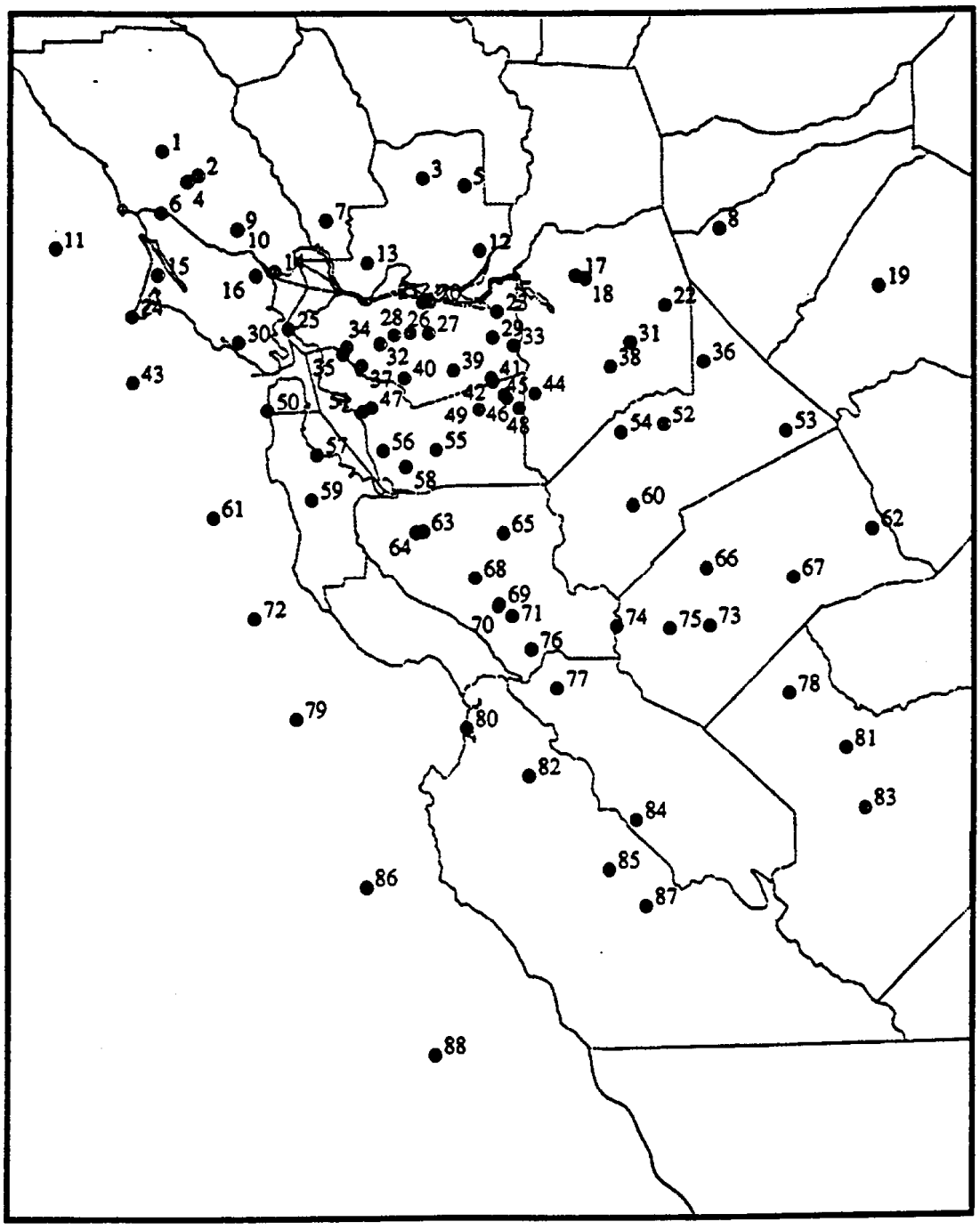

FIGURE 3-9. Map showing surface wind sites for trajectories.

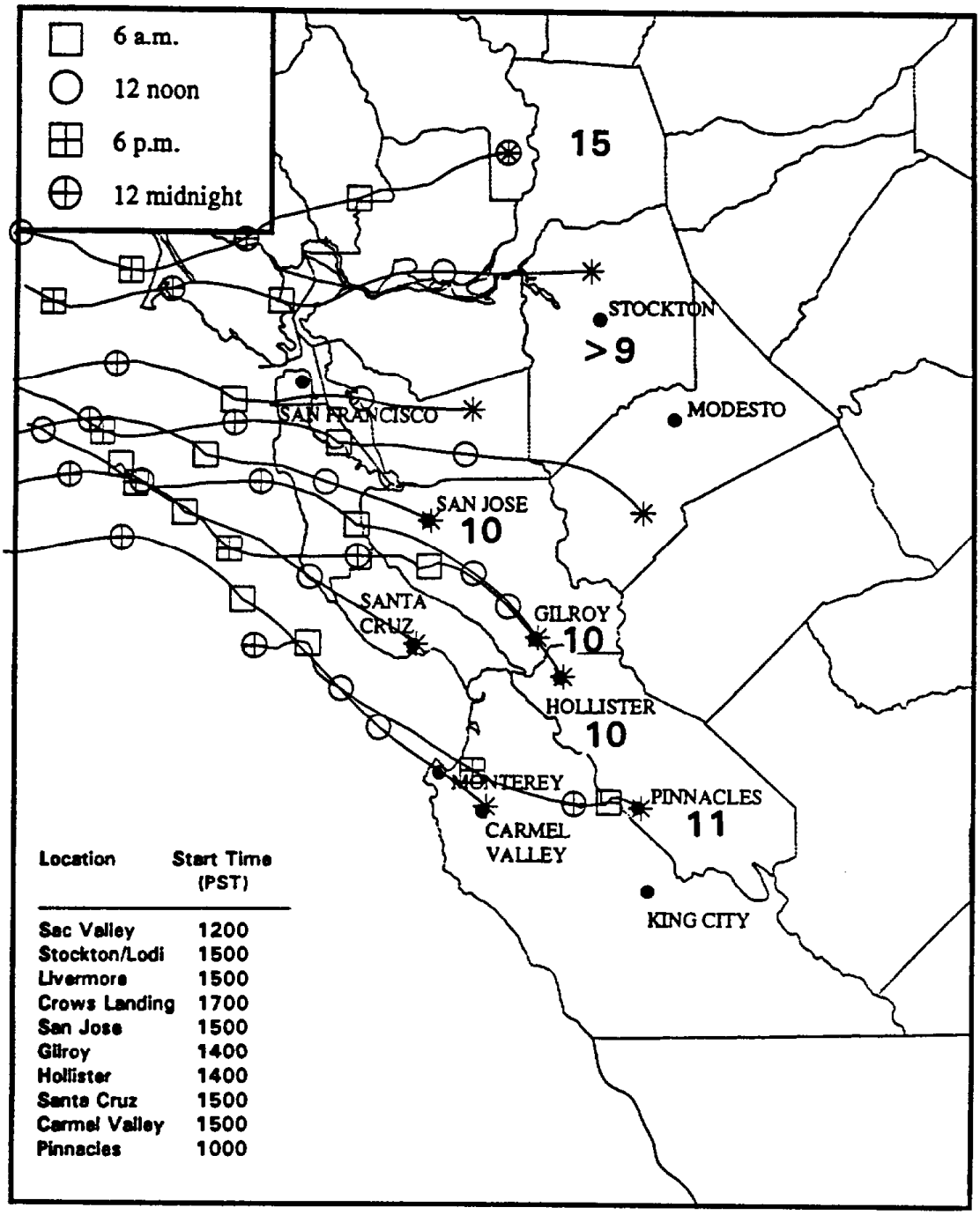

FIGURE 3-10. Backward trajectories from various locations and start times on 11 July 1990. Exceedance ozone concentrations (pphm) are shown on the map. These trajectories resemble northwesterly flow without convergence.

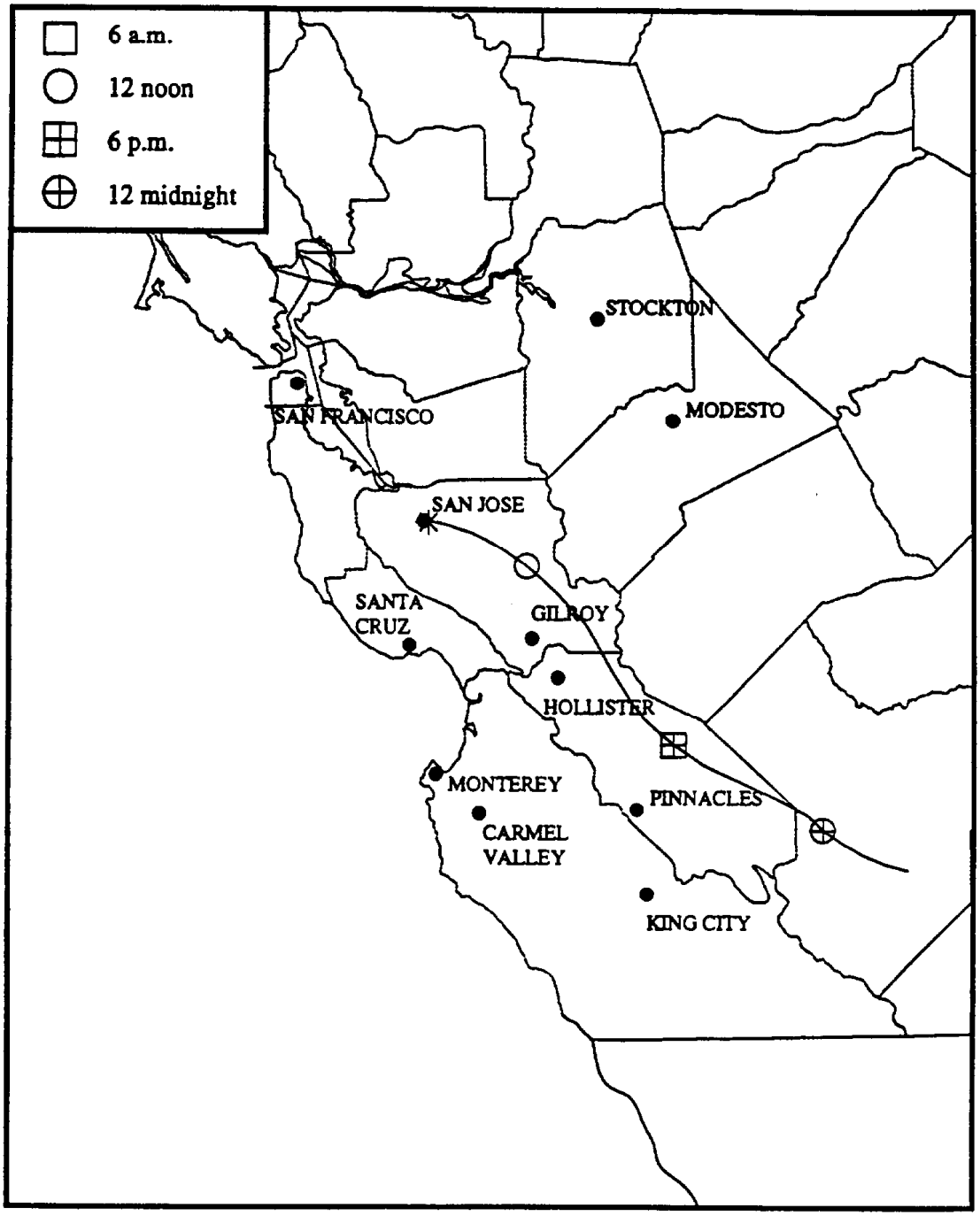

FIGURE 3-11. Forward trajectory from San Jose on 11 July 1990 at 0700 PST.

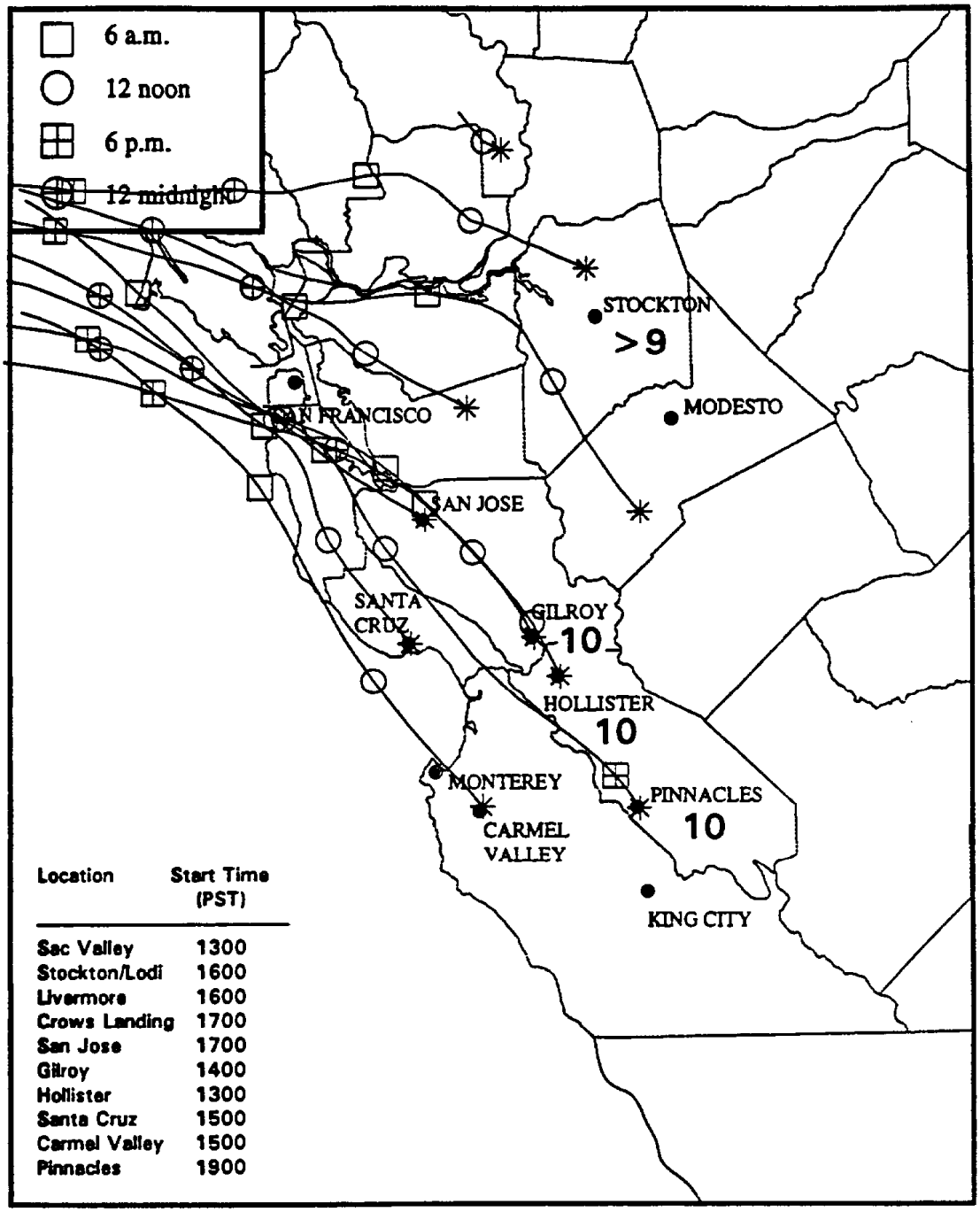

FIGURE 3-12. Backward trajectories from various locations and start times on 5 August 1990. Exceedance ozone concentrations (pphm) are shown on the map. These trajectories resemble northwesterly flow without convergence.